1728

UNIVERSITY of
NOTRE DAME

NASA/USRA UNIVERSITY ADVANCED DESIGN PROGRAM 1988-1989

Final Design Proposal

THE DELTA MONSTER

An RPV Designed to Investigate
the Aerodynamics of a Delta Wing Planform

Department of Aerospace and Mechanical Engineering
University of Notre Dame
Notre Dame, IN 46556

AERODYNAMIC DATA ACQUISTION FOR A DELTA WING MODEL USING A REMOTELY PILOTED VEHICLE

AE441: AIRCRAFT SYSTEMS DESIGN
4 MAY 1989

GROUP B

KRISTEN CONNOLLY
MIKE FLYNN
RANDY GALLAGHER
CHRIS GREEK
MARC KOZLOWSKI
BRIAN McDONALD
MATT McKENNA
RICH SELLAR
ANDY SHEARON

TABLE OF CONTENTS

CHAPTER 1

EXECUTIVE INFORMATION

EXECUTIVE SUMMARY

The mission requirements for the performance of aerodynamic tests on a delta wing planform posed some very unique problems, these included aerodynamic interference, structural support, data acquisition and transmission instrumentation, aircraft stability and control, and propulsion system implementation. However, since the overall integrity of the aircraft is of primary importance the preliminary design work outlined in this document was performed in order to arrive at a fundamentally solid design suitable for further development. This specifications of this design is summarized in Table 1.1.

The proposed aircraft is a test bed for a delta wing planform model used in aerodynamic testing. Presently, the overall aerodynamic configuration of the proposed aircraft incorporates twin tail booms, a low horizontal tail, twin vertical tails, a relatively large fuselage, and a low-mounted, rectangular-planform wing (see Figure 1.1). With the exception of the twin tail booms, which are the result of concerns over the dissipation of the vortices shed from the delta wing model, all of the configurational components are relatively conventional.

This aircraft is uniquely suited for the acquisition of aerodynamic data from a delta wing planform model because it was design for this purpose. The data acquisition system incorporated in this design has the advantage of being extremely fast. It can read 100 pressure ports virtually simultaneously! During each test flight the test engineer will be able to test any of 20 angles of attack in the Reynold's number range of 550,000 to 1,650,000 and 28 tests are possible during each flight due to an average flight duration of 30 minutes.

This aircraft will be catapult launched so as to expend minimal fuel and also to allow for an extremely short take-off distance. Once in the air the aircraft will be manually controlled until the test altitude is reached, at which time control will be transferred to a computer-based, automatic control system. This will allow for the standardization of the data acquisition procedure. As a safety feature the test engineer (or technician) always reserves the right to override the automatic system and resume manual control. After the flight (average duration of 30

minutes) the proposed aircraft will land on the deployed spring-loaded landing gear.

The propulsion system proposed for this design utilizes a ducted fan unit housed in the rear of the fuselage. This system was chosen and developed because of concerns over the quality of flow over the test model. By removing flow from the propulsion unit from the upper surface of the aircraft (wings, forward end of fuselage, rear end of fuselage, etc.), good flow quality should be ensured.

The overall structural integrity of the aircraft is quite sound. The results of the preliminary design studies revealed that conventional, light-weight, low cost materials could be utilized for the fabrication of this aircraft. Hence, the entire aircraft will be constructed of balsa, spruce, and a shear carrying thin plastic covering (*e.g.* Monokote™).

The aerodynamic integrity of the aircraft is also quite sound. Because of the twin tail boom configuration, potentially disrupted flow from the test model will not be allowed to impinge upon the tail control surfaces. Also, the model will be mounted in a region above the fuselage out of the boundary layer.

From a stability and control point of view this aircraft is also quite attractive. Due to the placement and size of the tail surfaces stability is assured, while the controllability of the aircraft remains intact. Also, due to the placement of the model above and slightly aft of the aircraft center of gravity the pitching moment created by the lift and drag on the model will work to cancel each other resulting a minimal net pitching moment.

Although this aircraft was design as a sort of "work-horse" aircraft, it still boasts some good performance characteristics. Since this type of data acquisition can only be accomplished in flight, a typical flight duration (30 minutes) is most appealing. The proposed aircraft is also able to climb efficiently expending minimal fuel. Finally, the flight ceiling allows for a diverse testing environment.

The proposed aircraft design, which evolved from a team concept selection study, seems to be fundamentally solid. This aircraft utilizes some relatively common aircraft technology at this stage in the design process, but could be easily adapted to incorporate more advanced technologies, especially in the areas of materials and data acquisition.

TABLE 1.1 SUMMARY OF SPECIFICATIONS

I. Overall Dimensions
   a. Total Weight.....25.0 pounds (with fuel)
   b. Dry Weight.....18.2 pounds
   c. Aircraft Width.....14 feet
   d. Aircraft Length.....5.22 feet
   e. Aircraft Height.....1.33 feet

II. Aerodynamics
   a. Wing Airfoil.....NACA 4415
   b. Wing Span.....14 feet
   c. Wing Chord.....1 foot
   d. Wing Area.....14 square feet
   e. Aspect Ratio.....14

III. Propulsion System
   a. Type.....Single ducted fan
   b. Power.....5 horsepower
   c. Fuel Capacity.....1.3 pounds
   d. Specific Fuel Consumption.....0.75 ounces/minute-SBhP

IV. Performance
   a. Range.....224.5 miles
   b. Endurance.....6.7 hours
   c. Ceiling.....25000 feet (absolute)
      23350 feet (service)
   d. Maximum Rate of Climb.....42.09 feet/second

V. Launch and Retrieval
   a. Launch System.....Catapult
   b. Landing System.....Spring-loaded Gear

VI. Data Acquisition System

a. 100 pressure ports
b. 2 inclinometers
c. 1 RCT-3 transmitter
d. 1 RCRI-1C receiver
e. 1 RTEI encoder
f. 1 RTDI decoder
g. 1 RTI1 telemetry interface
h. 10 Tattletale Model 5 data acquisition systems
i. 120 pressure tubes
j. 1 yaw indicator
k. 1 heading indicator

VII. Materials

a. Wing.....Spruce/Balsa/Monokote™
b. Tail Booms.....Spruce
c. Fuselage.....Spruce/Balsa
d. Tail Surfaces.....Spruce/Balsa/Monokote™

VIII. Loadings

a. Overall.....2g
b. Wing.....4.08 pounds/square foot

IX. Estimated Cost.....$15,260.00

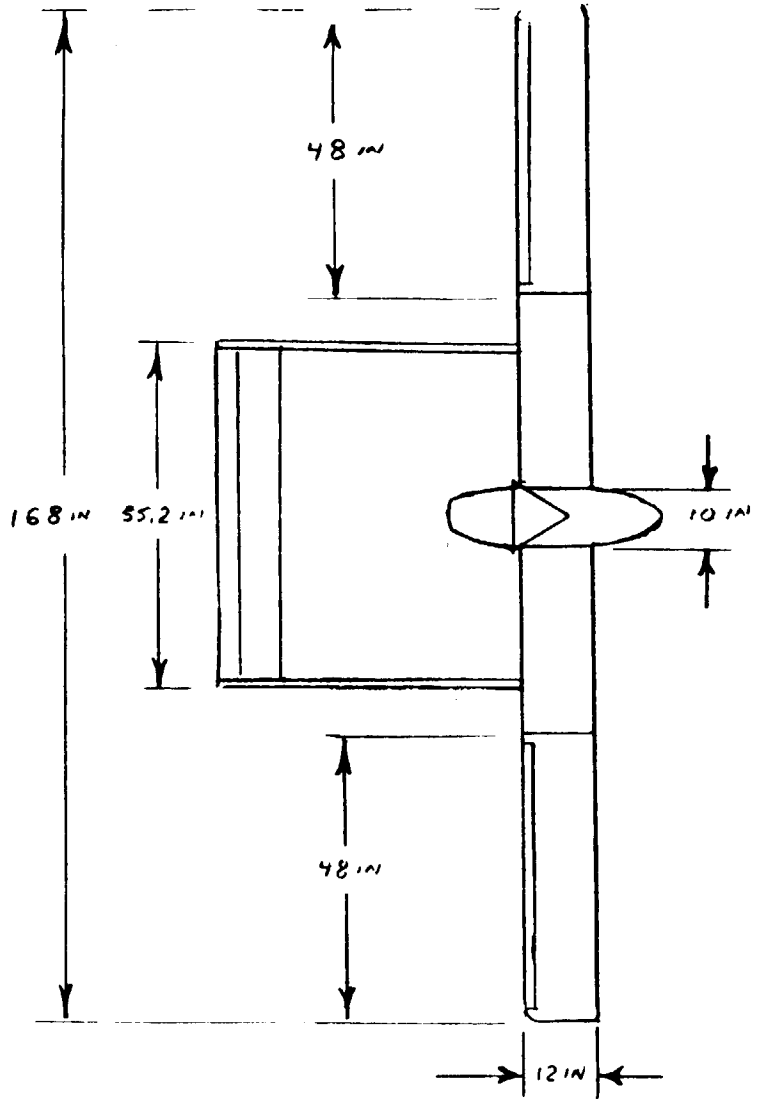

FIGURE 1.1

3-VIEW FINAL DESIGN DRAWING

SCALE 3/8 IN = 1.0 FT

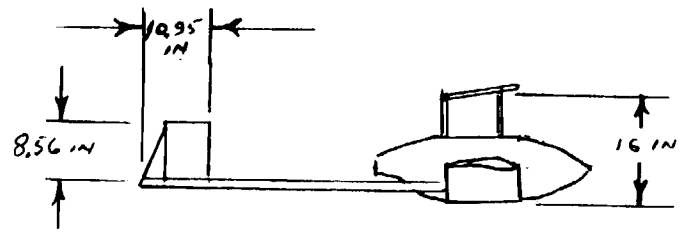

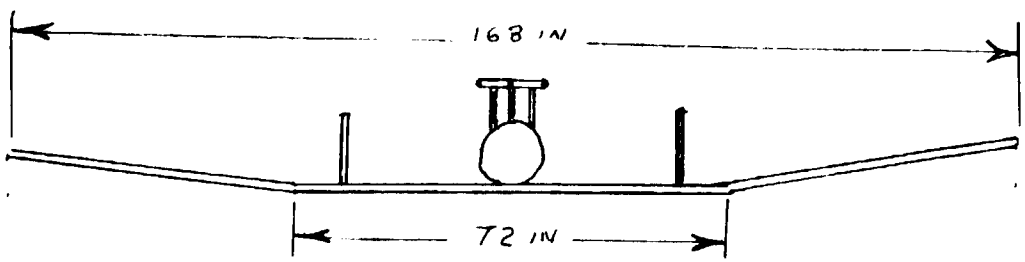

CHAPTER 2

MISSION DEFINITION

THE DELTA MONSTER MISSION

To eliminate the problems of wall interference, free stream turbulence, and the difficulty of achieving dynamic similarity between the test and actual flight aircraft that are associated with aerodynamic testing in wind tunnels, the concept of the remotely piloted vehicle (RPV) as a flying test bed was pursued. The design of a remotely piloted vehicle which can perform a basic aerodynamic study on a delta wing was the main objective for the Green mission - the Delta Monster. Since sweep angle has a significant influence on the performance of the delta wing sweep angles of greater than 45 degrees were to be considered for this mission. The constraints on testing dictated that the delta wing was to be capable of attaining angles of attack of +40 degrees over a Reynold's number range of 40,000 to 1,000,000. To perform similar aerodynamic studies to those performed in the wind tunnel, the delta wing would need to be highly instrumented. Instrumentation to study the formation and location of the leading edge vortex was the major concern for the mission, however, an attempt at flow field visualization would also be feasible. Other measurement requirements include airspeed, angle of attack, altitude, rate of climb, and the control surface position to maintain the integrity of the systems described.

The proposed RPV was also subject to other design constraints. First, all testing of the RPV was to be accomplished within the line-of-sight of the test pilot. Secondly, the takeoff and landing was to be accomplished in a circular area of 150 foot radius with a 50 foot obstacle clearance. Finally, the RPV was to be fully self-contained and capable of being assembled and launched in 30 minutes by two people. These requirements have been summarized in Table 2.1.

The proposed Delta Monster will incorporate the capabilities to achieve the above stated goals. It will be catapulted using a 20 foot launch system which will accelerate the aircraft to 50 ft/s in under 1 second (a 2g acceleration). Since a majority of the flight will be straight and level, 2g's (during launch) was considered to be the maximum loading on the Monster . The primary test altitude will be 800 feet and the RPV will be manually flown to this altitude. To initiate the testing sequence,

the pilot will position the Delta Monster at a specified starting position in the test loop and switch to an automatic control system. This system, composed of hundreds of sensors, several gyroscopic position indicators, and various other instruments, will then stabilize the velocity of the RPV, maintain the proper angle of the delta wing, and fly straight and level for 30 seconds. Since the initial 15 seconds of steady, level flight will be used for velocity and angle of attack adjustments, the actual flight data on the delta wing will be taken for only half of the 30 second straight flight time . The course will be an oval "race" course with a minimum length of 3000 ft (0.568 miles) at the minimum testing velocity of 50 ft/s, and a maximum length of 9000 ft (1.7 miles) at 150 ft/s. Test data will be collected from the delta wing and other instruments during the straight portions of the course while maintaining the delta wing at a constant angle of attack. However, during each subsequent test leg the velocity is increased by 5 ft/s. One hundred pressure ports will be controlled by the control system and data collection will begin when the flight conditions have stabilized. Allowing for the full minute for each of the straight legs, and 30 seconds for each turn around, the total flight duration will be approximately thirty minutes. The landing will be accomplished with remotely activated, pop-out, tripod landing gear. The flight will then be repeated after downloading the information from the onboard computers, performing delta wing adjustments, and refueling. This allows for several tests on a good day.

The design goal of performing basic aerodynamic studies of the flow over the delta wing is accomplished using the 100 pressure ports on the wing. The Delta Monster is instrumented to sweep through delta wing angles of attack while maintaining test velocity. Using a delta wing root chord of ten inches, the Reynold's number range specified from the onset of the mission was determined to be unrealistic. The range that can be tested with the Delta Monster was narrowed to 350,000 to 1,000,000. Finally, the ease with which the models can be interchanged makes the design compatible with wind tunnel testing.

THE DELTA MONSTER

MISSION REQUIREMENTS

DESIGN GOAL -

The use of a remotely piloted vehicle for the collection of aerodynamic data at low Reynold's numbers for a low aspect ratio delta wing.

OBJECTIVES -

- Perform basic aerodynamic studies on a delta wing with a sweep angle greater than 45 degrees.

- Perform these studies at various angles of attack and Reynold's numbers:

Angles	0 to 40°	**Reynold's Number**	350,000 to 1,000,000

- Instrument the delta wing to determine the primary leading edge vortex formation and location, using pressure measurements and/or flow visualization.

- Provide an data acquisition system to collect all necessary data including airspeed, angle of attack, etc.

Table 2.1

CHAPTER 3

CONCEPT SELECTION STUDY

CONCEPT SELECTION STUDY

Since the mission definition for the proposed aircraft required the capability to perform aerodynamic tests on delta wing planforms, a delta wing surface needed to be incorporated into the design. The selection of the final aerodynamic configurational concept was accomplished based on three primary competing concepts. These concepts were 1) a main delta wing acting as the primary lifting surface and also a test surface, 2) a delta wing canard acting as a control surface and a test surface, and 3) a delta wing model mounted on top of a test bed aircraft.

The first concept, which is depicted in sketch form in Figure 3.1, provided for the testing of an actual main lifting surface with a delta wing planform. This concept also included a fuselage in order to avoid a flying wing configuration (with its inherent stability problems) and also to house the data acquisition and transmission equipment. Also, this concept included an aft tail assembly comprised of the horizontal and vertical tail surfaces (stabilizers and control surfaces) in order to move the control surfaces off the testing surface thereby eliminating any abrupt discontinuities on this surface. This proposed aircraft concept would launch with the aid of a catapult and glide to a belly landing upon completion of its flight.

Unfortunately, there were some concerns with the overall integrity of the first concept. First, due to the main delta wing planform, the aircraft weight would be high. Secondly, according to the mission definition, this aircraft would need to fly at high angles of attack, which, with a main delta wing, would necessitate the use of an extremely powerful propulsion system. Thirdly, because the leading edge vortices on a delta wing planform are comprised of violently swirling air cones which break down into turbulent flow and drift aft off of the main wing, it would be possible for the tail surfaces to have been in regions of disrupted flow. This condition could have possibly led to loss of control power. Lastly, since high angles of attack needed to be tested, this configuration would have needed to be in a climb while taking data. Because the ambient conditions (temperature, density, and static pressure) vary in the atmosphere with altitude they would have been changing during the data

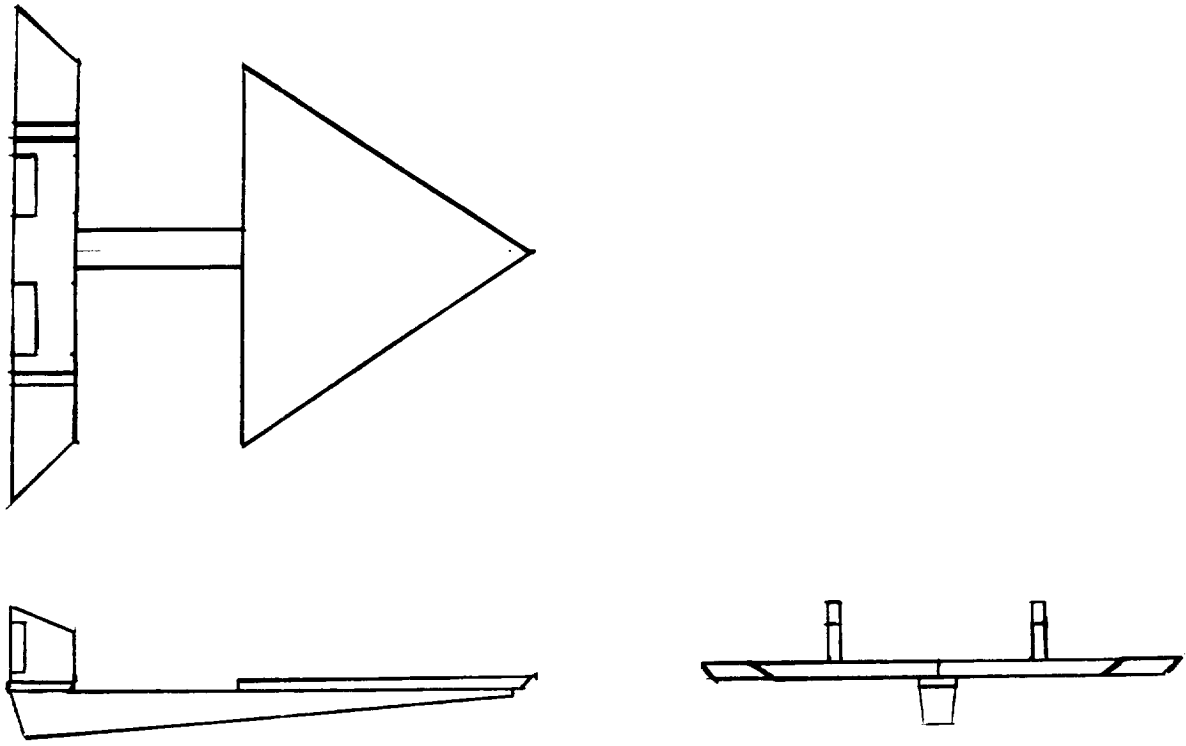

FIGURE 3.1

CONCEPT NO. 1 MAIN DELTA WING

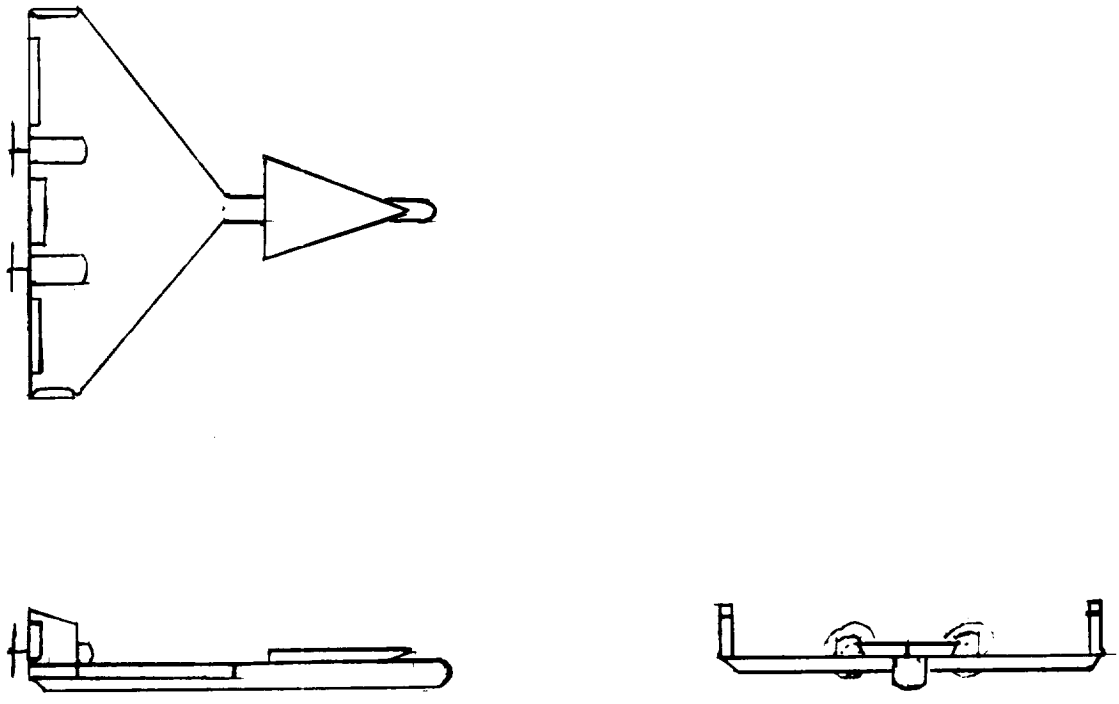

FIGURE 3.2

CONCEPT NO. 2 CANARD DELTA WING

acquisition. This would have produced less than optimum data and eliminated the possible comparison with existing wind tunnel data.

The second competing concept, depicted in sketch form in Figure 3.2, provided for the testing of a delta wing surface which also served as a control surface. This concept allowed for a weight savings due to the dual purpose delta wing surface (one surface instead of two). Also, since the canard is a forward mounted surface, the freestream would be assumed to be somewhat free from disruption. The concept also included a tapered main delta wing with an elevator, ailerons, twin vertical stabilizers with rudders, and a twin turbo-prop propulsion system.

Again, there were disadvantages associated with this conceptual configuration. First, two delta wing surfaces would have provided for very high weight and drag which would again necessitate the use of an extremely powerful propulsion system and would also add to the already high weight. Secondly, the flow into the turbo-prop engines could have been disrupted providing for a disrupted freestream over the test surface. Thirdly, the presence of the fuselage between the two halves of the test surface/canard would have immediately eliminated possible comparisons with existing wind tunnel data. Fourthly, there would have been an inherent conflict between the test surface angle of attack needed for testing and that needed to trim the aircraft. Also, again, the control surfaces located at the rear of the main wing could possibly have been in regions of broken flow allowing for the possible loss of control power. Lastly, the high angle of attack data would have been taken in a climb with changing ambient conditions which would have provided less than optimum data.

The third and final competing configurational concept, shown in sketch form in Figure 3.3, involved a test bed aircraft with a delta wing model mounted on top near the center of gravity of the aircraft/model system. This concept featured a twin tail construction in order to provide space for the leading edge vortices to escape without impinging upon the tail structure or the control surfaces. Also incorporated into this concept was a low horizontal tail surface which allowed for this surface to have seen the freestream even in a climb (no blockage due to the remainder of the aircraft), a low wing which would have moved the circulation distribution of the wing away from the test surface, a large fuselage to

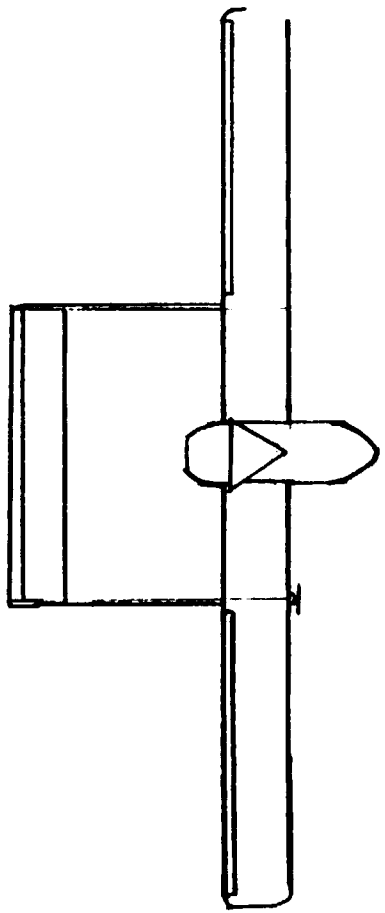

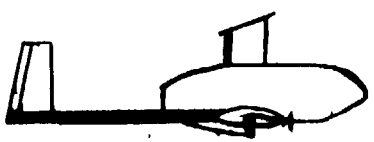

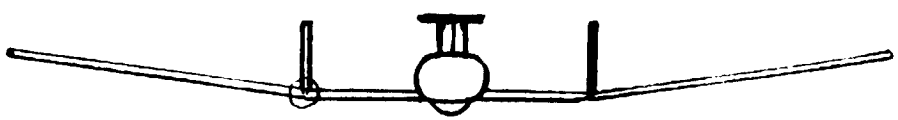

FIGURE 3.3

CONCEPT NO. 3 FINAL CONCEPT

house all of the data acquisition and transmission equipment, a single ducted fan propulsion unit to remove the possibility of propeller flow near the test surface, and a tripod mounting support for the test surface which positioned the model above and slightly aft of the center of gravity of the aircraft providing for some cancellation of the effects of the lift and drag produced by the model on the moment about the center of gravity of the entire system.

This third concept was eventually chosen to be developed further due primarily to its three major advantages. First, since the tail surfaces and structures were positioned away from the disrupted flow from the leading edge vortices, the pilot would always be assured controllability of the aircraft. Second, the data would be able to be collected in steady, level flight providing for constant ambient conditions and the best possible data. Last, because the model was to be mounted on top of a test bed aircraft and not integrated into the aircraft's primary systems, different models could be mounted on this test bed and tested.

CHAPTER 4

AERODYNAMICS

AERODYNAMIC DESIGN

DRAG PREDICTION

Drag prediction was the primary focus of the aerodynamics group in the design stage of the aircraft. In order to calculate the drag on the aircraft a drag polar was found using the drag breakdown method. With this method the drag contribution of each component of the aircraft was found and incorporated into the drag polar for the entire vehicle. The drag breakdown technique is described in Brendel and Nelson[1].

The zero lift drag coefficient, or the profile drag coefficient, CDo, is calculated in the following manner:

$$CDo = \Sigma CD_{\pi} A_{\pi} / S.$$

The CD_{π} terms are the induced drag coefficients of each component based on experimental research. Normalizing the calculations for a wing planform area of 14 square feet the zero lift drag calculation for each component of the aircraft resulted in:

WING: $CD_{\pi} = 0.0030$, $A_{\pi} = 2S$

FUSELAGE: $CD_{\pi} = 0.0024$, $A_{\pi} = 0.75 \pi d l$

TAIL: $CD_{\pi} = 0.0025$, $A_{\pi} = 2(Sh+Sv)$

DELTA WING: $CDo = 0.006$

From this breakdown, a zero lift drag coefficient of 0.0146 was found. The zero lift drag coefficient for the delta wing test specimen was calculated using simple flat plate theory for a 45° sweep delta wing modelled as a triangular flat plate at zero angle of attack. This analysis

was assumed to suffice as a "worst case" delta wing induced drag coefficient.

A span efficiency factor of e = 0.85 was assumed for the aircraft based on a data bank of similarly sized aircraft. This leads to an induced drag coefficient of 0.027 CL^2. The resulting drag polar is CD = 0.0146 + 0.027 CL^2 (shown in Figure 4.1).

This drag polar results in a minimum drag force of 1.12 lbs. at 50 ft/s and a maximum drag force of 5.61 lbs. at a velocity of 150 ft/s. These velocities represent the velocity range of our aircraft.

The drag breakdown technique is advantageous for developing a preliminary drag estimation in its consideration of each component of the aircraft and for its relative ease of application to the overall configuration of the aircraft.

AIRFOIL SELECTION

The criteria used for selecting the airfoil for this vehicle are the following:

1. High Cl
2. High L/D
3. Low CDo
4. Low pitching moment
5. Moderately small maximum thickness
6. Suitable shape for modelling

The NACA 44 series airfoils were considered and found to meet the specified criteria. Two of the airfoils considered adequate for our mission requirements were the NACA 4412 and the NACA 4415. Both airfoils were considered for their camber, a rather blunt leading edge, their relatively flat bottom surfaces, and their section characteristics.

The NACA 4415 was the airfoil eventually selected for our aircraft. Its heavier weight, due to its large maximum thickness, was necessary due to landing requirements. Data for the NACA 4412 and the NACA 4415 is represented in Table 4.1:

FIGURE 4.1

DRAG POLAR

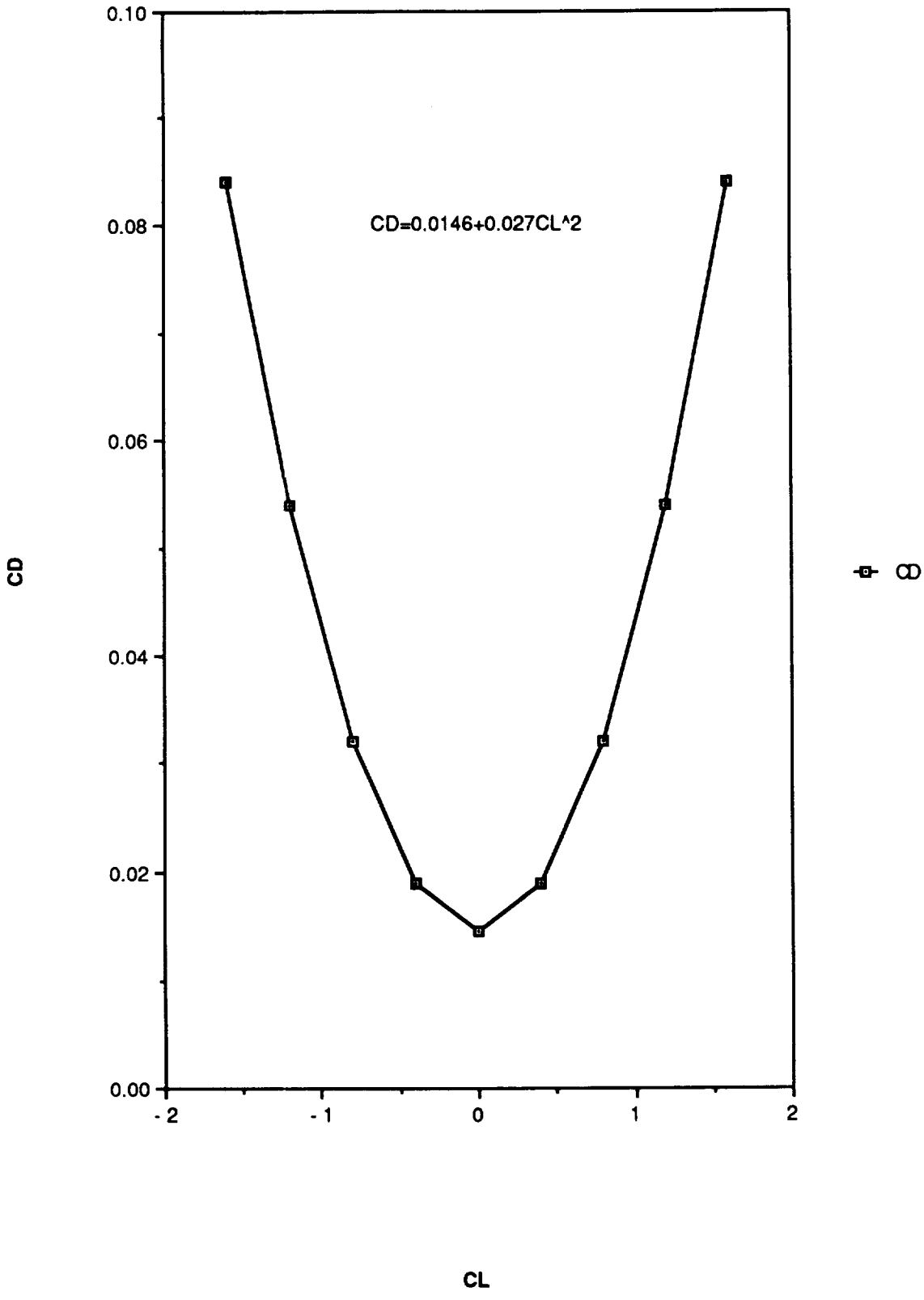

Table 4.1

	NACA 4412	NACA 4415
α (L=0)	-3.8 degrees	-4.3 degrees
Cmo	-0.093	-0.093
Clα	.105 / degree	.105 / degree
a. c.	.247c	.245c
α (Cl max)	14 degrees	15 degrees
Cl max	1.67	1.64
α (stall)	7.5 degrees	8 degrees
maximum thickness	0.12c	0.15c

The coefficients presented here are section coefficients for the airfoils obtained from Nicolai[2]. The lift curves as well as the variation of Cd with Cl for the airfoil sections are found in Figures 4.2 & 4.3 (taken from Anderson[3]).

WING DESIGN

The present design calls for a low mounted wing with a span of 14 feet. A dihedral of 8 degrees will be located outboard of the wing-fuselage juncture. This will provide the necessary roll stability for the aircraft.

The wing is to be low mounted so that it does not produce an induced flow field around the delta wing test surface. This aircraft has been designed to collect aerodynamic data and information concerning the vortex breakdown on the delta wing test surface. In order to get better results it is necessary that the flow over the delta wing be uninterrupted. A high mounted wing would interrupt the flow over the delta wing, thus the boundary layer and separation at high velocities and high angles of attack would result in turbulent flow over the delta wing. This would result in poor results. A low mounted wing, therefore, provides an undisturbed flow field over the delta wing enabling the design to meet the necessary mission requirements.

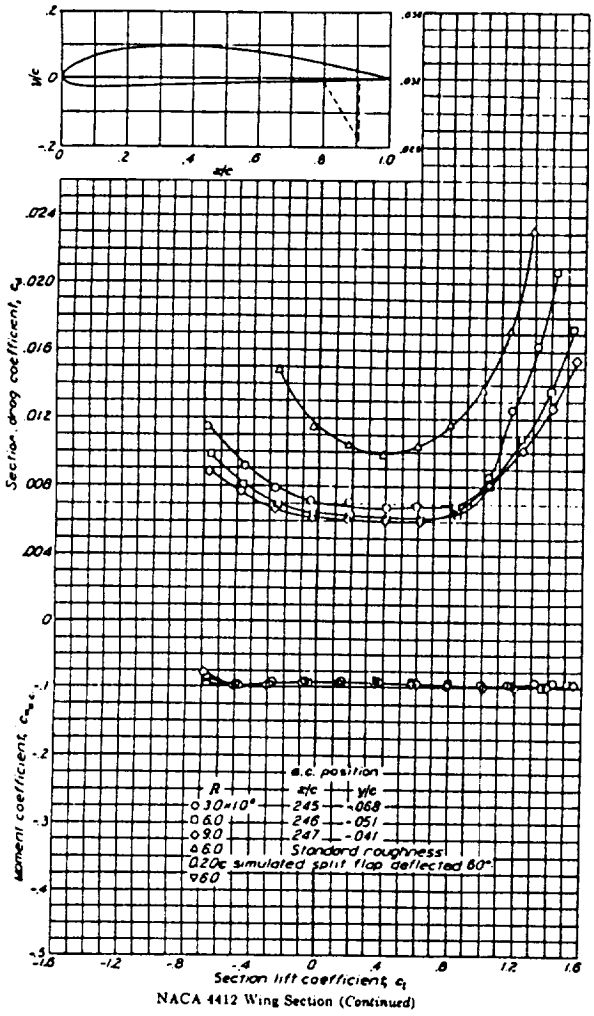

NACA 4412 Wing Section (Continued)

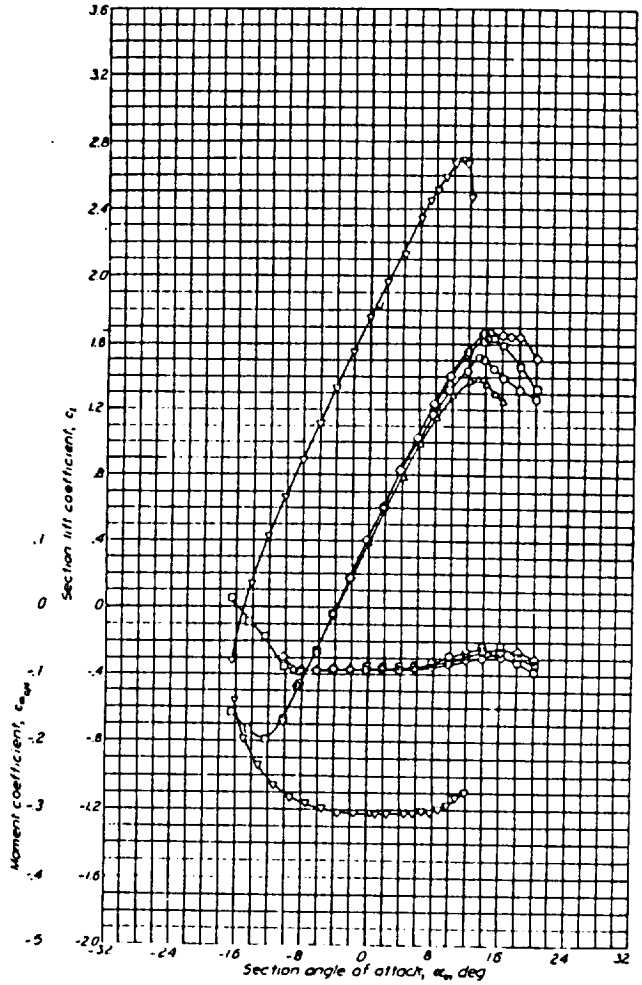

NACA 4412 Wing Section

Figure 4.2 (from reference 3)

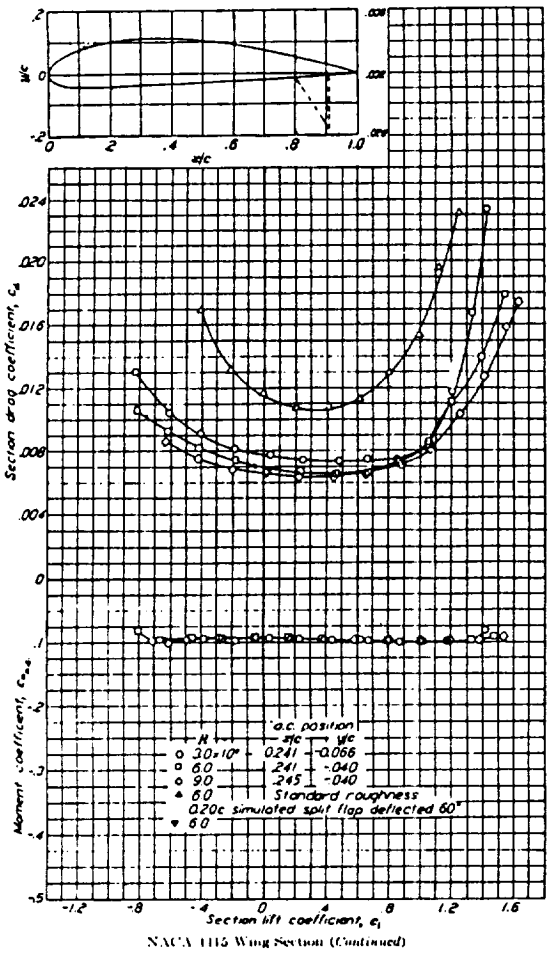

NACA 4415 Wing Section (Continued)

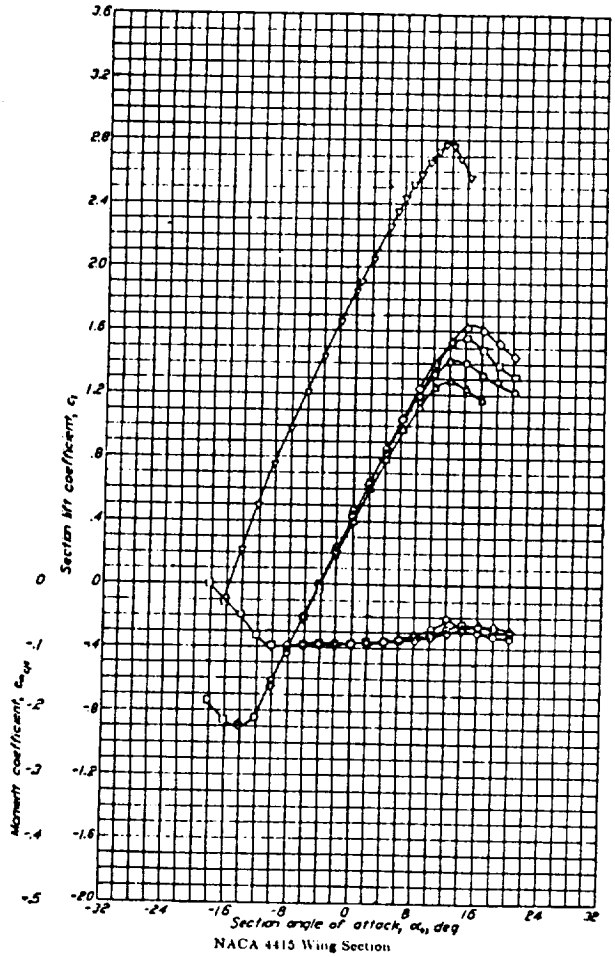

NACA 4415 Wing Section

Figure 4.3 (from reference 3)

DELTA WING

A delta wing test surface with a root chord of 10 inches will be mounted above the fuselage of the aircraft. The design calls for a tripod mounting system which, by activating a servo changes the angle of attack of the delta wing. The mission requirements stipulate that an angle of attack range of 0 to 40 degrees for the delta wing be attainable.

At large angles of attack it is found that large lift coefficients are generated on the delta wing. At an angle of attack of 25 degrees for a 45° sweep delta a CL of 1.73 results from the equation:

$$CL = KP \sin\alpha \cos^2\alpha + KV \cos\alpha \sin^2\alpha$$

where KP and KV are constants relating to the flow around the delta wing. For a worst case analysis (delta sweep of 45°) KP and KV are both equal to 3.4. Therefore, at large angles of attack, lift must be "dumped" by the elevator control surfaces. The elevators therefore needed to be sized to compensate for this additional lift.

The lift provided by the delta wing also varies with the sweep angle. A range of sweep angles from 50 to 75 degrees has been proposed for the test wing. Preliminary studies using the Lin-Air™ program suggest that the delta wing will provide approximately 1 to 2% of the total lift of the aircraft at low angles of attack. From this range of sweep angles, the best sweep angle will be chosen according to constraints proposed in further studies by the aerodynamics group.

Drag on the delta wing also decreases as the sweep angle is increased. The lift and drag contributions of the delta wing decrease with increasing sweep angle partly because of the decreasing planform area of the delta wing. With a constant root chord, the planform area decreases as sweep increases.

The delta wing will be mounted near the aircraft's center of gravity so that it contributes a minimal moment about the center of gravity.

REFERENCES

1. Atmospheric Flight Mechanics, Brendel and Nelson, 1989
2. Fundamentals of Aircraft Design, Leland M. Nicolai, 1975
3. Introduction to Flight, John D. Anderson, 1985

CHAPTER 5

PROPULSION

PROPULSION

DESIGN OBJECTIVE

The purpose of this study was to design and analyze the performance of a ducted fan. A ducted fan is essentially a multibladed propeller encased by a shroud. Because very little technical information on ducted fans was available, a computer program was developed to perform this analysis.

REASONS FOR THE DUCTED FAN

The main reason for choosing the ducted fan as a propulsion unit is that it satisfies mission requirements. Because it is necessary to have a relatively steady flow over the mounted delta wing, flow acceleration and flow interference from the propulsion system are not desirable. A ducted fan satisfies this requirement by taking air and accelerating it through a duct to produce thrust. Conventional propulsion systems including propellers, turbofans, and turbojets are not viable alternatives for various reasons. A propeller would cause an unsteady flow over the delta wing, while turbofans and turbojets are characterized by excessive weight, fuel consumption, and thrust.

THEORY OF DUCTED FANS

One of the main advantages of using a ducted fan instead of a propeller is size. Because a ducted fan has a small diameter, it must take a relatively small amount of air and accelerate it quickly to produce thrust. Because of the low aspect ratio of the fan blades, the induced flow is considerable. However, the tip losses caused by the induced flow are negated because of the shroud. Furthermore, the fan must spin at a high number of revolutions per minute to produce thrust. This causes an inefficient use of engine power at low velocities (a similar analogy is trying to start a car in third gear as opposed to first gear). However, as the aircraft begins to move faster, the efficiency of the fan increases (see Figure 5.1). Thus, an aircraft using a ducted fan needs a greater takeoff distance or a catapult to provide the necessary takeoff

FIGURE 5.1

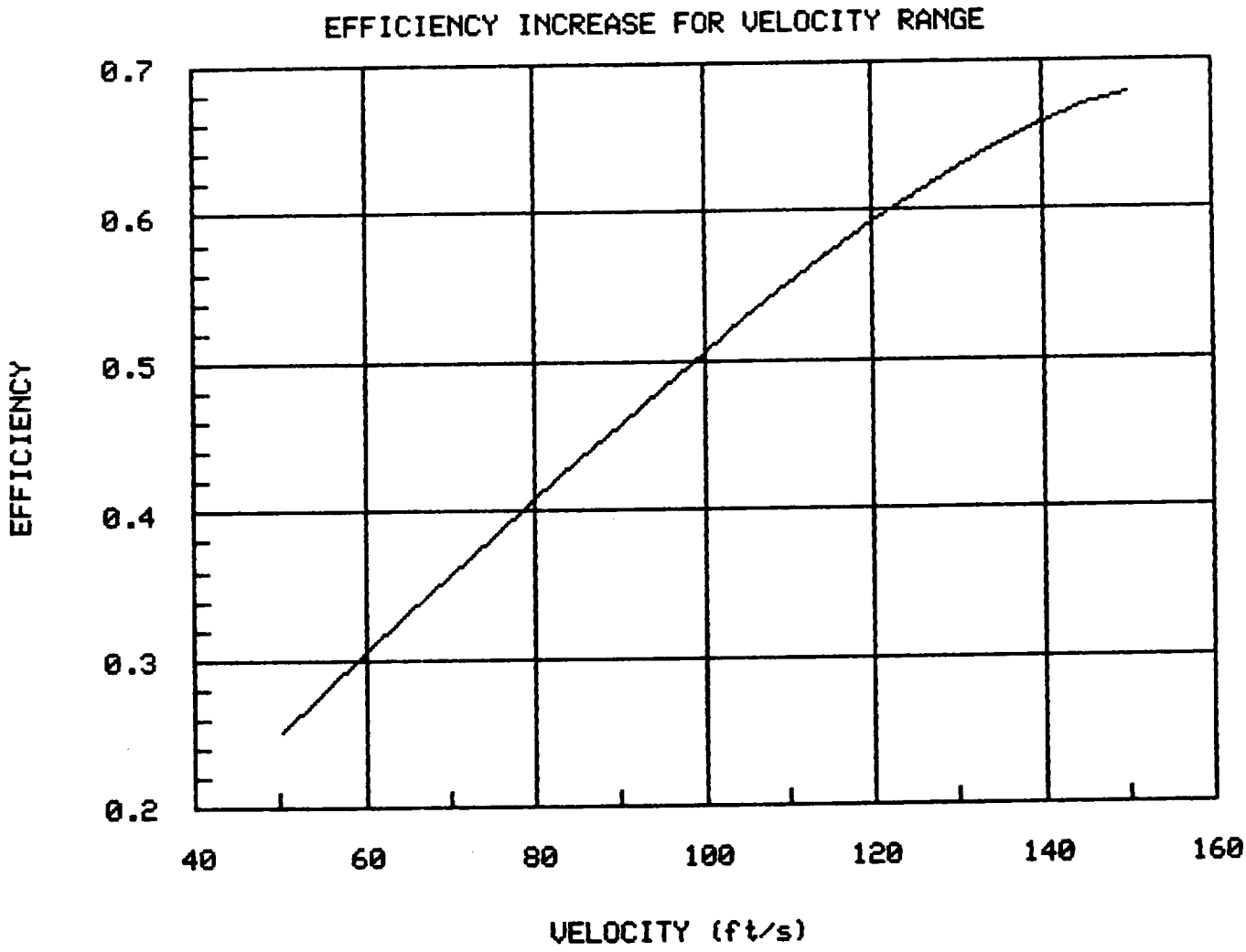
EFFICIENCY INCREASE FOR VELOCITY RANGE
EFFICIENCY
0.7
0.6
0.5
0.4
0.3
0.2
40
60
80
100
120
140
160
VELOCITY (ft/s)

acceleration.

PROBLEMS WITH ANALYSIS

The biggest problem in analyzing the performance of the ducted fan is modelling the three dimensional effects which introduce significant error in the calculations. Instead of using a complex analysis technique such as cascade flow theory to account for blade interference, a simple model was used. The absolute angle of attack that each discrete airfoil section sees is strongly dependent on blade solidity, which is defined as the ratio of the total fan swept area to the total blade area. Because ducted fans are multibladed and operate at a high RPM setting, blade interference lowers the available thrust and engine power required. Furthermore, only a small absolute angle of attack is necessary to produce a sufficient amount of thrust. The effect of increasing the solidity of the fan reduces the absolute angle of attack (and therefore the thrust and power required) by increasing the induced angle of attack. Thus, to account for blade interference, the fan was modelled as having an infinite number of blades, with the solidity becoming the ratio of the swept volume of the blades to the total blade swept area, giving it a value equivalent to the mean chord of the blade.

COMPUTER PROGRAM

The computer program that was developed to analyze the design is given in Appendix 5.1. The program uses a simple blade element model (see Figure 5.2), and corrects for altitude, compressibility, and the induced angle of attack using the method described in the previous section. In the program, the rpm setting is entered and remains a fixed parameter. The program then goes through the range of flight velocities, calculating the thrust and power required at each of the nine equidistant radial stations. From these calculations, the thrust and power coefficients are plotted as a function of advance ratio. In addition, the program has as option to print the local section parameters. These are used to analyze the aerodynamic performance of the blade over the range of flight velocities. Appendix 5.2 lists the local section parameters for the final design.

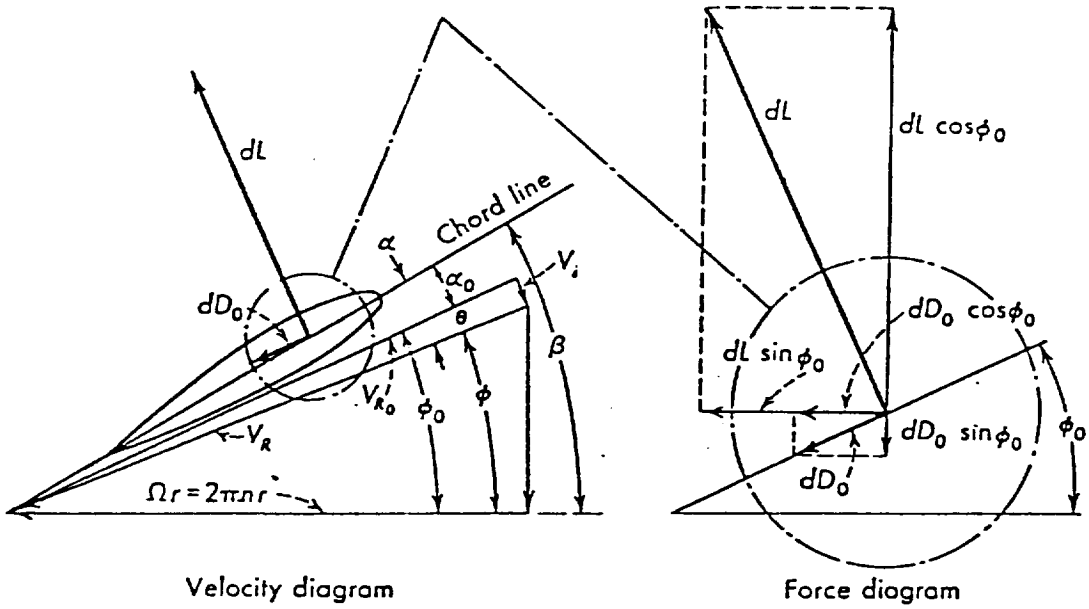

Velocity diagram

Force diagram

FIGURE 5.2

(from ref. 1)

RESULTS

From the computer program, a blade design was developed for the ducted fan. For the final design, a NACA 0006 was selected for the airfoil section. This airfoil provides an excellent lift to drag ratio for the full range of velocities from blade root to tip. The section lift and drag coefficients for the NACA 0006 are given in Figures 5.3 and 5.4. In addition, the fan has 5 blades and the diameter of the fan is 6 inches. The hub has a radius of 1 inch, and the blade has a span of 2 inches. The blade itself is shown in Figure 5.5, and has a linear twist of -20 degrees (40 degree pitch at the root and 20 degree pitch at the tip). The fan unit operates at a fixed value of 19500 revolutions per minute (325 rev/sec). The results for this blade design are listed in Table 5.1 (thrust is given in pounds and power required in horsepower), and thrust and power coefficient curves are plotted in Figures 5.6 and 5.7.

Because this design did not take into account inlet ram drag, fuselage interference, or the presence of nondirected flow within the duct, these results were reduced by a conservative, arbitrary value of 50%, and are given in Table 5.2. Plots of the thrust and power coefficient curves are given in Figures 5.8 and 5.9. These are the results used in the performance calculations, and they represent the expected results from an empirical analysis.

CONCLUSIONS AND RECOMMENDATIONS

This analysis was performed to give estimates of the thrust and engine power required for a ducted fan unit. Although the results are relatively accurate (based on the thrust produced and power required by similar commercial fan units), it is now necessary to either fabricate or purchase a ducted fan and run empirical tests in a wind tunnel to substantiate the analytic results produced by this study.

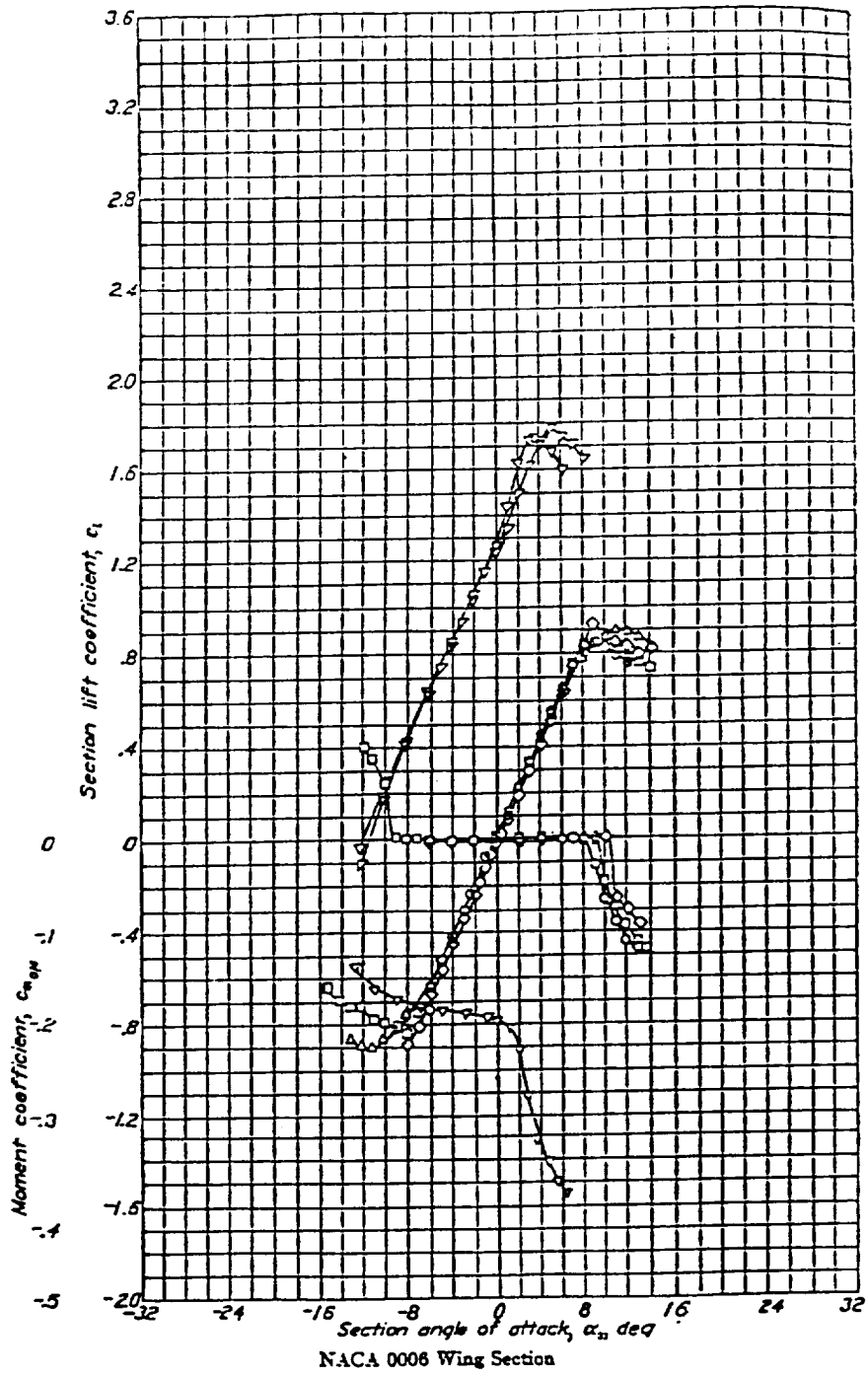

NACA 0006 Wing Section

FIGURE 5.3

(from ref.2)

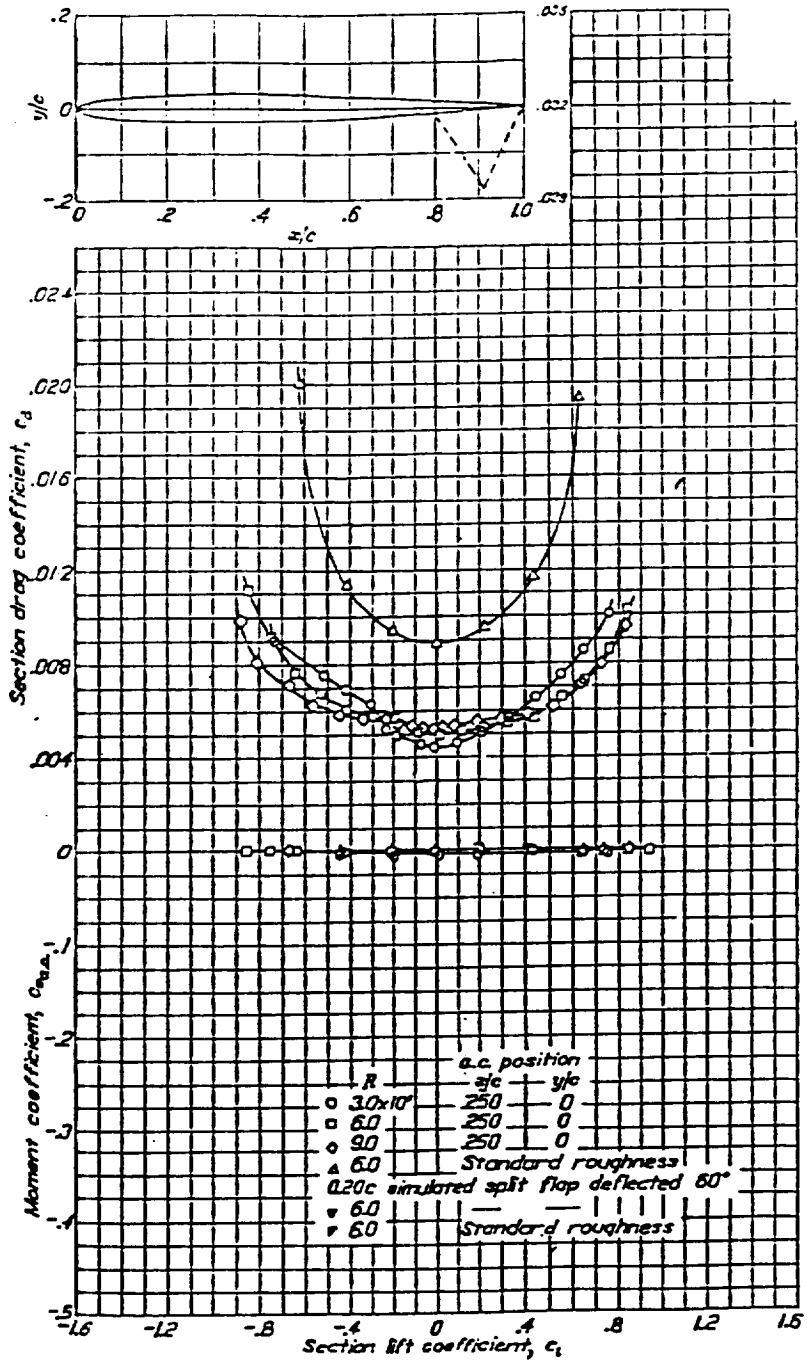

NACA 0006 Wing Section

FIGURE 5.4

(from ref.2)

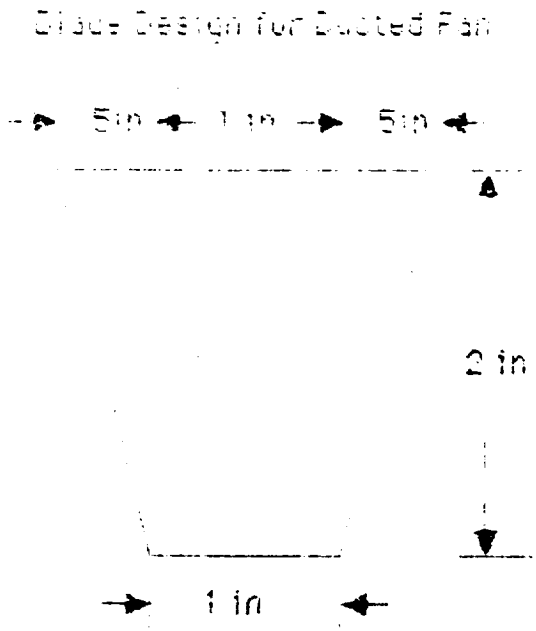

FIGURE 5.5

FAN SPEED (REV/SEC) = 325.000

BLADE PITCH SETTING (DEGREES) = 50.0000

ALTITUDE (FT) = 0.000000E+00

BLADE ELEMENT WIDTH (IN) = 0.250000

ANALYSIS INCLUDES INDUCED FLOW

ADVANCE RATIO	THRUST	POWER REQUIRED	CT	CP	EFFICIENCY
0.30769	22.4	8.1	1.42922	1.74641	0.25181
0.33846	22.9	8.2	1.45749	1.77667	0.27766
0.36923	23.7	8.5	1.51050	1.83259	0.30434
0.40000	24.3	8.7	1.55164	1.87616	0.33081
0.43077	24.8	8.8	1.58134	1.90793	0.35703
0.46154	25.1	8.9	1.60006	1.92841	0.38295
0.49231	25.2	9.0	1.60823	1.93810	0.40852
0.52308	25.2	9.0	1.60629	1.93744	0.43367
0.55385	25.0	8.9	1.59467	1.92686	0.45836
0.58462	24.7	8.8	1.57379	1.90676	0.48253
0.61538	24.2	8.7	1.54407	1.87751	0.50609
0.64615	23.6	8.5	1.50592	1.83946	0.52899
0.67692	22.9	8.3	1.45973	1.79295	0.55112
0.70769	22.1	8.1	1.40590	1.73828	0.57238
0.73846	21.1	7.8	1.34480	1.67574	0.59262
0.76923	20.0	7.4	1.27680	1.60562	0.61170
0.80000	18.9	7.1	1.20226	1.52819	0.62938
0.83077	17.6	6.7	1.12152	1.44368	0.64538
0.86154	16.2	6.3	1.03492	1.35234	0.65932
0.89231	14.8	5.8	0.94278	1.25440	0.67064
0.92308	13.3	5.3	0.84542	1.15006	0.67856

TABLE 5.1

FIGURE 5.6

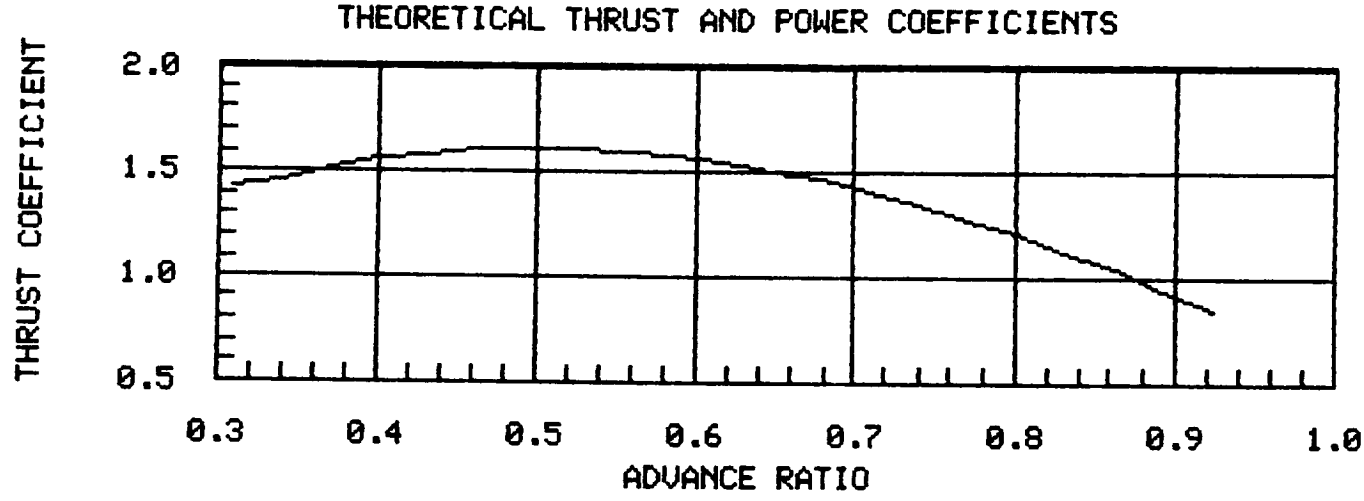

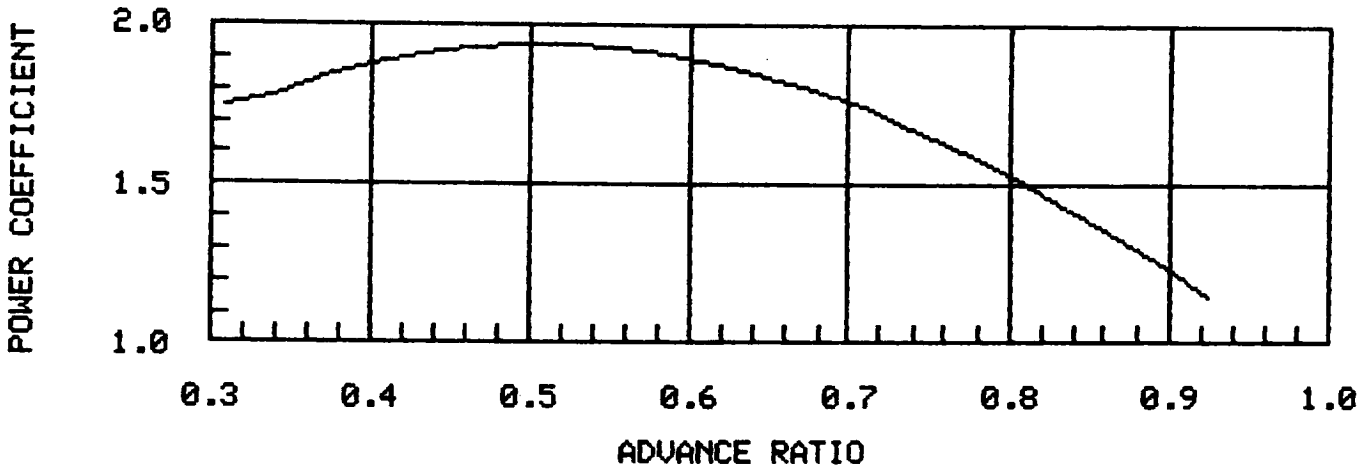

FIGURE 5.7

FAN SPEED (REV/SEC) = 325.000

BLADE PITCH SETTING (DEGREES) = 30.0000

ALTITUDE (FT) = 0.000000E+00

BLADE ELEMENT WIDTH (FT) = 0.250000

ANALYSIS INCLUDES INDUCED FLOW

ADVANCE RATIO	THRUST	POWER REQUIRED	CT	CP	EFFICIENCY
0.30769	11.2	4.0	0.71461	0.87321	0.25181
0.33846	11.4	4.1	0.72875	0.88833	0.27766
0.36923	11.9	4.2	0.75826	0.91630	0.30434
0.40000	12.2	4.3	0.77582	0.93808	0.33081
0.43077	12.4	4.4	0.79067	0.95396	0.35703
0.46154	12.6	4.5	0.80003	0.96421	0.38295
0.49231	12.6	4.5	0.80412	0.96905	0.40852
0.52308	12.6	4.5	0.80314	0.96872	0.43367
0.55385	12.5	4.5	0.79733	0.96343	0.45836
0.58462	12.3	4.4	0.78690	0.95338	0.48253
0.61538	12.1	4.4	0.77204	0.93876	0.50609
0.64615	11.8	4.3	0.75296	0.91973	0.52899
0.67692	11.5	4.2	0.72987	0.89647	0.55112
0.70769	11.0	4.0	0.70295	0.86914	0.57238
0.73846	10.6	3.9	0.67240	0.83787	0.59262
0.76923	10.0	3.7	0.63840	0.80281	0.61170
0.80000	9.4	3.5	0.60113	0.76409	0.62938
0.83077	8.8	3.3	0.56076	0.72184	0.64538
0.86154	8.1	3.1	0.51746	0.67617	0.65932
0.89231	7.4	2.9	0.47139	0.62720	0.67064
0.92308	6.6	2.7	0.42271	0.57503	0.67856

TABLE 5.2

FIGURE 5.8

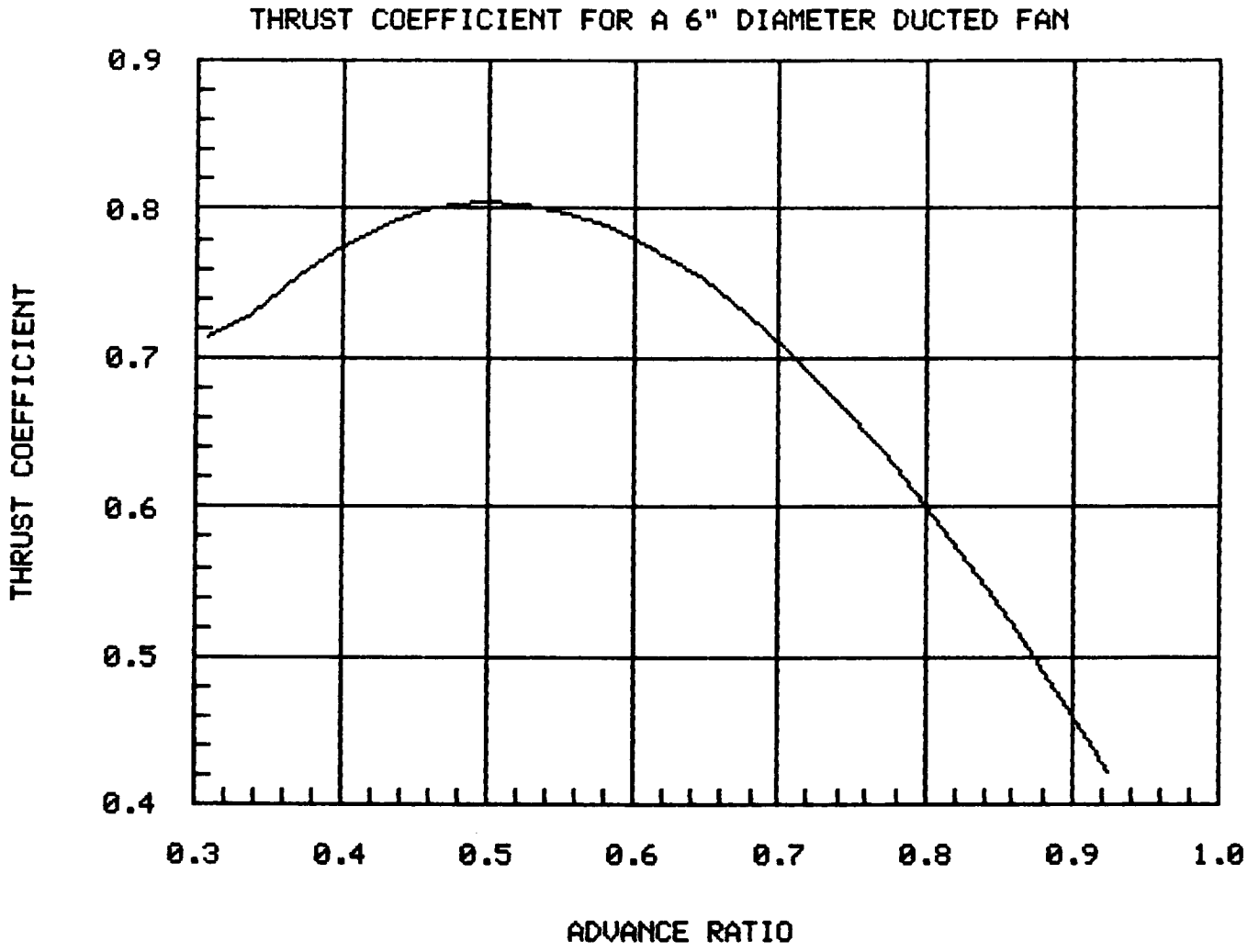
THRUST COEFFICIENT FOR A 6" DIAMETER DUCTED FAN
THRUST COEFFICIENT
0.9
0.8
0.7
0.6
0.5
0.4
0.3
0.4
0.5
0.6
0.7
0.8
0.9
1.0
ADVANCE RATIO

FIGURE 5.9

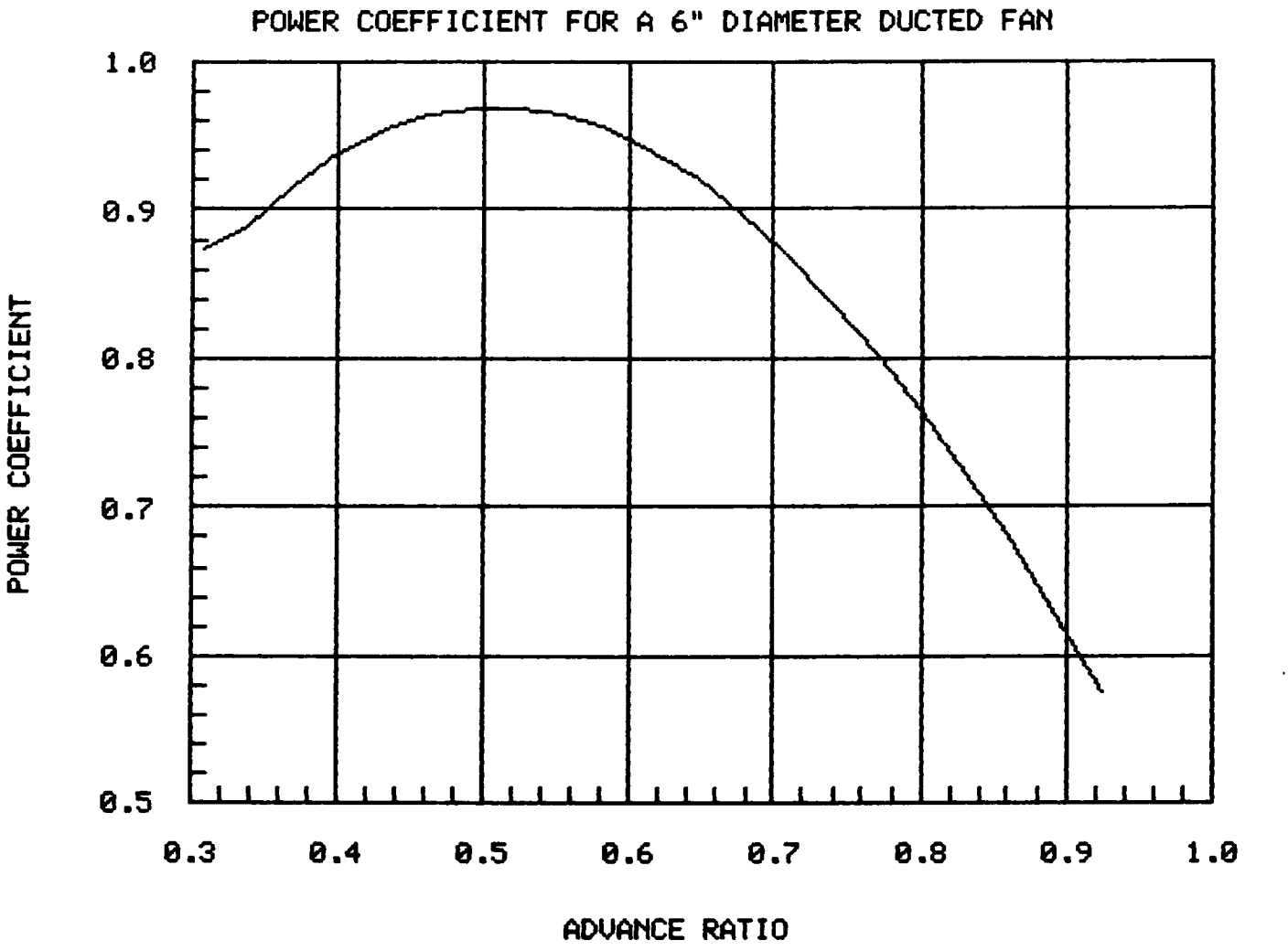
POWER COEFFICIENT FOR A 6" DIAMETER DUCTED FAN
1.0
0.9
0.8
0.7
0.6
0.5
POWER COEFFICIENT
0.3
0.4
0.5
0.6
0.7
0.8
0.9
1.0
ADVANCE RATIO

REFERENCES

1. Dommasch, Daniel O., Sydney S. Sherby, and Thomas F. Connally, Airplane Aerodynamics, Pitman Publishing Corporation, New York, 4th edition, 1967, p. 226.

2. Abbott, Ira H., and Albert E. von Doenhoff, Thoery of Wing Sections, Dover Publications, Inc., New York, 2nd edition, 1959, pp. 452-453.

APPENDIX 5.1

```
0001              LIBRARY 'PLOTLIB'
0002              DIMENSION THRUST(21),POWER(21),TCOEFF(21),PCOEFF(21),ARJ(21),
0003             +          EFF(21),HPOWER(21),V(21)
0004              REAL M
0005              INR=6
0006              WRITE(1,*)'ENTER DESIRED FAN RPM '
0007              READ(1,*) RN
0008              WRITE(1,*)'ENTER FINITE BLADE ELEMENT WIDTH'
0009              READ(1,*) DR
0010              WRITE(1,*)'ENTER FLIGHT ALTITUDE (IN FEET)  '
0011              READ(1,*) H
0012              WRITE(1,*)'ENTER 1 FOR SIMPLE BLADE ELEMENT MODEL, 2 FOR INDUCED
0013             +LOW EFFECTS '
0014              READ(1,*) K
0015              WRITE(1,*)'ENTER BLADE PITCH AT ROOT (DEGREES)'
0016              READ(1,*) PITCH
0017              WRITE(1,*)'ENTER 1 TO BYPASS INCREMENTAL PRINT OPTION, 2 TO PRIN
0018             +INCREMENTAL ANALYSIS'
0019              READ(1,*) N
0020              PHI=0.0
0021              BETA=0.0
0022              BETAR=0.0
0023              THETA=0.0
0024              ALPHA=0.0
0025              CL=0.0
0026              CD=0.0
0027              VR=0.0
0028              QINF=0.0
0029              DL=0.0
0030              DD=0.0
0031              DT=0.0
0032              RN=RN/60.0
0033              RHO=0.0023769
0034              RHO1=0.0
0035              PI=3.141592654
0036              CC=0.16666667
0037              D=0.5
0038              A=-0.0035662
0039              RAIR=1716.0
0040              SIGMA=2.0
0041              TEMP=58.0
0042              G=32.2
0043              A0=6.11155
0044        C     ******************************************************
0045        C     *STANDARD ATMOSPHERIC MODEL ALTITUDE CORRECTIONS*
0046        C     ******************************************************
0047              TEMP=TEMP+A*H
0048              TEMP=TEMP+460.0
0049              RHO1=RHO*EXP(-(G*H)/(RAIR*TEMP))
0050              J=0
0051              DO 20 VINF=50.0,151.0,5.0
0052.01           I=0
0053.01           J=J+1
0054.01           T=0.0
0055.01           Q=0.0
0056.01           PHI=0.0
0057.01           PHID=0.0
0058.01     C
0059.01           DO 10 RR=1.0,3.0,DR
0060.02           DRR=DR/12.0
0061.02           R=RR/12.0
0062.02           C=CC-2.0*(0.25*((RR-1.0)/12.0))
0063.02           BETA=0.0
0064.02           I=I+1
0065.02           PHI=ATAN(VINF/(2.0*PI*RN*R))
0066.02           PHID=PHI*180.0/PI
0067.02     C     *****************
0068.02     C     * PITCH SETTING *
0069.02     C     *****************
0070.02           BETA=PITCH - 10.0*RR
0071.02     C     *****************
0072.02           IF(K.EQ.1) THEN
0073.03           ALPHA=BETA-PHID
0074.03     C     ***************************
0075.03     C     *INDUCED FLOW CORRECTIONS*
```

```
0076.03  C     ************************
0077.03         ELSEIF(K.EQ.2) THEN
0078.03         BETAR=BETA*PI/180.0
0079.03         THETA=(BETAR-PHI)/(1.0+((8.0*R*SIN(PHI))/(0.5*A0*D*SIGMA)))
0080.03         PHI=PHI+THETA
0081.03         PHID=PHI*180.0/PI
0082.03         ALPHA=BETA-PHID
0083.03         ENDIF
0084.02         IF(ALPHA .LT. -10.0 .AND. ALPHA .GT. -32.0) THEN
0085.03         ALPHA=ALPHA+10.0
0086.03         CL=-0.9-(.04091*ALPHA)
0087.03         ELSEIF(ALPHA .LT. 10.0) THEN
0088.03         CL=.10*ALPHA
0089.03         ELSEIF(ALPHA .LT. 32.0) THEN
0090.03         ALPHA=ALPHA-10.0
0091.03         CL=0.9-(.04091*ALPHA)
0092.03         ELSE
0093.03         CL=0.0
0094.03         ENDIF
0095.02         CD=0.005+(0.00397*(CL**2))
0096.02         VR=2.0*PI*RN*R/(COS(PHI))
0097.02         M=VR/SQRT(1.4*RAIR*TEMP)
0098.02  C     ***********************************
0099.02  C     *ISENTROPIC COMPRESSIBILITY CORRECTION*
0100.02  C     ***********************************
0101.02         IF(M.GT.0.3) THEN
0102.03         RHO=RHO1/((1.0+(0.2*M**2))**2.5)
0103.03         ENDIF
0104.02         QINF=0.5*RHO*(VR**2)
0105.02         DL=CL*QINF*C*DR
0106.02         DD=CD*QINF*C*DR
0107.02         DT=DL*COS(PHI)-DD*SIN(PHI)
0108.02         DQ=(DL*SIN(PHI)+DD*COS(PHI))*R
0109.02         T=T+DT
0110.02         Q=Q+DQ
0111.02         IF(N.NE.2) GO TO 10
0112.02         IF(I.EQ.1) THEN
0113.03         WRITE(IWR,*)'   '
0114.03         WRITE(IWR,*)'   '
0115.03         WRITE(IWR,*)'   '
0116.03         WRITE(IWR,*)'FREESTREAM VELOCITY (FT/SEC) = ',VINF
0117.03         WRITE(IWR,*)'   '
0118.03         ENDIF
0119.03  C     ************************
0120.03  C     *INCREMENTAL PRINT OPTION*
0121.03  C     ************************
0122.02         IF(I.EQ.1) THEN
0123.03         WRITE(IWR,100)
0124.03    100  FORMAT('  ',4X,'R',8X,'PHI',8X,'BETA',6X,'ALPHA',6X,'CL',8X,'CD',8
0125.03        +,'DL',8X,'DD',8X,'DT',8X,'DQ')
0126.03         WRITE(IWR,105)
0127.03    105  FORMAT('   ')
0128.03         ENDIF
0129.02         WRITE(IWR,110)R,PHID,BETA,ALPHA,CL,CD,DL,DD,DT,DQ
0130.02    110  FORMAT('  ',10F10.5)
0131.02     10  CONTINUE
0132.01         ARJ(J)=VINF/(RN*D)
0133.01         THRUST(J)=5.0*T
0134.01         POWER(J)=5.0*(2.0*PI*RN*Q)
0135.01         HPOWER(J)=POWER(J)/550.0
0136.01         V(J)=VINF
0137.01         TCOEFF(J)=THRUST(J)/(RHO1*(RN**2)*(D**4))
0138.01         PCOEFF(J)=(POWER(J)/(RHO1*(RN**3)*(D**5)))
0139.01         EFF(J)=(TCOEFF(J)/PCOEFF(J))*ARJ(J)
0140.01     20  CONTINUE
0141            WRITE(IWR,*)'   '
0142            WRITE(IWR,*)'   '
0143            WRITE(IWR,*)'   '
0144            WRITE(IWR,*)'   '
0145            WRITE(IWR,*)'   '
0146            WRITE(IWR,*)'FAN SPEED (REV/SEC) = ',RN
0147            WRITE(IWR,*)'   '
0148            WRITE(IWR,*)'BLADE PITCH SETTING (DEGREES) = ',PITCH
0149            WRITE(IWR,*)'   '
0150            WRITE(IWR,*)'ALTITUDE (FT) = ',H
0151            WRITE(IWR,*)'   '
0152            WRITE(IWR,*)'BLADE ELEMENT WIDTH (IN) = ',DR
0153            WRITE(IWR,*)'   '
0154            IF(K.EQ.1) THEN
0155.01         WRITE(IWR,*)'SIMPLE BLADE ELEMENT MODEL'
```

```
0156.01           ELSEIF(K.EQ.2) THEN
0157.01           WRITE(IWR,*)'ANALYSIS INCLUDES INDUCED FLOW'
0158.01           ENDIF
0159              WRITE(IWR,*)'   '
0160              WRITE(IWR,*)'   '
0161              WRITE(IWR,130)
0162          130 FORMAT(' ',1X,'ADVANCE RATIO',5X,'THRUST',5X,'POWER REQUIRED',7X
0163             +CT',12X,'CP',8X,'EFFICIENCY')
0164              WRITE(IWR,*)'   '
0165              WRITE(IWR,140)(ARJ(I),THRUST(I),HPOWER(I),TCOEFF(I),PCOEFF(I),EF
0166             +I), I=1,21)
0167          140 FORMAT(' ',F10.5,2F15.1,3F15.5)
0168              NP=21
0169              ND=21
0170              NF=1
0171              IOPT=-111
0172              CALL TPLACE('UPH')
0173              CALL TPLOT(IOPT,ARJ,TCOEFF,NP,ND,NF)
0174              CALL TLABEL('ADVANCE RATIO','THRUST COEFFICIENT')
0175              CALL TPLACE('LOH')
0176              CALL TPLOT(IOPT,ARJ,PCOEFF,NP,ND,NF)
0177              CALL TLABEL('ADVANCE RATIO','POWER COEFFICIENT')
0178              CALL TITLE('THEORETICAL THRUST AND POWER COEFFICIENTS')
0179        C     CALL TPLOT(IOPT,V,EFF,NP,ND,NF)
0180        C     CALL TLABEL('VELOCITY (ft/s)','EFFICIENCY')
0181        C     CALL TITLE('EFFICIENCY INCREASE FOR VELOCITY RANGE')
0182              STOP
0183              END
```

APPENDIX 5.2

FREESTREAM VELOCITY (FT/SEC) = 50.0000

R	PHI	BETA	ALPHA	CL	CD	DL	DD	DT	DG
0.08333	38.60113	40.00000	1.36887	0.13689	0.00507	0.32166	0.01192	0.24383	0.01751
0.10417	35.97433	37.50000	1.42567	0.14257	0.00508	0.45841	0.01634	0.36089	0.02949
0.12500	33.58449	35.00000	1.41551	0.14155	0.00508	0.57580	0.02066	0.46825	0.04197
0.14583	31.13429	32.50000	1.36571	0.13657	0.00507	0.63382	0.02355	0.53035	0.05073
0.16667	28.70926	30.00000	1.29074	0.12907	0.00507	0.67993	0.02669	0.58353	0.05834
0.18750	26.30114	27.50000	1.19886	0.11989	0.00506	0.69261	0.02922	0.60796	0.06245
0.20833	23.90487	25.00000	1.09513	0.10951	0.00505	0.67378	0.03106	0.60340	0.06280
0.22917	21.51722	22.50000	0.98278	0.09828	0.00504	0.62697	0.03214	0.57148	0.05955
0.25000	19.13604	20.00000	0.86396	0.08640	0.00503	0.55696	0.03242	0.51555	0.05330

FREESTREAM VELOCITY (FT/SEC) = 55.0000

R	PHI	BETA	ALPHA	CL	CD	DL	DD	DT	DG
0.08333	38.61112	40.00000	1.38888	0.13889	0.00508	0.29084	0.01063	0.22063	0.01582
0.10417	36.03000	37.50000	1.47000	0.14700	0.00509	0.42098	0.01456	0.33189	0.02702
0.12500	33.52712	35.00000	1.47288	0.14729	0.00509	0.53353	0.01842	0.43459	0.03876
0.14583	31.07110	32.50000	1.42890	0.14289	0.00508	0.66231	0.02355	0.55513	0.05279
0.16667	28.64503	30.00000	1.35497	0.13550	0.00507	0.71294	0.02669	0.61289	0.06087
0.18750	26.23915	27.50000	1.26085	0.12608	0.00506	0.72770	0.02922	0.63980	0.06524
0.20833	23.84747	25.00000	1.15253	0.11525	0.00505	0.70852	0.03106	0.63547	0.06560
0.22917	21.46614	22.50000	1.03386	0.10339	0.00504	0.65914	0.03215	0.60165	0.06213
0.25000	19.09257	20.00000	0.90743	0.09074	0.00503	0.58471	0.03243	0.54194	0.05547

FREESTREAM VELOCITY (FT/SEC) = 60.0000

R	PHI	BETA	ALPHA	CL	CD	DL	DD	DT	DG
0.08333	38.60813	40.00000	1.39187	0.13919	0.00508	0.29146	0.01063	0.22112	0.01585
0.10417	36.00090	37.50000	1.49910	0.14991	0.00509	0.42903	0.01456	0.33852	0.02750
0.12500	33.48322	35.00000	1.51678	0.15168	0.00509	0.54891	0.01842	0.44765	0.03977
0.14583	31.01986	32.50000	1.48014	0.14801	0.00509	0.68536	0.02355	0.57521	0.05445
0.16667	28.59147	30.00000	1.40853	0.14085	0.00508	0.74041	0.02670	0.63735	0.06296
0.18750	26.18675	27.50000	1.31325	0.13132	0.00507	0.75731	0.02923	0.66668	0.06758
0.20833	23.79874	25.00000	1.20126	0.12013	0.00506	0.73797	0.03107	0.66268	0.06796
0.22917	21.42292	22.50000	1.07708	0.10771	0.00505	0.68633	0.03215	0.62716	0.06431
0.25000	19.05626	20.00000	0.94374	0.09437	0.00504	0.60787	0.03243	0.56397	0.05728

FREESTREAM VELOCITY (FT/SEC) = 65.0000

R	PHI	BETA	ALPHA	CL	CD	DL	DD	DT	DG
0.08333	38.62089	40.00000	1.37911	0.13791	0.00508	0.28891	0.01063	0.21909	0.01572
0.10417	35.98624	37.50000	1.51376	0.15138	0.00509	0.43308	0.01457	0.34187	0.02774
0.12500	33.45225	35.00000	1.54775	0.15478	0.00510	0.55974	0.01843	0.45686	0.04049
0.14583	30.98017	32.50000	1.51983	0.15198	0.00509	0.70318	0.02356	0.59074	0.05573
0.16667	28.54825	30.00000	1.45175	0.14517	0.00508	0.76254	0.02670	0.65707	0.06465
0.18750	26.14368	27.50000	1.35632	0.13563	0.00507	0.78161	0.02923	0.68876	0.06949
0.20833	23.75845	25.00000	1.24155	0.12416	0.00506	0.76228	0.03107	0.68516	0.06991
0.22917	21.38738	22.50000	1.11262	0.11126	0.00505	0.70866	0.03216	0.64813	0.06609
0.25000	19.02695	20.00000	0.97305	0.09731	0.00504	0.62655	0.03244	0.58174	0.05873

FREESTREAM VELOCITY (FT/SEC) = 70.0000

R	PHI	BETA	ALPHA	CL	CD	DL	DD	DT	DG
0.08333	38.64814	40.00000	1.35186	0.13519	0.00507	0.28343	0.01063	0.21471	0.01544
0.10417	35.98520	37.50000	1.51480	0.15148	0.00509	0.43338	0.01457	0.34212	0.02775
0.12500	33.43364	35.00000	1.56636	0.15664	0.00510	0.56625	0.01843	0.46240	0.04092
0.14583	30.95160	32.50000	1.54840	0.15484	0.00510	0.71599	0.02356	0.60192	0.05665
0.16667	28.51506	30.00000	1.48494	0.14849	0.00509	0.77951	0.02671	0.67220	0.06593
0.18750	26.10967	27.50000	1.39033	0.13903	0.00508	0.80078	0.02924	0.70619	0.07100
0.20833	23.72638	25.00000	1.27362	0.12736	0.00506	0.78162	0.03108	0.70305	0.07145
0.22917	21.35931	22.50000	1.14069	0.11407	0.00505	0.72629	0.03216	0.66469	0.06748
0.25000	19.00446	20.00000	0.99554	0.09955	0.00504	0.64087	0.03244	0.59538	0.05984

FREESTREAM VELOCITY (FT/SEC) = 75.0000

R	PHI	BETA	ALPHA	CL	CD	DL	DD	DT	DQ
0.08333	38.68865	40.00000	1.31135	0.13113	0.00507	0.27525	0.01064	0.20820	0.01503
0.10417	35.99695	37.50000	1.50305	0.15031	0.00509	0.43016	0.01457	0.33946	0.02756
0.12500	33.42681	35.00000	1.57319	0.15732	0.00510	0.56865	0.01843	0.46444	0.04108
0.14583	30.93373	32.50000	1.56627	0.15663	0.00510	0.72399	0.02356	0.60890	0.05722
0.16667	28.49157	30.00000	1.50843	0.15084	0.00509	0.79151	0.02671	0.68291	0.06684
0.18750	26.08445	27.50000	1.41555	0.14156	0.00508	0.81498	0.02924	0.71911	0.07211
0.20833	23.70231	25.00000	1.29769	0.12977	0.00507	0.79612	0.03108	0.71647	0.07260
0.22917	21.33854	22.50000	1.16146	0.11615	0.00505	0.73932	0.03217	0.67693	0.06852
0.25000	18.98864	20.00000	1.01136	0.10114	0.00504	0.65095	0.03244	0.60497	0.06062

FREESTREAM VELOCITY (FT/SEC) = 80.0000

R	PHI	BETA	ALPHA	CL	CD	DL	DD	DT	DQ
0.08333	38.74118	40.00000	1.25882	0.12588	0.00506	0.26462	0.01064	0.19974	0.01449
0.10417	36.02068	37.50000	1.47932	0.14793	0.00509	0.42364	0.01457	0.33407	0.02718
0.12500	33.43118	35.00000	1.56882	0.15688	0.00510	0.56714	0.01843	0.46315	0.04098
0.14583	30.92613	32.50000	1.57387	0.15739	0.00510	0.72739	0.02356	0.61187	0.05746
0.16667	28.47743	30.00000	1.52257	0.15226	0.00509	0.79873	0.02671	0.68935	0.06739
0.18750	26.06775	27.50000	1.43225	0.14323	0.00508	0.82437	0.02925	0.72766	0.07285
0.20833	23.68600	25.00000	1.31400	0.13140	0.00507	0.80594	0.03109	0.72556	0.07338
0.22917	21.32486	22.50000	1.17514	0.11751	0.00505	0.74790	0.03217	0.68500	0.06920
0.25000	18.97931	20.00000	1.02069	0.10207	0.00504	0.65689	0.03244	0.61063	0.06108

FREESTREAM VELOCITY (FT/SEC) = 85.0000

R	PHI	BETA	ALPHA	CL	CD	DL	DD	DT	DQ
0.08333	38.80455	40.00000	1.19545	0.11954	0.00506	0.25175	0.01065	0.18951	0.01384
0.10417	36.05556	37.50000	1.44444	0.14444	0.00508	0.41402	0.01457	0.32614	0.02661
0.12500	33.44617	35.00000	1.55383	0.15538	0.00510	0.56192	0.01843	0.45871	0.04063
0.14583	30.92836	32.50000	1.57164	0.15716	0.00510	0.72640	0.02356	0.61100	0.05739
0.16667	28.47230	30.00000	1.52770	0.15277	0.00509	0.80135	0.02671	0.69169	0.06759
0.18750	26.05928	27.50000	1.44072	0.14407	0.00508	0.82914	0.02925	0.73200	0.07322
0.20833	23.67723	25.00000	1.32277	0.13228	0.00507	0.81122	0.03109	0.73045	0.07380
0.22917	21.31808	22.50000	1.18192	0.11819	0.00506	0.75216	0.03217	0.68900	0.06953
0.25000	18.97630	20.00000	1.02370	0.10237	0.00504	0.65880	0.03245	0.61245	0.06123

FREESTREAM VELOCITY (FT/SEC) = 90.0000

R	PHI	BETA	ALPHA	CL	CD	DL	DD	DT	DQ
0.08333	38.87761	40.00000	1.12239	0.11224	0.00505	0.23685	0.01066	0.17770	0.01308
0.10417	36.10079	37.50000	1.39921	0.13992	0.00508	0.40152	0.01457	0.31583	0.02587
0.12500	33.47119	35.00000	1.52881	0.15288	0.00509	0.55319	0.01843	0.45129	0.04006
0.14583	30.93998	32.50000	1.56002	0.15600	0.00510	0.72120	0.02356	0.60646	0.05702
0.16667	28.47583	30.00000	1.52417	0.15242	0.00509	0.79955	0.02671	0.69008	0.06745
0.18750	26.05878	27.50000	1.44122	0.14412	0.00508	0.82942	0.02925	0.73225	0.07324
0.20833	23.67576	25.00000	1.32424	0.13242	0.00507	0.81211	0.03109	0.73127	0.07387
0.22917	21.31800	22.50000	1.18200	0.11820	0.00506	0.75221	0.03217	0.68904	0.06954
0.25000	18.97944	20.00000	1.02056	0.10206	0.00504	0.65681	0.03244	0.61055	0.06107

FREESTREAM VELOCITY (FT/SEC) = 95.0000

R	PHI	BETA	ALPHA	CL	CD	DL	DD	DT	DQ
0.08333	38.95928	40.00000	1.04072	0.10407	0.00504	0.22012	0.01067	0.16446	0.01222
0.10417	36.15556	37.50000	1.34444	0.13444	0.00507	0.38634	0.01457	0.30334	0.02497
0.12500	33.50565	35.00000	1.49435	0.14943	0.00509	0.54115	0.01843	0.44106	0.03926
0.14583	30.96053	32.50000	1.53947	0.15395	0.00509	0.71198	0.02356	0.59842	0.05636
0.16667	28.48769	30.00000	1.51231	0.15123	0.00509	0.79349	0.02671	0.68468	0.06699
0.18750	26.06596	27.50000	1.43404	0.14340	0.00508	0.82538	0.02925	0.72858	0.07293
0.20833	23.68136	25.00000	1.31864	0.13186	0.00507	0.80874	0.03109	0.72815	0.07360
0.22917	21.32442	22.50000	1.17558	0.11756	0.00505	0.74818	0.03217	0.68526	0.06922
0.25000	18.98856	20.00000	1.01144	0.10114	0.00504	0.65100	0.03244	0.60502	0.06063

FREESTREAM VELOCITY (FT/SEC) = 100.000

R	PHI	BETA	ALPHA	CL	CD	DL	DD	DT	DQ
0.08333	39.04853	40.00000	0.95147	0.09515	0.00504	0.20175	0.01068	0.14995	0.01128
0.10417	36.21909	37.50000	1.28091	0.12809	0.00507	0.36868	0.01458	0.28882	0.02392
0.12500	33.54898	35.00000	1.45102	0.14510	0.00508	0.52598	0.01843	0.42818	0.03826
0.14583	30.98960	32.50000	1.51040	0.15104	0.00509	0.69895	0.02356	0.58705	0.05543
0.16667	28.50752	30.00000	1.49248	0.14925	0.00509	0.78337	0.02671	0.67564	0.06623
0.18750	26.08054	27.50000	1.41946	0.14195	0.00508	0.81717	0.02925	0.72111	0.07229
0.20833	23.69380	25.00000	1.30620	0.13062	0.00507	0.80125	0.03109	0.72121	0.07301
0.22917	21.33715	22.50000	1.16285	0.11628	0.00505	0.74020	0.03217	0.67775	0.06859
0.25000	19.00348	20.00000	0.99652	0.09965	0.00504	0.64150	0.03244	0.59597	0.05989

FREESTREAM VELOCITY (FT/SEC) = 105.000

R	PHI	BETA	ALPHA	CL	CD	DL	DD	DT	DQ
0.08333	39.14439	40.00000	0.85561	0.08556	0.00503	0.18192	0.01069	0.13434	0.01026
0.10417	36.29066	37.50000	1.20934	0.12093	0.00506	0.34871	0.01458	0.27244	0.02272
0.12500	33.60061	35.00000	1.39939	0.13994	0.00508	0.50786	0.01843	0.41281	0.03705
0.14583	31.02673	32.50000	1.47327	0.14733	0.00509	0.68227	0.02355	0.57252	0.05423
0.16667	28.53498	30.00000	1.46502	0.14650	0.00509	0.76933	0.02670	0.66312	0.06516
0.18750	26.10225	27.50000	1.39775	0.13978	0.00508	0.80496	0.02924	0.71000	0.07133
0.20833	23.71285	25.00000	1.28715	0.12872	0.00507	0.78977	0.03108	0.71060	0.07210
0.22917	21.35598	22.50000	1.14402	0.11440	0.00505	0.72838	0.03217	0.66665	0.06765
0.25000	19.02404	20.00000	0.97596	0.09760	0.00504	0.62840	0.03244	0.58350	0.05888

FREESTREAM VELOCITY (FT/SEC) = 110.000

R	PHI	BETA	ALPHA	CL	CD	DL	DD	DT	DQ
0.08333	39.24594	40.00000	0.75406	0.07541	0.00502	0.16078	0.01071	0.11774	0.00917
0.10417	36.36951	37.50000	1.13049	0.11305	0.00505	0.32662	0.01459	0.25435	0.02140
0.12500	33.65997	35.00000	1.34003	0.13400	0.00507	0.48698	0.01843	0.39512	0.03566
0.14583	31.07150	32.50000	1.42850	0.14285	0.00508	0.66213	0.02355	0.55498	0.05278
0.16667	28.56972	30.00000	1.43028	0.14303	0.00508	0.75155	0.02670	0.64727	0.06381
0.18750	26.13079	27.50000	1.36921	0.13692	0.00507	0.78888	0.02924	0.69537	0.07007
0.20833	23.73827	25.00000	1.26173	0.12617	0.00506	0.77445	0.03108	0.69642	0.07088
0.22917	21.38073	22.50000	1.11927	0.11193	0.00505	0.71284	0.03216	0.65206	0.06642
0.25000	19.05008	20.00000	0.94992	0.09499	0.00504	0.61181	0.03243	0.56772	0.05759

FREESTREAM VELOCITY (FT/SEC) = 115.000

R	PHI	BETA	ALPHA	CL	CD	DL	DD	DT	DQ
0.08333	39.35236	40.00000	0.64764	0.06476	0.00502	0.13851	0.01073	0.10030	0.00801
0.10417	36.45496	37.50000	1.04504	0.10450	0.00504	0.30259	0.01460	0.23470	0.01995
0.12500	33.72653	35.00000	1.27347	0.12735	0.00506	0.46349	0.01843	0.37525	0.03408
0.14583	31.12347	32.50000	1.37653	0.13765	0.00508	0.63871	0.02355	0.53460	0.05108
0.16667	28.61141	30.00000	1.38859	0.13886	0.00508	0.73019	0.02670	0.62824	0.06218
0.18750	26.16589	27.50000	1.33411	0.13341	0.00507	0.76908	0.02923	0.67738	0.06851
0.20833	23.76983	25.00000	1.23017	0.12302	0.00506	0.75542	0.03107	0.67881	0.06936
0.22917	21.41119	22.50000	1.08881	0.10888	0.00505	0.69370	0.03216	0.63408	0.06489
0.25000	19.08141	20.00000	0.91859	0.09186	0.00503	0.59183	0.03243	0.54871	0.05603

FREESTREAM VELOCITY (FT/SEC) = 120.000

R	PHI	BETA	ALPHA	CL	CD	DL	DD	DT	DQ
0.08333	39.46285	40.00000	0.53715	0.05371	0.00501	0.11524	0.01075	0.08213	0.00680
0.10417	36.54633	37.50000	0.95367	0.09537	0.00504	0.27677	0.01462	0.21365	0.01839
0.12500	33.79976	35.00000	1.20024	0.12002	0.00506	0.43757	0.01844	0.35336	0.03234
0.14583	31.18222	32.50000	1.31778	0.13178	0.00507	0.61217	0.02355	0.51153	0.04916
0.16667	28.65970	30.00000	1.34030	0.13403	0.00507	0.70541	0.02669	0.60618	0.06029
0.18750	26.20729	27.50000	1.29271	0.12927	0.00507	0.74571	0.02923	0.65615	0.06666
0.20833	23.80730	25.00000	1.19270	0.11927	0.00506	0.73279	0.03107	0.65790	0.06755
0.22917	21.44717	22.50000	1.05283	0.10528	0.00504	0.67108	0.03215	0.61285	0.06309
0.25000	19.11787	20.00000	0.88213	0.08821	0.00503	0.56856	0.03243	0.52658	0.05421

FREESTREAM VELOCITY (FT/SEC) = 125.000

R	PHI	BETA	ALPHA	CL	CD	DL	DD	DT	DQ
0.08333	39.57673	40.00000	0.42327	0.04233	0.00501	0.09110	0.01078	0.06335	0.00553
0.10417	36.64303	37.50000	0.85697	0.08570	0.00503	0.24932	0.01463	0.19132	0.01672
0.12500	33.87913	35.00000	1.12087	0.11209	0.00505	0.40937	0.01844	0.32959	0.03044
0.14583	31.24735	32.50000	1.25265	0.12526	0.00506	0.58268	0.02355	0.48594	0.04701
0.16667	28.71427	30.00000	1.28573	0.12857	0.00507	0.67735	0.02669	0.58124	0.05814
0.18750	26.25470	27.50000	1.24530	0.12453	0.00506	0.71891	0.02922	0.63181	0.06454
0.20833	23.85046	25.00000	1.14954	0.11495	0.00505	0.70671	0.03106	0.63380	0.06545
0.22917	21.48848	22.50000	1.01152	0.10115	0.00504	0.64507	0.03215	0.58846	0.06101
0.25000	19.15930	20.00000	0.84070	0.08407	0.00503	0.54209	0.03242	0.50143	0.05213

FREESTREAM VELOCITY (FT/SEC) = 130.000

R	PHI	BETA	ALPHA	CL	CD	DL	DD	DT	DQ
0.08333	39.69332	40.00000	0.30668	0.03067	0.00500	0.06623	0.01081	0.04406	0.00422
0.10417	36.74442	37.50000	0.75558	0.07556	0.00502	0.22039	0.01465	0.16784	0.01496
0.12500	33.96416	35.00000	1.03584	0.10358	0.00504	0.37905	0.01845	0.30407	0.02838
0.14583	31.31845	32.50000	1.18155	0.11815	0.00506	0.55039	0.02355	0.45795	0.04466
0.16667	28.77478	30.00000	1.22522	0.12252	0.00506	0.64618	0.02668	0.55354	0.05574
0.18750	26.30785	27.50000	1.19215	0.11921	0.00506	0.68881	0.02922	0.60452	0.06215
0.20833	23.89907	25.00000	1.10093	0.11009	0.00505	0.67729	0.03106	0.60664	0.06308
0.22917	21.53492	22.50000	0.96508	0.09651	0.00504	0.61581	0.03214	0.56103	0.05865
0.25000	19.20553	20.00000	0.79447	0.07945	0.00503	0.51254	0.03242	0.47335	0.04980

FREESTREAM VELOCITY (FT/SEC) = 135.000

R	PHI	BETA	ALPHA	CL	CD	DL	DD	DT	DQ
0.08333	39.81204	40.00000	0.18796	0.01880	0.00500	0.04073	0.01084	0.02434	0.00287
0.10417	36.84996	37.50000	0.65004	0.06500	0.00502	0.19012	0.01467	0.14334	0.01310
0.12500	34.05437	35.00000	0.94563	0.09456	0.00504	0.34675	0.01846	0.27695	0.02618
0.14583	31.39513	32.50000	1.10487	0.11049	0.00505	0.51547	0.02355	0.42774	0.04209
0.16667	28.84092	30.00000	1.15908	0.11591	0.00505	0.61203	0.02668	0.52324	0.05310
0.18750	26.36648	27.50000	1.13352	0.11335	0.00505	0.65555	0.02921	0.57438	0.05950
0.20833	23.95292	25.00000	1.04708	0.10471	0.00504	0.64465	0.03105	0.57653	0.06044
0.22917	21.58631	22.50000	0.91369	0.09137	0.00503	0.58340	0.03214	0.53066	0.05603
0.25000	19.25639	20.00000	0.74361	0.07436	0.00502	0.47999	0.03242	0.44245	0.04723

FREESTREAM VELOCITY (FT/SEC) = 140.000

R	PHI	BETA	ALPHA	CL	CD	DL	DD	DT	DQ
0.08333	39.93236	40.00000	0.06764	0.00676	0.00500	0.01471	0.01087	0.00430	0.00148
0.10417	36.95912	37.50000	0.54088	0.05409	0.00501	0.15863	0.01470	0.11792	0.01116
0.12500	34.14928	35.00000	0.85072	0.08507	0.00503	0.31263	0.01848	0.24835	0.02385
0.14583	31.47701	32.50000	1.02299	0.10230	0.00504	0.47807	0.02356	0.39542	0.03933
0.16667	28.91236	30.00000	1.08764	0.10876	0.00505	0.57505	0.02668	0.49047	0.05023
0.18750	26.43033	27.50000	1.06967	0.10697	0.00505	0.61926	0.02921	0.54153	0.05659
0.20833	24.01178	25.00000	0.98822	0.09882	0.00504	0.60892	0.03105	0.54359	0.05753
0.22917	21.64245	22.50000	0.85755	0.08576	0.00503	0.54793	0.03213	0.49745	0.05316
0.25000	19.31173	20.00000	0.68827	0.06883	0.00502	0.44454	0.03242	0.40880	0.04440

FREESTREAM VELOCITY (FT/SEC) = 145.000

R	PHI	BETA	ALPHA	CL	CD	DL	DD	DT	DQ
0.08333	40.05379	40.00000	-0.05379	-0.00538	0.00500	-0.01174	0.01091	-0.01600	0.00007
0.10417	37.07140	37.50000	0.42860	0.04286	0.00501	0.12607	0.01473	0.09171	0.00914
0.12500	34.24849	35.00000	0.75151	0.07515	0.00502	0.27680	0.01850	0.21839	0.02138
0.14583	31.56372	32.50000	0.93628	0.09363	0.00503	0.43832	0.02357	0.36114	0.03639
0.16667	28.98881	30.00000	1.01119	0.10112	0.00504	0.53537	0.02669	0.45536	0.04713
0.18750	26.49913	27.50000	1.00087	0.10009	0.00504	0.58007	0.02921	0.50610	0.05343
0.20833	24.07544	25.00000	0.92456	0.09246	0.00503	0.57022	0.03105	0.50795	0.05437
0.22917	21.70316	22.50000	0.79684	0.07968	0.00503	0.50953	0.03213	0.46153	0.05002
0.25000	19.37139	20.00000	0.62861	0.06286	0.00502	0.40627	0.03242	0.37252	0.04133

FREESTREAM VELOCITY (FT/SEC) = 150.000

R	PHI	BETA	ALPHA	CL	CD	DL	DD	DT	DQ
0.08333	40.17590	40.00000	-0.17590	-0.01759	0.00500	-0.03851	0.01095	-0.03649	-0.00137
0.10417	37.18635	37.50000	0.31365	0.03137	0.00500	0.09253	0.01476	0.06479	0.00705
0.12500	34.35155	35.00000	0.64845	0.06484	0.00502	0.23941	0.01852	0.18720	0.01880
0.14583	31.65489	32.50000	0.84511	0.08451	0.00503	0.39638	0.02358	0.32503	0.03326
0.16667	29.06995	30.00000	0.93005	0.09300	0.00503	0.49314	0.02669	0.41805	0.04382
0.18750	26.57265	27.50000	0.92735	0.09274	0.00503	0.53810	0.02921	0.46820	0.05003
0.20833	24.14368	25.00000	0.85632	0.08563	0.00503	0.52865	0.03105	0.46970	0.05095
0.22917	21.76826	22.50000	0.73174	0.07317	0.00502	0.46829	0.03213	0.42298	0.04664
0.25000	19.43520	20.00000	0.56480	0.05648	0.00501	0.36529	0.03242	0.33368	0.03803

CHAPTER 6

WEIGHTS AND BALANCE

WEIGHT AND BALANCE

In order for an aircraft to be controllable, the center of gravity (cg) must be located in a favorable position. In regular transport planes the cg can be greatly effected by passengers or cargo placement. However, for this test vehicle the cg travels only slightly because the equipment is positioned permanently. Therefore, the only consideration for cg travel is the consumption of fuel throughout the flight.

The major factor in determining the shape of the fuselage was the accommodation of the ducted fan unit, while the fuselage size was determined by the volume of equipment being used. The resulting size of the fuselage was 36 inches in length with a maximum diameter of 10 inches tapering to six inches. The cg of the fuselage had to be located between 16 and 20 inches from the forward end in order for the aircraft to be stable. Since the quarter chord of the wing falls within this range the equipment was positioned so that the cg of the fuselage was close to the quarter chord.

The fan and engine were positioned at the rear of the fuselage so that the propulsion system could exhaust directly out the back. A scoop was positioned slightly below the fuselage to increase the airflow to the fan unit, and the throttle servo was located above the engine inside the fuselage so that it could be easily connected to the engine.

Another system located at the rear of the fuselage was the pressure measurement system. This system contains two banks of pressure transducers, one on each side of the fuselage. Since the delta wing was positioned slightly aft of the cg and above the main wing, having the pressure transducers at the rear allowed the pressure tubes to be run directly up the rear struts of the delta wing support structure to the pressure taps located on the surface of the wing.

The computer system, which consists of the data acquisition equipment and the communications pack, was located near the center of the fuselage. Since the data from the pressure banks needed be relayed to the data acquisition equipment the two systems were placed near each other to reduce the amount of wiring running through the fuselage.

Finally, the guidance system was located in the forward section of the

fuselage. Included in this system were two inclinometers, a heading indicator, and a yaw indicator. Since these components were relatively heavy they were placed in the forward portion so they could counteract the weight of the engine in the rear. In addition, there was a battery pack and a nose wheel located in the forward section (see Figure 6.1).

The remainder of the aircraft weight consisted of the fuel system. This system was contained in the wings and was to be comprised of two 0.25 gallon tanks.

By using weight estimations for single engine RPVs the weights of the aircraft components were determined. This analysis resulted in a total aircraft weight estimate of 28 pounds which was used for all design calculations.

The weights for each part of the structure were determined by using the size and density of the material for that section. Since balsa and spruce (two woods) were found to be sufficiently strong to support the anticipated loadings the resulting weight of the aircraft was less than expected. This reduced RPV total weight was 19.5 pounds. Since the weight varied significantly from the initial estimate the center of gravity position was altered. The fuselage cg was found to be 21.27 inches from the forward edge of the fuselage due to the necessary location of the instrumentation.

With the determined fuel and component weights, the center of gravity for the RPV was determined to be 24 inches from the forward-most point of the aircraft. Since the cg should be located near the wing quarter chord, the allowable cg travel was determined to be from 18 to 20 inches from the same reference point. Therefore, the cg was at least 4 inches too far aft. Because the cg would travel as fuel was burned it would eventually reach 25.3 inches. The only way to compensate for this problem was to place ballast in the nose of the RPV. Since the initial estimate was greater than the proposed design weight, ballast could be added in the nose in order to adjust the center of gravity.

In order to locate the center of gravity at an optimal location (18 inches), 7.06 pounds of ballast was required in the nose. Upon depletion of the fuel the cg would have traveled 0.1 inches. An alternative was to locate the cg at 19 inches with a resulting travel of 0.3 inches and 5.5 pounds of ballast in the nose. This results in a favorable design.

FIGURE 6.1

INTERNAL CONFIGURATION

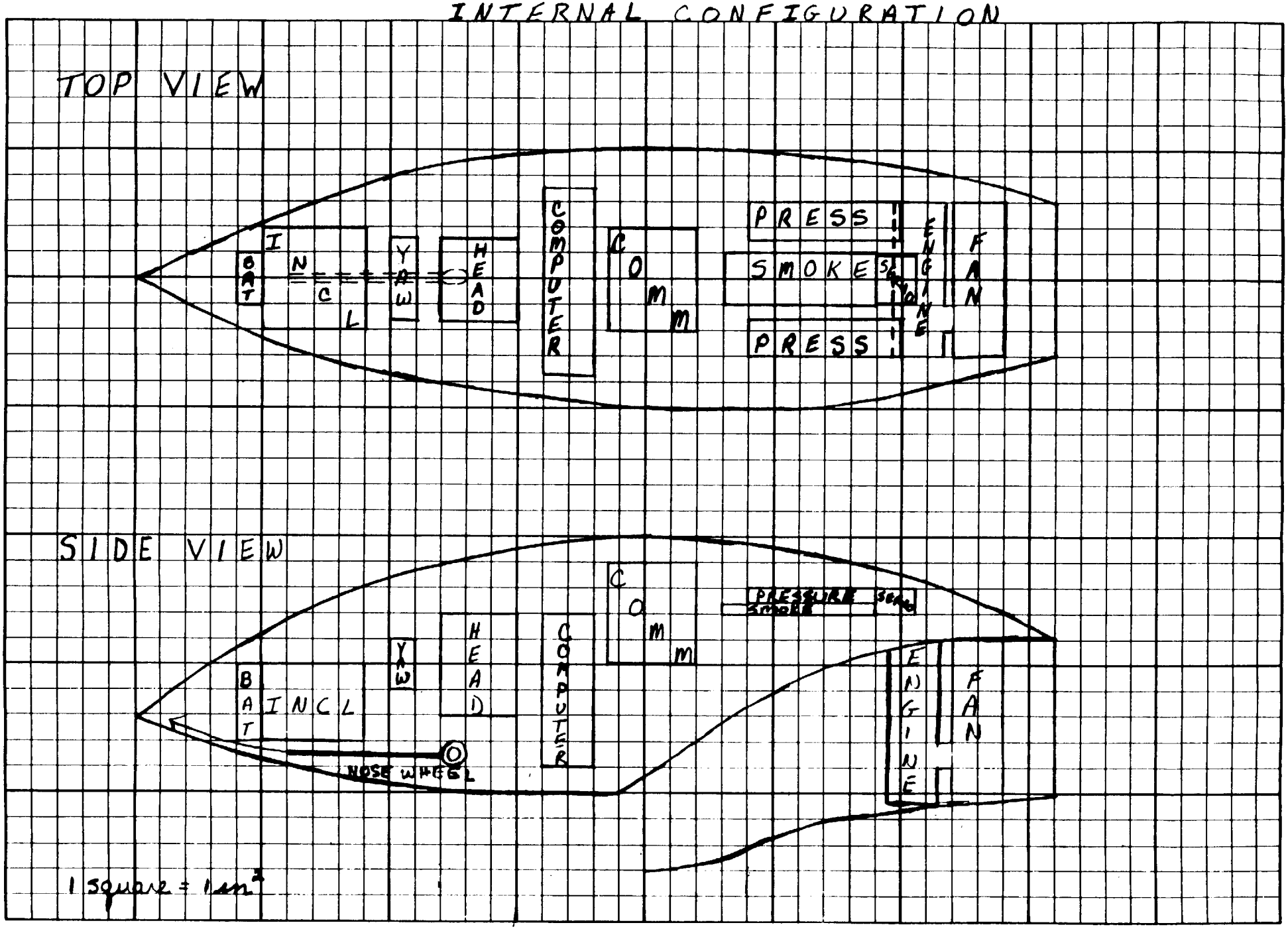

CHAPTER 7

STABILITY AND CONTROL

STABILITY AND CONTROL

STABILITY

The first concern in dealing with the proposed data collection vehicle was to design the aircraft so that it is stable without the presence of a delta wing.

The main stability mode analyzed for the aircraft was longitudinal stability. Since many of the physical parameters associated with longitudinal stability had already been established through other flight requirements the longitudinal mode was examined with respect to center of gravity position (x_{cg}) and length from the wing aerodynamic center to the tail aerodynamic center (l_t).

From longitudinal stability it was determined that the aircraft must have a natural pitch up motion ($c_{m_o} > 0$) and must restore itself to equilibrium when disturbed ($c_{m_\alpha} < 0$). In order for this to occur with the current flight configuration a tail length of at least three feet was required (Figures 7.1 & 7.2). This would insure stability for the entire range of center of gravity position chosen (x_{cg} = 0.23c to 0.32 c).

A factor of concern for the vehicle in general was the overall weight. In order to keep the weight low while maintaining an acceptable degree of longitudinal stability it was thought that a tail length of around 3.3 feet would be appropriate for a center of gravity position near 0.28c.

With the preliminary estimates made, a series of delta wings were added to the aircraft to determine their effect on stability and the feasibility of testing many different wings.

The first thing to note about this analysis is that a c_{do} of 0.006 was assumed for all delta wing planforms. This number was calculated for a delta wing sweep of 45° and since all subsequent calculations are based on delta wing sweep angles varying from 45° to 75° this was taken as a valid approximation. The effect of the delta wing c_{do} on aircraft c_{m_o} was to reduce it from about 0.1 to 0.002; thus, for a sweep angle higher than 45° the aircraft c_{m_o} would fall somewhere between these values.

Two parameters which now arose in the stability determination were the delta wing sweep angle and the position of the delta wing with

Figure 7.1 The Effect of Tail Length on Pitching Moment

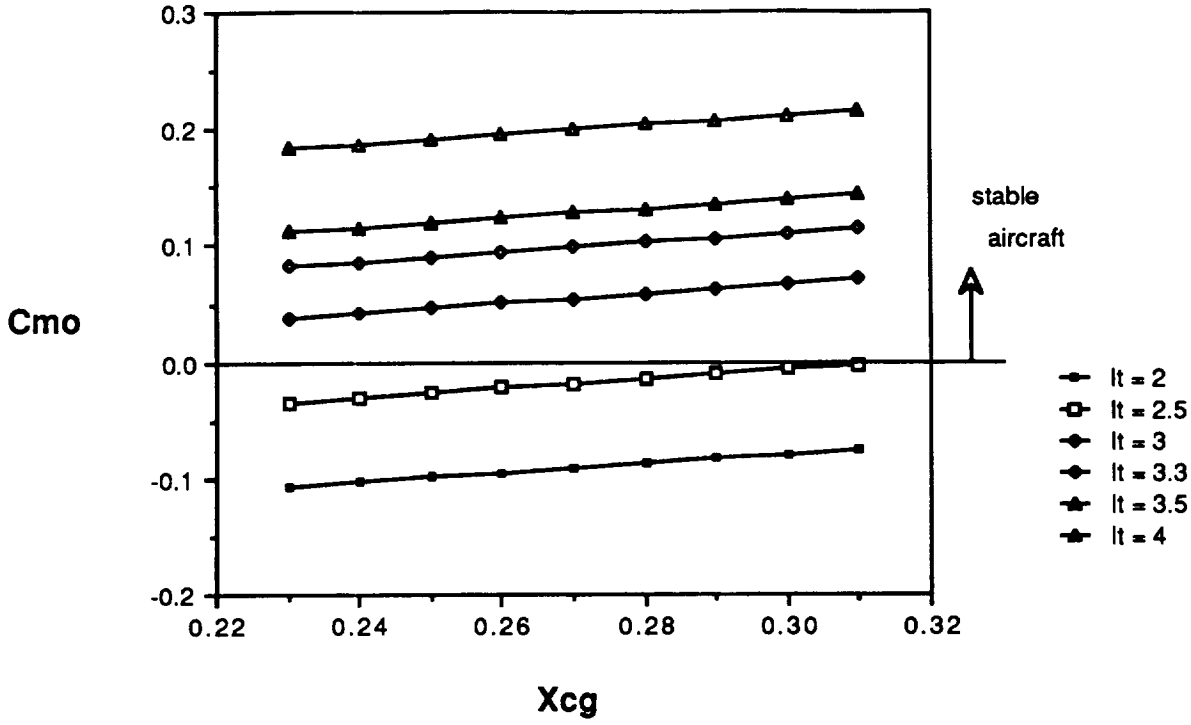

Figure 7.2 Tail Length Effect on Aircraft Stability

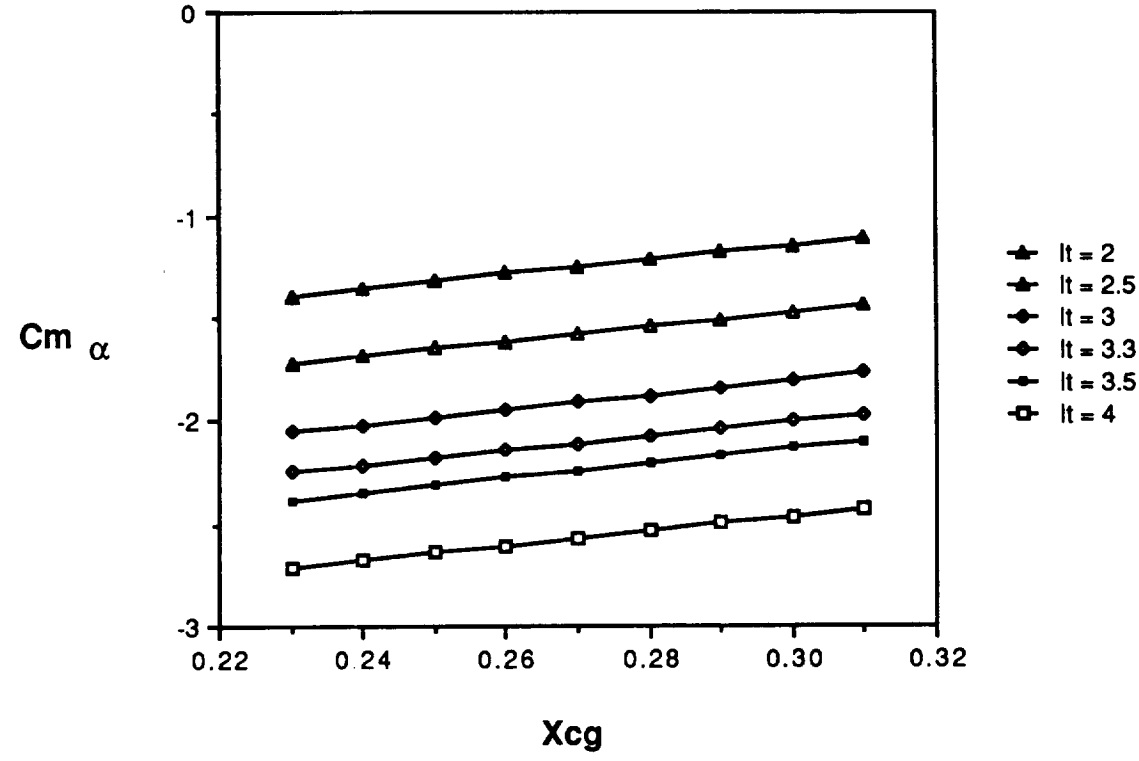

respect to the main wing aerodynamic center. By examining Figure 7.3 it is evident that for all delta wings chosen the aircraft will be longitudinally stable.

Two other interesting points should be observed. The first is that as the delta wing aerodynamic center approaches the vehicle's center of gravity it has less of an effect on longitudinal stability. The other is that as the delta wing sweep angle is increased c_{m_α} for the entire aircraft is less varied over a range of delta wing placements (see Table 7.1).

Initial indications are that the aircraft is feasibly longitudinally stable both with and without the delta wing present. This is important in the delta wing testing and is discussed under the topic of the delta wing.

Calculation was also done which showed the aircraft was also directionally stable. A point which needs to be addressed at this time is roll stability. It is hoped that a wing dihedral of approximately 7° or 8° will provide sufficient roll control of the vehicle.

CONTROL

As far as primary aircraft control is concerned, both longitudinal and directional modes were examined. From the aerodynamic parameters determined an elevator trim angle at cruise was determined. For a cruise c_l of approximately 0.25 this angle was found to be in the range of -0.5° to -1.0°. These values are reasonable and leave sufficient elevator power to control the aircraft in non-cruise conditions.

For directional control a rudder control effectiveness on the order of -0.2 was found. Again this seems to be a reasonable value.

Also noteworthy in the area of control is the aircraft control during data acquisition. Since the delta wing(s) are to be tested at many angles of attack over a wide range of flight velocities it was of interest to determine whether it would be easier to vary flight velocity or delta wing angle of attack during testing. From Figure 7.4 it can be seen that varying the delta wing angle of attack over its entire range will produce only a minor change in angle of attack of the primary wing. However, by varying flight velocity during the test the primary wing angle of attack will

change almost 13 times more. Consequently the decision was made that the delta wing angle will be varied in flight and the fight velocity will be held constant.

Figure 7.3 Delta Wing Effect on Stability

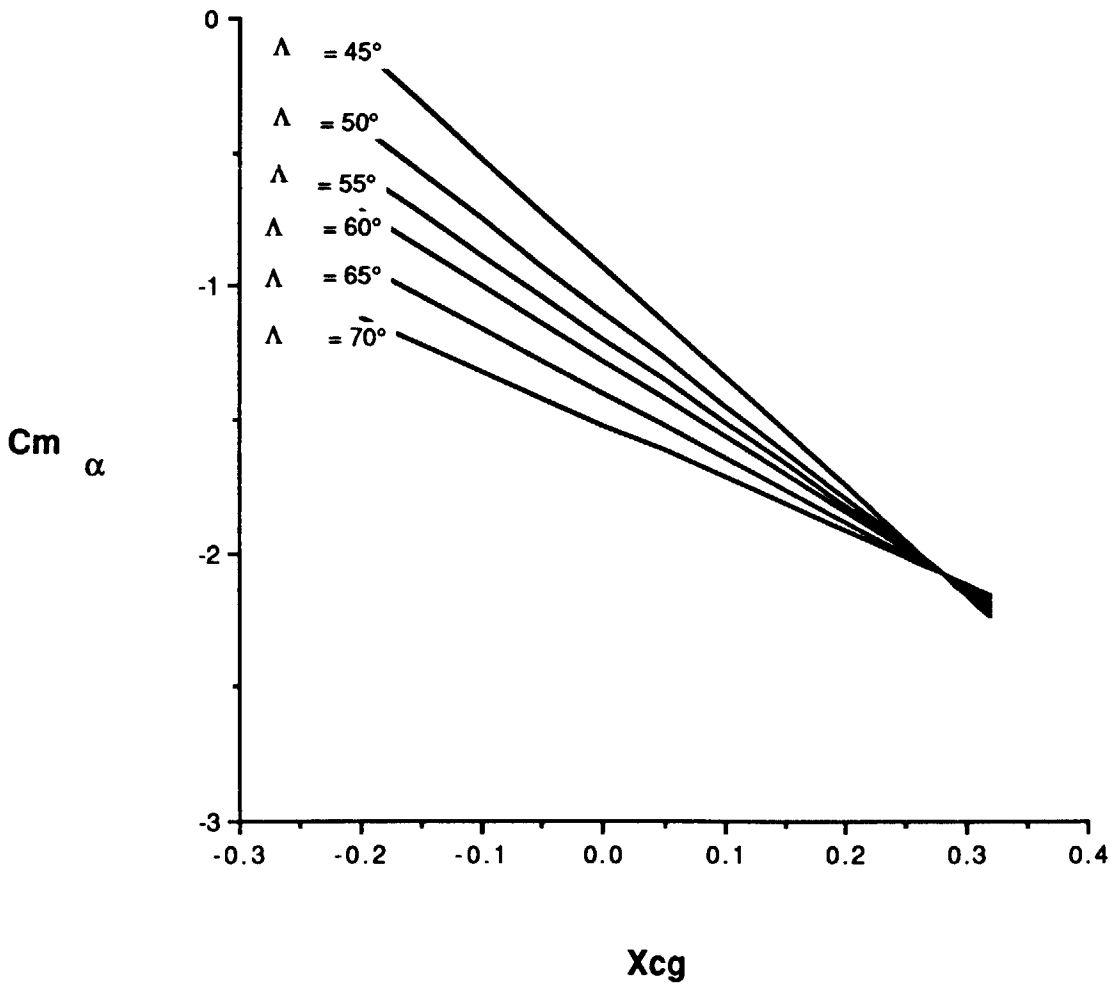

Table 7.1

Delta Wing ac position (xdac)*c	Delta Sweep 45° Cma	Delta Sweep 50° Cma	Delta Sweep 55° Cma	Delta Sweep 60° Cma	Delta Sweep 65° Cma	Delta Sweep 70° Cma
-0.2	-0.112695	-0.400695	-0.573495	-0.717495	-0.919095	-1.120695
-0.15	-0.316695	-0.574695	-0.729495	-0.858495	-1.039095	-1.219695
-0.1	-0.520695	-0.748695	-0.885495	-0.999495	-1.159095	-1.318695
-0.05	-0.724695	-0.922695	-1.041495	-1.140495	-1.279095	-1.417695
0	-0.928695	-1.096695	-1.197495	-1.281495	-1.399095	-1.516695
0.05	-1.132695	-1.270695	-1.353495	-1.422495	-1.519095	-1.615695
0.1	-1.336695	-1.444695	-1.509495	-1.563495	-1.639095	-1.714695
0.15	-1.540695	-1.618695	-1.665495	-1.704495	-1.759095	-1.813695
0.2	-1.744695	-1.792695	-1.821495	-1.845495	-1.879095	-1.912695
0.25	-1.948695	-1.966695	-1.977495	-1.986495	-1.999095	-2.011695
0.26	-1.989495	-2.001495	-2.008695	-2.014695	-2.023095	-2.031495
0.27	-2.030295	-2.036295	-2.039895	-2.042895	-2.047095	-2.051295
0.28	-2.071095	-2.071095	-2.071095	-2.071095	-2.071095	-2.071095
0.29	-2.111895	-2.105895	-2.102295	-2.099295	-2.095095	-2.090895
0.3	-2.152695	-2.140695	-2.133495	-2.127495	-2.119095	-2.110695
0.31	-2.193495	-2.175495	-2.164695	-2.155695	-2.143095	-2.130495
0.32	-2.234295	-2.210295	-2.195895	-2.183895	-2.167095	-2.150295

FIGURE 7.4

Primary wing angle of attack as a function of Delta wing angle

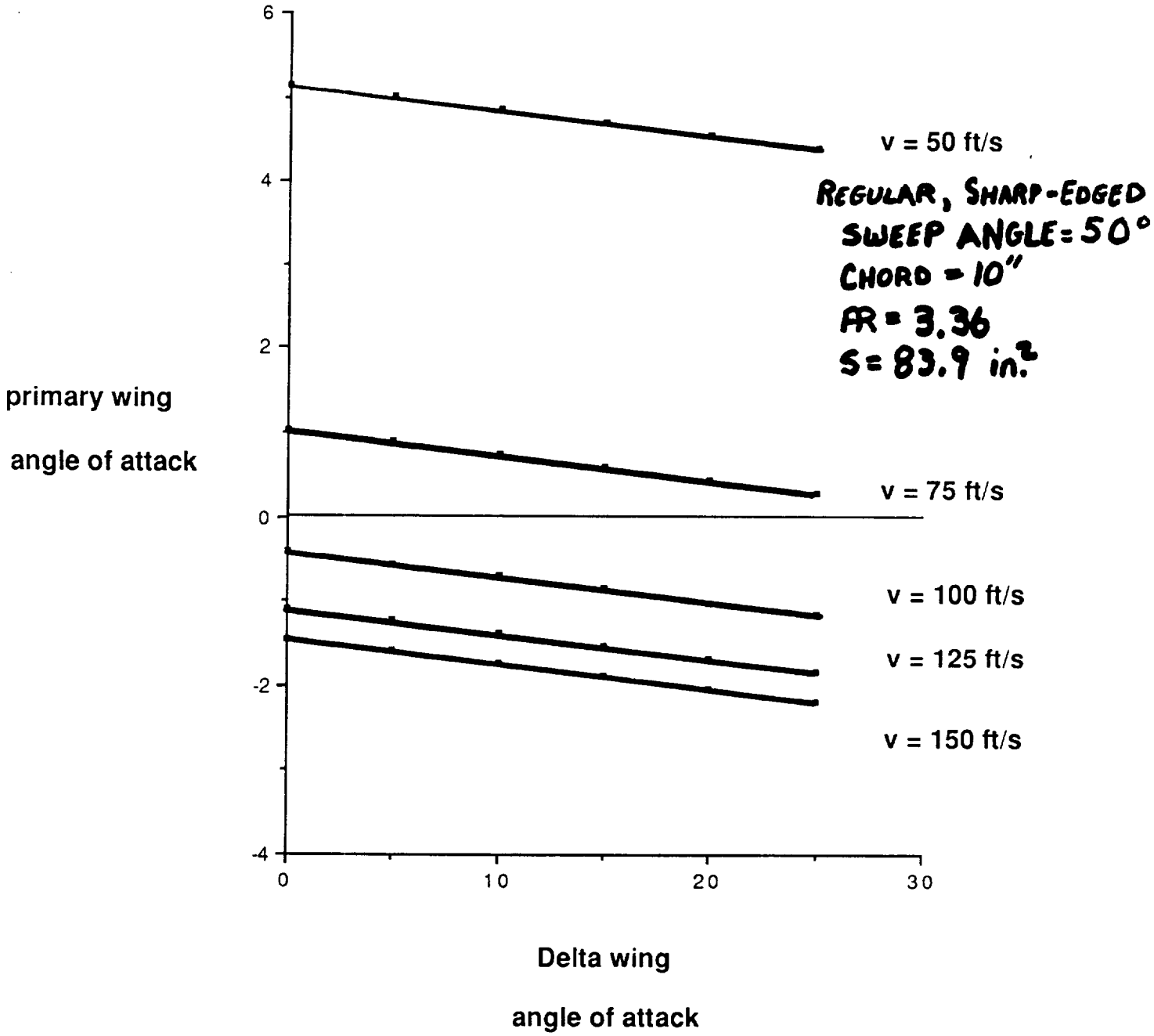

CHAPTER 8

PERFORMANCE ESTIMATION

PERFORMANCE

Primarily designed to operate at low level altitudes, the Delta Monster achieves its maximum glide performance at speeds below the primary operating speeds. If the speed is reduced at altitude to achieve a maximum $Cl^{3/2}/Cd$ = 26.84, the maximum glide distance for a given altitude can be obtained from Figure 8.1. If the power system fails or landing system becomes damaged during flight, the glide performance becomes critical. Energy dissipation can be maximized through use of Figure 8.2. At a max Cl/Cd = 25.87, the minimum rate of descent at altitude can be obtained from this graph.

For the desired testing mission, the minimum amount of fuel expended for a 28 minute test run is 1.323 lbs of fuel. This value was obtained by using varied propellor efficiencies and a thrust specific fuel consumption of 0.75 oz fuel/(min-shaft brake horsepower). Allowing for a one minute and twenty second sweep at each 5 ft/sec increment in velocity, the change in weight of the aircraft was computed as a function of velocity and can be found in Figure 8.3. The variation of $Cl^{3/2}/Cd$ and Cl/Cd with velocity and change in weight is also charted (Figure 8.4).

The climbing performance of the Delta Monster at low level altitudes of concern is shown in Figure 8.5. This graph displays static rates of climb variation with velocities in the testing range. The maximum rates of climb at each altitude are plotted in Figure 8.6. This curve sets the absolute ceiling of the Delta Monster at 25000 ft and the service ceiling at 23,350 ft.

The maximum range and endurance were calculated using the Breguet formulas for velocities of 50 ft/sec, 100 ft/sec, and 150 ft/sec. These values are listed in Appendix 8 along with the formulas. The power coefficient was assumed to be a typical value of 0.5 lbs fuel/hp-hour again with varied propellor efficiency of 0.7. Note these values are at the typical operating speeds and not at the velocities for maximum range and endurance.

Fig. 8.1: Maximum Glide Performance

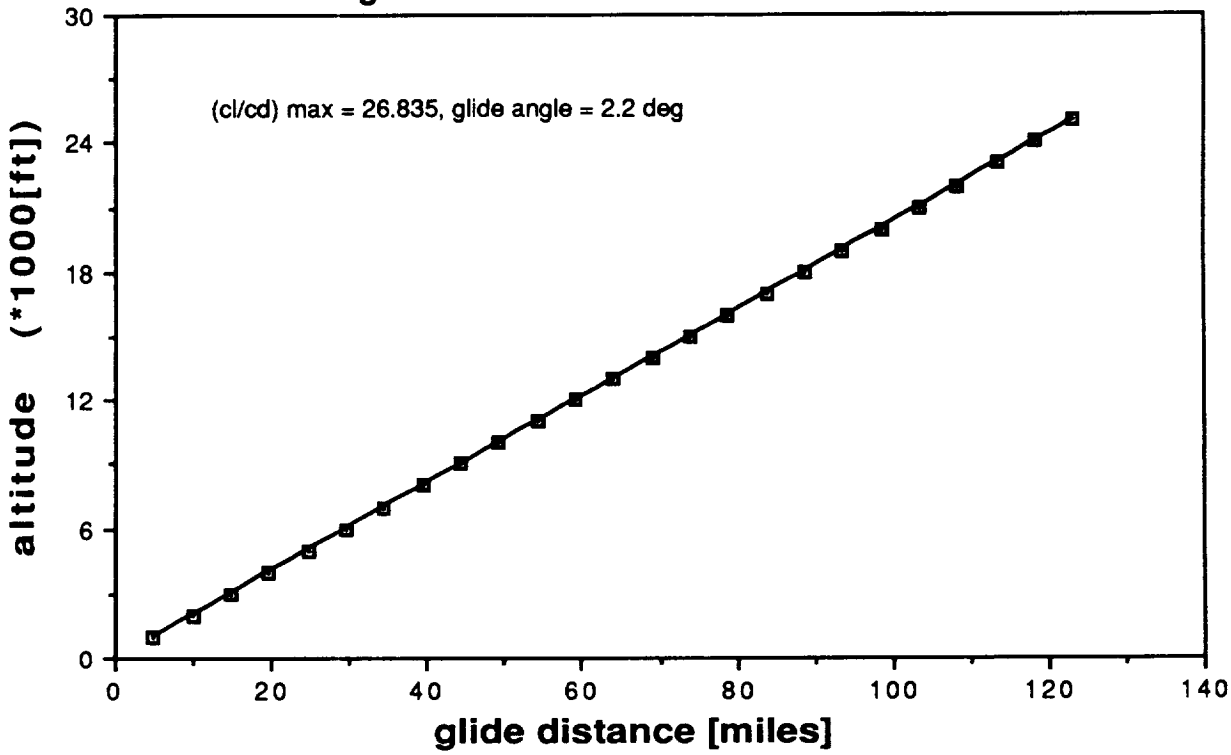

Fig. 8.2: Maximizing Glide Endurance

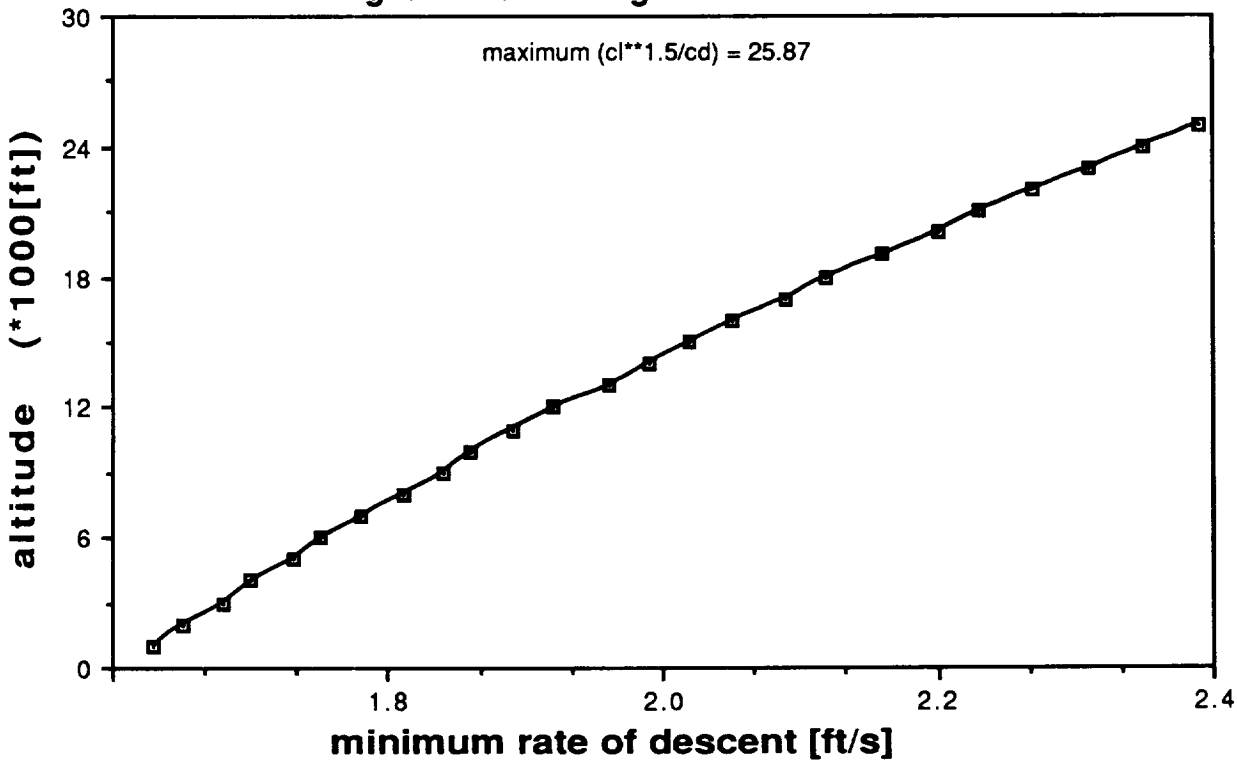

Fig. 8.3: Weight Loss Over Testing Phase

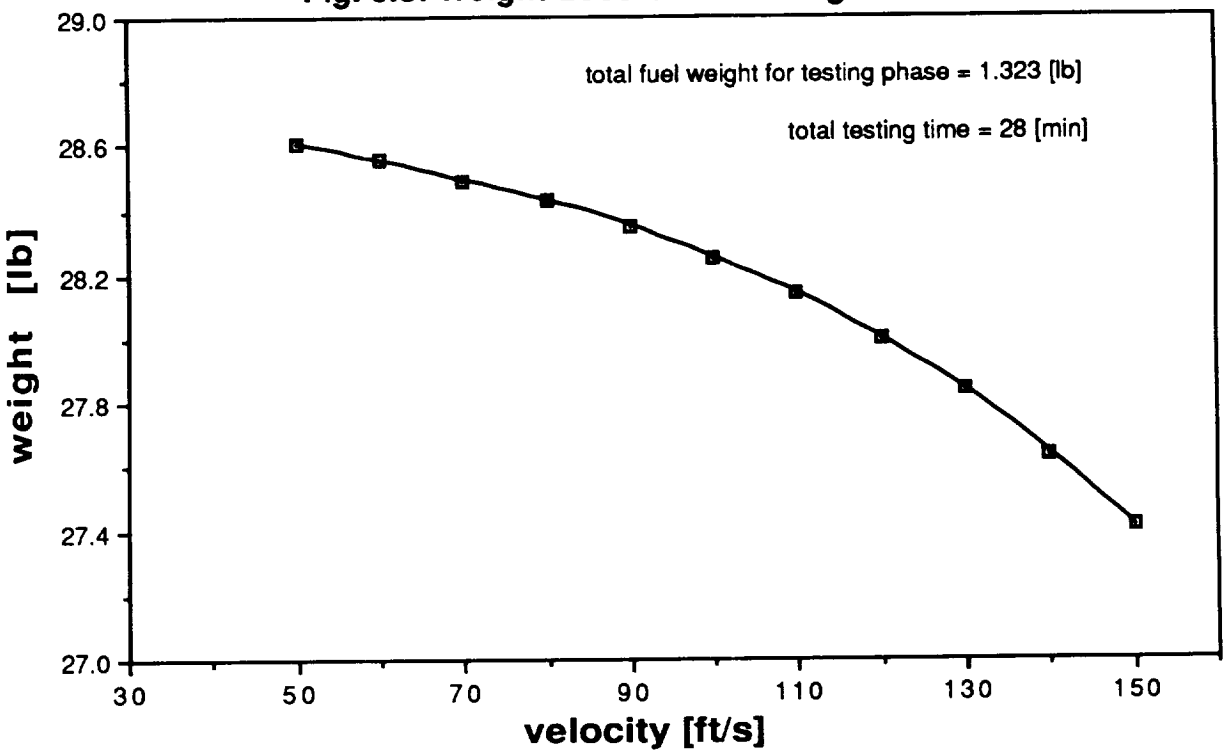

Fig. 8.4: Lift and Drag Coefficients as Functions of Velocity

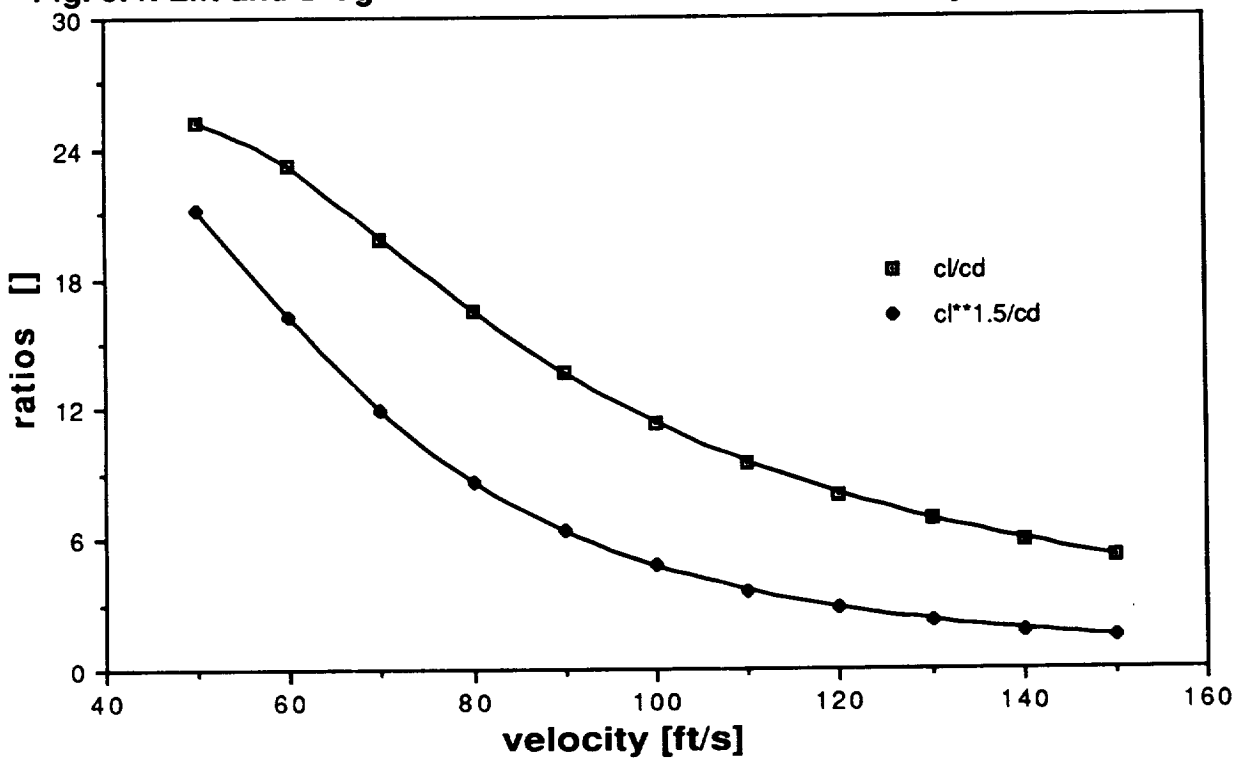

Fig. 8.5: Climbing Performance

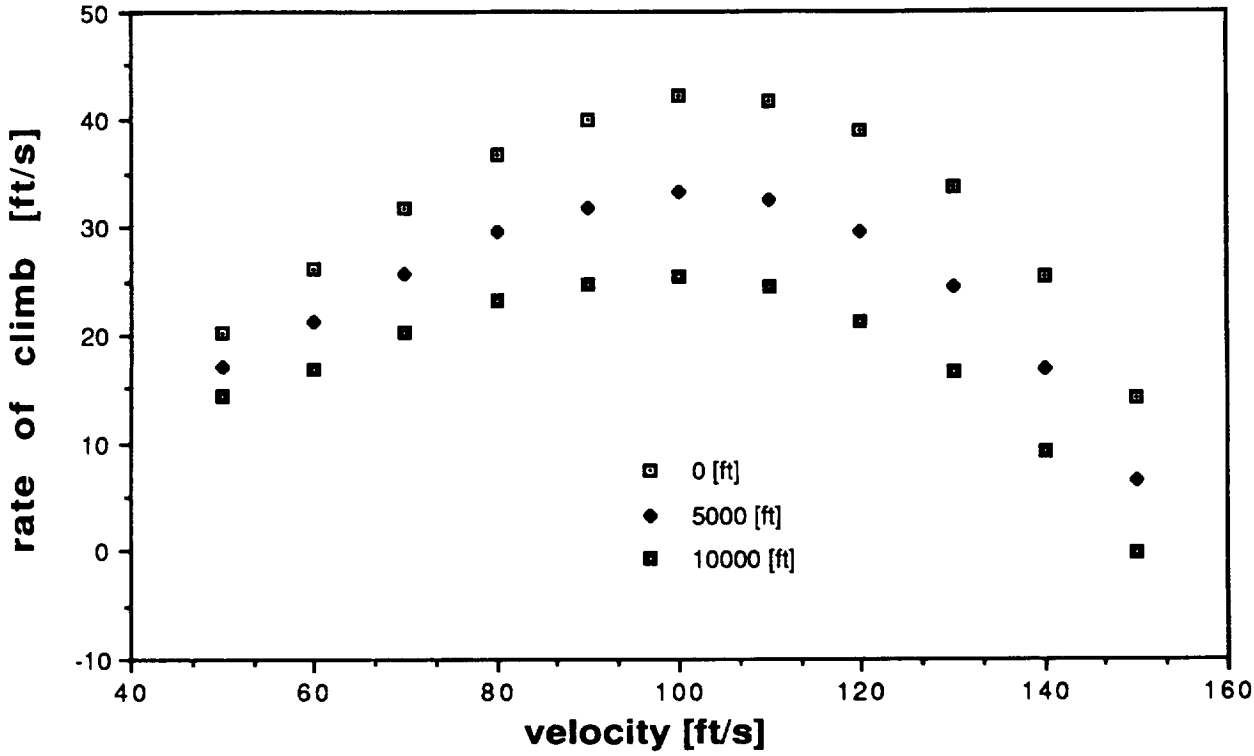

Fig. 8.6: Ceiling Calculation

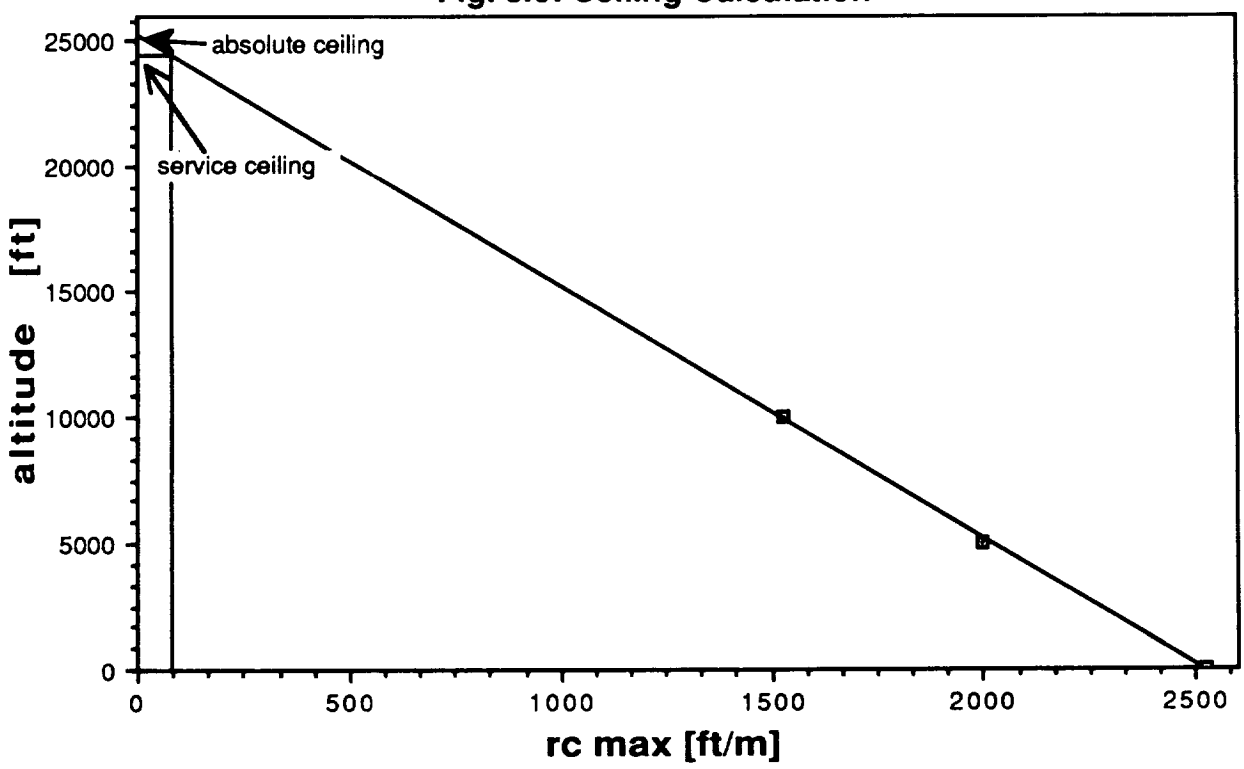

APPENDIX 8

Performance Parameters

Flight Velocity v [ft/s]	Propeller Efficiency η [ ]	Range R [miles]	Endurance E [hours]
50	0.25	224.5	6.7
100	0.51	202.3	3.0
150	0.68	122.2	1.2

Breguet Formulas

1. Endurance (propeller):

$$E = (\eta / cp) (C_L^{1.5} / C_D) (2\rho s)^{1/2} \quad (1/(W_f^{1/2}) - 1/(W_i^{1/2}))$$

2. Range (propeller):

$$R = (\eta / cp) (C_L / C_D) \ln(W_i/W_f)$$

Source

Nelson, R.C., and M. Brendel, Atmospheric Flight Mechanics, pp. 4.47 - 4.57, 1988.

CHAPTER 9

SYSTEM OPERATION

SYSTEM OPERATION

LAUNCH / TAKEOFF

The proposed Delta Monster is to be catapult launched from a 20 ft. rail. This length allows a constant acceleration of 64.4 ft/s^2, taking the craft from rest to 50 ft/s (see Figure 9.1). Since, the stall velocity is 40 ft/s, this margin is reasonable. If the Monster could be built for higher loads, it could possibly be launched at 100 ft/s, the optimum launch velocity, which would maximize rate of climb, and time to climb to the mission altitude of 800 ft (Figures 9.2 & 9.3). Note that the 10 ft/s above stall velocity will allow the craft to climb, and allow the self-propulsion system to catch-up and stabilize.

The rail is to be inclined at 10 degrees to the horizontal. This will launch the craft at the angle necessary to clear a 50 ft obstacle in 300 ft. An additional benefit is the 3.5 ft that the launcher end is elevated. This gives the Monster a small margin in case the self-propulsion system can not obtain the necessary power just off the rail.

DATA COLLECTION AND INSTRUMENTATION

Three competing concepts were analyzed for use in obtaining in-flight data and for flight control of the aircraft. Complete autonomous RPV control, a ground link capable of full information transfer from the RPV to a ground station, and limited information transfer between the aircraft and the ground station were studied in order to determine the optimal data acquisition package for the mission requirements. In addition, the instrumentation required for the data acquisition was studied for both flight control and data acquisition. The parameters used as criterion for these studies were, accuracy, weight, volume, and cost. Finally, the integration of the data analysis routine into the flight mission profile was defined (see Figure 9.4).

Fig. 9.1: Launch Velocity

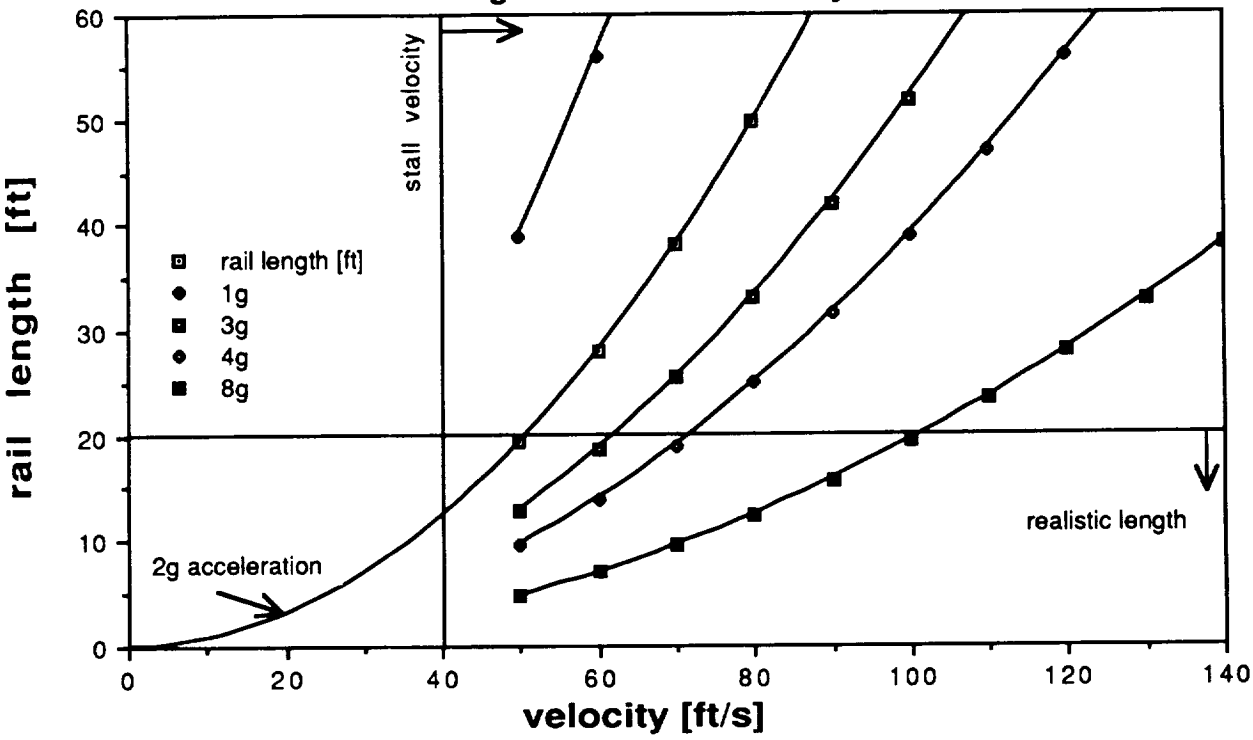

Fig. 9.2: Power Curves

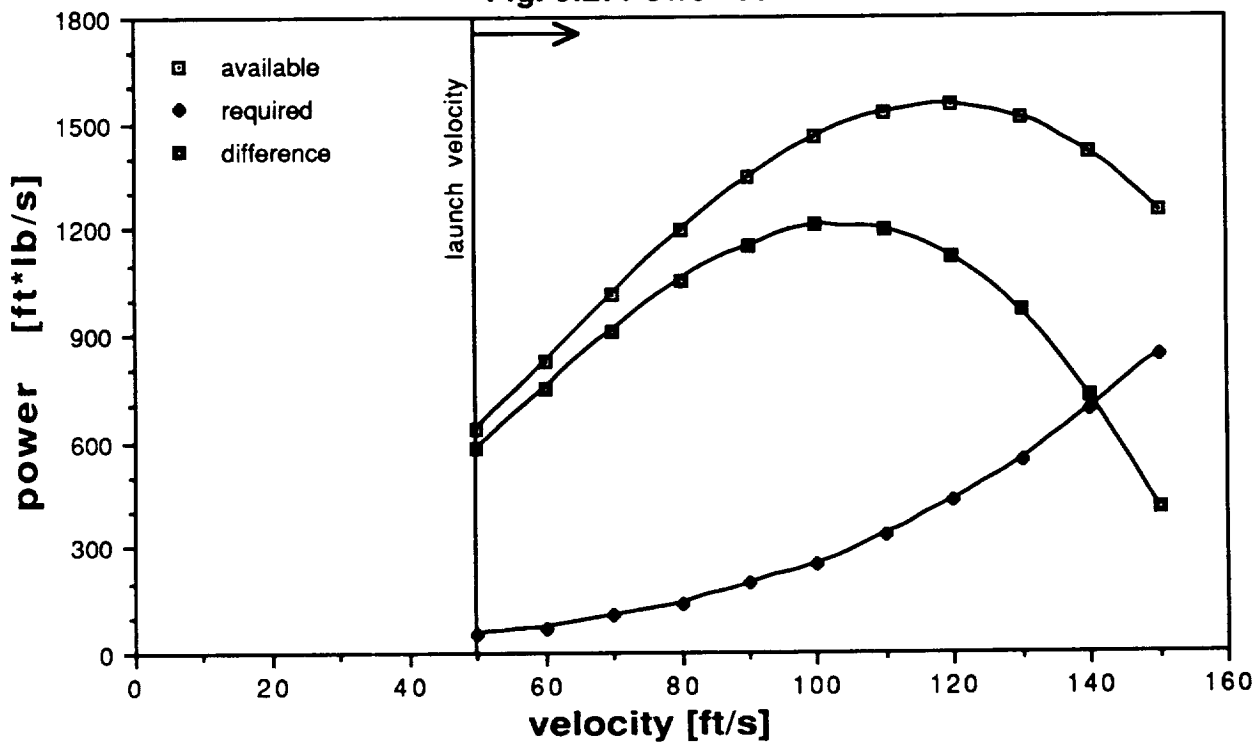

Fig. 9.3: Rate of Climb and Time to Climb

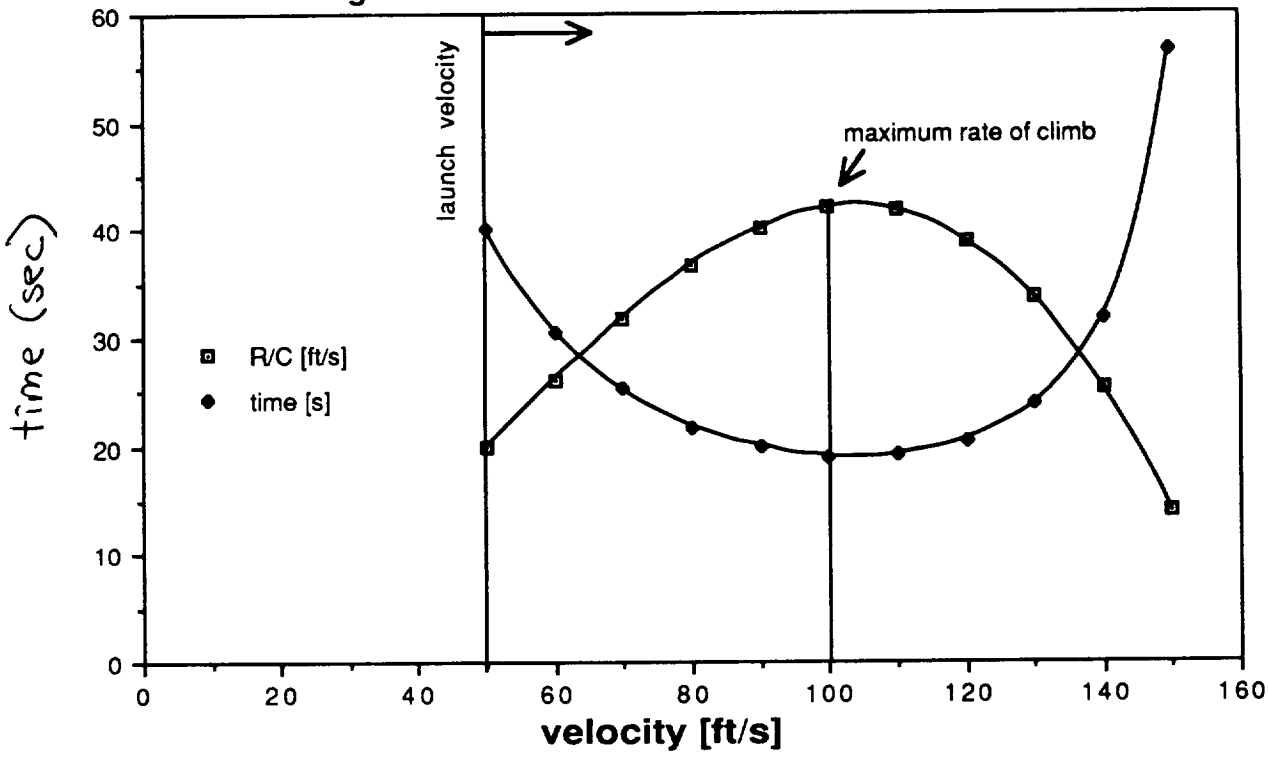

MISSION

Flight Duration = 30 minutes

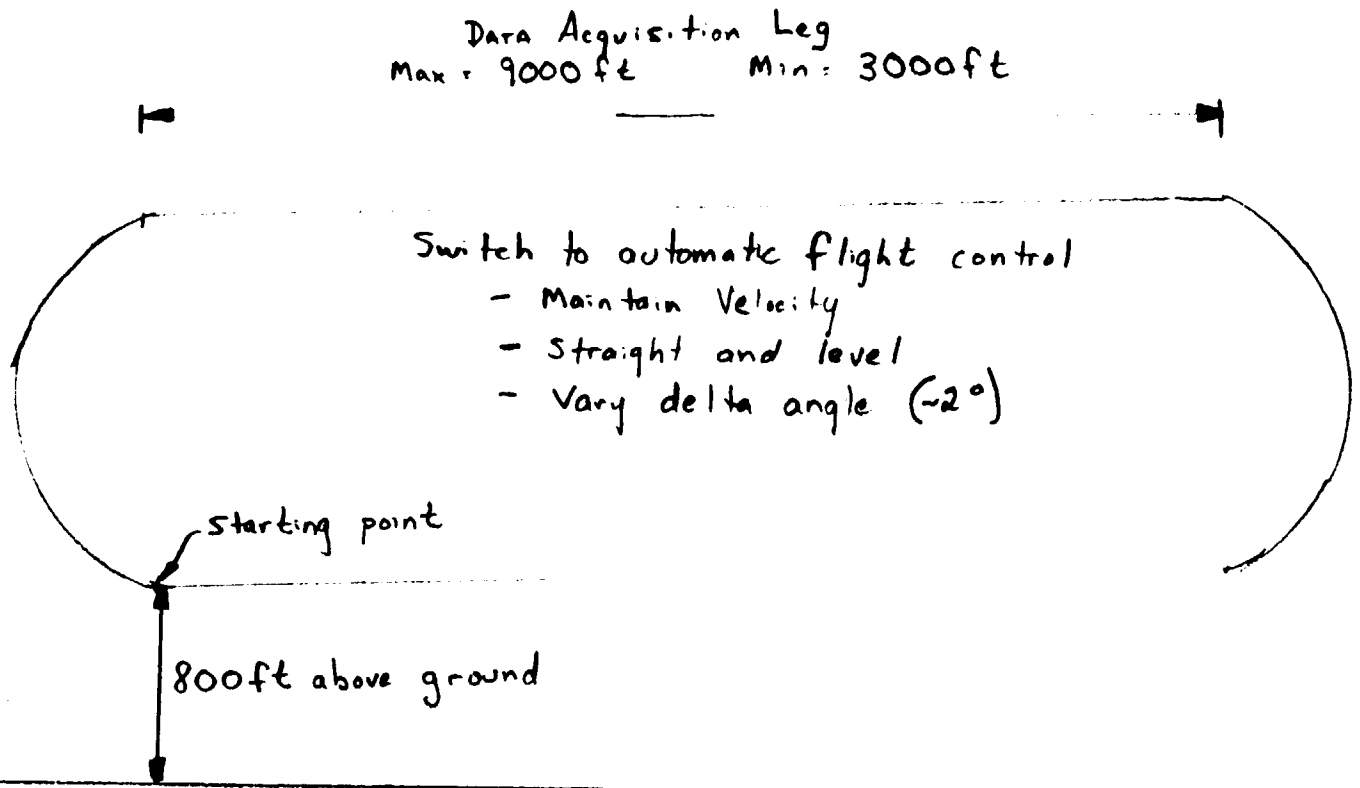

FIGURE 9.4

LAUNCH

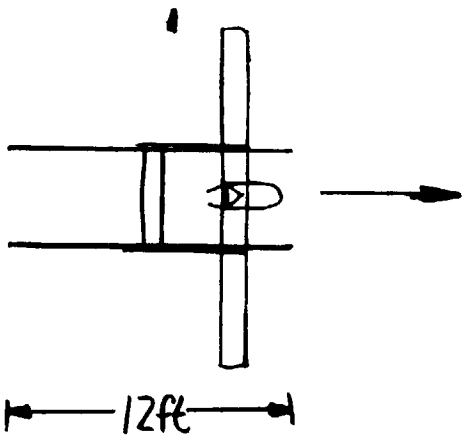

$V_{To} = 50 ft/s$

LANDING

$V_{Land} \cong 55 ft/s$

FLIGHT CONTROL INSTRUMENTATION

Six critical flight indicators were determined to be adequate for control of the RPV, whether by an onboard computer or a ground link system. It was determined that control of the RPV would be accomplished by knowing aircraft angle of attack, roll angle, yaw angle, heading, velocity, and altitude. The integrated use of these indicators would not only allow automatic control of the aircraft but also would ensure aircraft stability during the critical data acquisition phases of the mission profile.

Several different methods for measuring angle of attack were available for the RPV. Some electronic angle measuring devices were cursorily examined for the use of angle of attack measurement, unfortunately, the settling time of these devices was more than a second, rendering their use for accurate flight attitude control insufficient. The use of a yaw tube was a strong possibility because of its high accuracy, but the need for durability, especially during landing and takeoff, precluded its use as it is required to be placed on a sting well away from the fuselage in order to obtain accurate readings.

The device that was chosen for the RPV was a windvane angle of attack sensor with motion being measured by a rotational variable differential transducer (RVDT), which has high accuracy. The RVDT is capable of measuring angle variations of as little as 0.15 degrees (output voltage .1 volt/°). The difficulty with this system is that it must be calibrated when installed to ensure that it reads the angle relative to the correct reference line. Additionally, since it is mounted on the side of the fuselage, a study should be done to determine effects of fuselage interference at various angles of attack.

The measurement of the roll angle will permit the operator (human or computer) to know if the aircraft is banked. Constraining the bank angle for accurate data acquisition would eliminate any instrumentation error due to the aircraft's acceleration. When not in the data acquisition mode this instrument could be used for turn control when coupled with a yaw indicator, the roll angle measured by an inclinometer. Although bulky this

instrument is highly accurate, capable of angle measurements of about 0.03°.

In conjunction with the roll indicator, a yaw indicator would be necessary in order to ensure coordinated turns and stable flight conditions for data acquisition. Since high accuracy of this device is not critical, a ball-type, liquid level such as that in general aviation aircraft could be coupled with an optical or magnetic sensor for the determination of ball location. Such a device could be manufactured in-house at little expense. Weight and volume could then be minimized by constructing the level with light-weight materials rather than purchasing such an off-the-shelf device. The use of a yaw indicator was deemed impractical for the same reasons as it could not be used as an angle of attack indicator.

The use of a heading indicator would be necessary in order for flight path control. Gyros used in private aviation have sufficient accuracy for use in the RPV. A system with more sophisticated gyros slaved to a magnetic heading indicator was deemed unnecessary. The gyro on the RPV would have to be adjusted during the powering of the onboard systems (before flight vehicle launch). Precession of the gyro was not expected to pose a problem as the estimated flight duration is 30 minutes. Precession during this period is predicted to be less than ten degrees as only gentle turning (no radical maneuvers, large contributors to precession) is expected. This deviation from the true heading would not be of concern as the flight vehicle would be within sight at all times. The heading indicator's primary use would be to ensure a constant heading during each data acquisition run.

Velocity of the aircraft would be measured with a simple pitot-static system. This would be located on the tip of one of the booms of the aircraft to ensure that fuselage effects are minimized. Although other systems, including a propeller velocity measurement device, were considered, the accuracy of the pitot system, its small weight, and its size precluded the use of another velocity measurement device. An additional benefit of the pitot-static system is that the static pressure can also be used for altitude control and for data reduction purposes.

By maintaining a set pressure altitude (as opposed to a radar sensing system or laser altitude system) one of the test parameters could be set, thereby maintaining at least one consistent parameter between individual tests. Additionally, space requirements for a pressure transducer would be minimal when compared to the other altitude sensing devices. Although actual altitude changes could be seen by the aircraft during its thirty minute flight because of a change in the ambient pressure, these would be minimal. The static pressure could also be used to measure rate of climb as long as some care is taken when differentiating the output signal from the pressure transducer (i.e. such as averaging old and new readings).

DATA ACQUISITION INSTRUMENTATION

The instrumentation required for accurate data acquisition of the delta wing can be divided into two groups: those that define the flight test conditions and those which read in the necessary data. Although the data acquisition system is designed to read most types of data for maximum test vehicle versatility, the focus of this section will be on the pressure distribution on the delta wing.

Instrumentation which will define the test conditions includes the velocity sensor, static pressure ports, ambient temperature sensor, and delta wing angle of attack sensor. Velocity and static pressure can be obtained from the flight control instrumentation. A thermocouple can be used for a temperature probe in order to obtain the temperature at altitude. This temperature can be quite different from the surface temperature depending on both the altitude of the RPV and the wind velocity and needs to be taken into account during data reduction. Lastly, a linear variable differential transducer (LVDT) will be required to measure the delta wing angle of attack. Used in conjunction with the aircraft angle of attack sensor, the delta wing's location with respect to the freestream can be accurately measured to within 0.2 degrees.

In order to maintain sufficient flexibility for testing, it has been determined that a maximum of 100 pressure taps will be required in order to fully instrument the top of a delta wing (with a worst case root chord of ten inches and a sweep angle of 45°). Keeping in mind the volume and

accuracy constraints, some miniature differential pressure transducers were found with maximum pressure differential readings of ±2 PSID with accuracies of ±0.05% full scale. These are ideal for this application as the pressures on the delta wing top when compared with the static pressure typically do not exceed one PSI. This pressure range allows the greatest accuracy for the tests. The combination of accuracy and small volume requirements at 13.4 pressure ports per cubic inch outweigh the high cost of the system at $100/port. The use of these ports allows a nearly simultaneous reading of all the ports by computer, yielding more precise pressure distributions than obtainable using a scanivalve device, especially when atmospheric disturbances make long term controlled test conditions nearly impossible.

DATA ACQUISITION/CONTROL SYSTEM

Three different systems were available: complete autonomous RPV control and data storage, a ground link capable of full information transfer from the RPV to a ground station, and limited information transfer between the aircraft and the ground station. Safety, weight and price of these three different systems were of primary concern.

The use of a control and data storage system in the RPV is advantageous in that the entire system is self-contained and does not require any ground link telemetry other than the manual control system used for takeoff and landing. This provides a drastic reduction in the cost of the system. However, safety considerations outweigh any monetary benefits gained through the use of this system. Once control is transferred to the test vehicle, the RPV is in the hands of the onboard computer. If this system malfunctions, there is the possibility that control will not be returned to the pilot on the ground. This presents a formidable safety problem, as an out of control 38 pound aircraft flying at 150 miles per hour is capable of doing an incredible amount of damage. Due to this dangerous possibility, this type of system was not considered past the early preliminary design stages.

The second system considered downlinked all the instrument readings to a ground based computer for instantaneous viewing. The flight

control data was then analyzed on the ground, and control information relayed to the aircraft to maintain the flight profile required for the particular test. This setup eliminated the safety problem inherent with the first system by transferring control from the computer to the manual transmitter in the event of a problem. This system would have the additional benefit of utilizing a redundant control system in case of failure of either system.

Once this system passed the safety concerns further research was done on alternate systems that could be used for this purpose. The result of this search was the development of a system that was capable of reading the 100 pressure ports, amplifying the signal for maximum accuracy, performing a 16-bit A/D conversion, converting these reading to pressures, and then sending the data to a transmitter for relay to the ground at 1200 baud. A data relay back to the RPV was capable of controlling the vehicle's flight and test conditions of the delta wing. The system was simple to use, compact, and highly accurate. It had the additional benefit that test data was almost instantaneously available for review. Unfortunately, the package weight of 17 pounds was far in excess of what was desired. This package would be an excellent option if the size of the test bed vehicle was not critical.

However, it was desired to keep the aircraft as light as possible, in order to allow the use of inexpensive construction materials. A hybrid of these two systems, utilizing an onboard computer for signal amplification, A/D conversion and data manipulation and storage with a ground link system for vehicle flight control combined the best features of both systems. This system has a redundant control system for safety and a small ground-linked system without the usual weight penalties associated with total data transfer.

The resulting system would be capable of transmitting 8 channels of data to the ground and back to the RPV. Angle of attack, roll angle, heading, yaw, velocity, and altitude could be transmitted to the ground for flight control with the other two channels being specified by the user before the flight. These signals would be read into a ground based computer which stored the control laws for the flight. The aircraft's

control surfaces could then be controlled by the ground based computer to achieve a desired flight condition. The ground based system would be able to control the elevator, rudder, ailerons, throttle, delta wing stepping motor (for angle of attack control), and a data acquisition trigger.

The onboard computer system would be ten computers hooked together in parallel which would be capable of reading eleven channels of data each with 10 bit A/D conversion possible. Each individual computer is capable of a conversion every 0.01 second, allowing a complete sweep of all pressure ports to be completed within a tenth of a second. The current data acquisition cycle calls for each port to be read 100 times, with the average and standard deviation of these readings then stored for retrieval on the ground. With 28K available for data storage, over one thousand test series could be stored before data would need to be downlinked to another computer.

DATA ACQUISITION DURING THE MISSION

The RPV is to be manually launched and controlled through climb to altitude after which control will be switched over to the ground based computer. Once this has been accomplished the computer will begin a series of "racetrack" ovals, with each circuit lasting two minutes. The straight legs of these ovals will be flown upwind or downwind, so that in the event of a strong headwind a manual correction could be entered into the computer to extend the upwind leg slightly to correct for drift and keep the RPV over the test range. Once the aircraft enters the first turn, it will begin the test cycle by adjusting the delta wing angle of attack and velocity for the first test condition. After completing the turn (within 30 seconds), the aircraft will be allowed fifteen seconds for the control system to assume a steady flight profile.

Upon completion of the waiting period, the data collection phase begins, with the ground based computer triggering the airborne computers to begin data collection. If any set limits on any of the flight control readings exceeds a set limit (such as a gust changing the angle of attack of the aircraft), data acquisition can be interrupted until the disturbance

passes or is corrected for by the ground based control system. Once the ten seconds necessary to read each port a hundred times is completed, the aircraft will begin its 180° turn. During the turn and settling phase, the onboard computer would be manipulating the readings and recording the average and standard deviation. This cycle then repeats up to nineteen more times, the maximum time allowed for data acquisition being twenty minutes. Control will then be returned to the ground pilot for entry into the traffic pattern and landing.

RETRIEVAL / LANDING

The proposed Delta Monster will execute a standard runway landing. The pilot will trigger a servo which will extend the landing gear. The craft will descend on a 10 degree path, which will allow for the clearance of a 50 ft obstacle 300 ft prior to touchdown. This descent could alternately occur in a gentle, banking circle if constrained by objects or visibility. Landing speed will be 45 ft/s, only slightly larger than stall speed of 40 ft/s. Very simple estimates of ground roll distance, assuming constant deceleration, maximum braking, and no skid, yielded a best case distance of 303 ft (Hale, p. 141).

Bibliography

Hale, Francis J., Introduction to Aircraft Performance, Selection, and Design, p. 141, John Wiley & Sons, New York, 1984.

CHAPTER 10

STRUCTURES

STRUCTURAL DESIGN

INTRODUCTION

The specific design challenge at hand poses some very special problems. First, since the aircraft is to be used as a test bed for aerodynamic tests on a delta wing planform model the structural integrity of the aircraft must be such as to allow for odd flying conditions and configurations. Secondly, in order to remain aloft for a reasonable period of time to obtain sufficient data, the aircraft must be especially light. And, thirdly, due to the dependence of the aerodynamic surfaces on their respective positions relative to the freestream, the supporting structure must be sufficiently stiff so as not to alter the performance of this vehicle. Also, all calculations were to be performed within the flight envelope shown in Figure 10.1a.

In response to the previously mentioned challenges and concerns, an aircraft sub-structure has been analyzed. The results of the analyses performed indicated that the structure for the aircraft under consideration will be a relatively lightly loaded, light weight structure.

The main wing of the aircraft (NACA 4412 airfoil, 1 foot chord, 14 foot span) will be constructed from spruce, balsa, and a thin outer coating of shear load carrying Monokote™. These lightweight low strength materials were chosen primarily due to the light loading on the aircraft. Since the main wing was a critical area, a large portion of the analysis was performed on this sub-structure.

Another critical area was the twin tail booms. Since performance of the tail surfaces (both horizontal and vertical) depends on their respective geometric angle of attack which, in turn, hinges on the stiffness of the tail booms, a parametric trade study was performed in this area. The results of this study indicated that these structural elements could most effectively be constructed of hollow circular cross section (outside diameter = 1.25 in., inside diameter = 0.5 in.) spruce at a length of 3.3 ft. For this design, the elements' performance is expected to be quite good.

The other structural elements, including the horizontal tail surface,

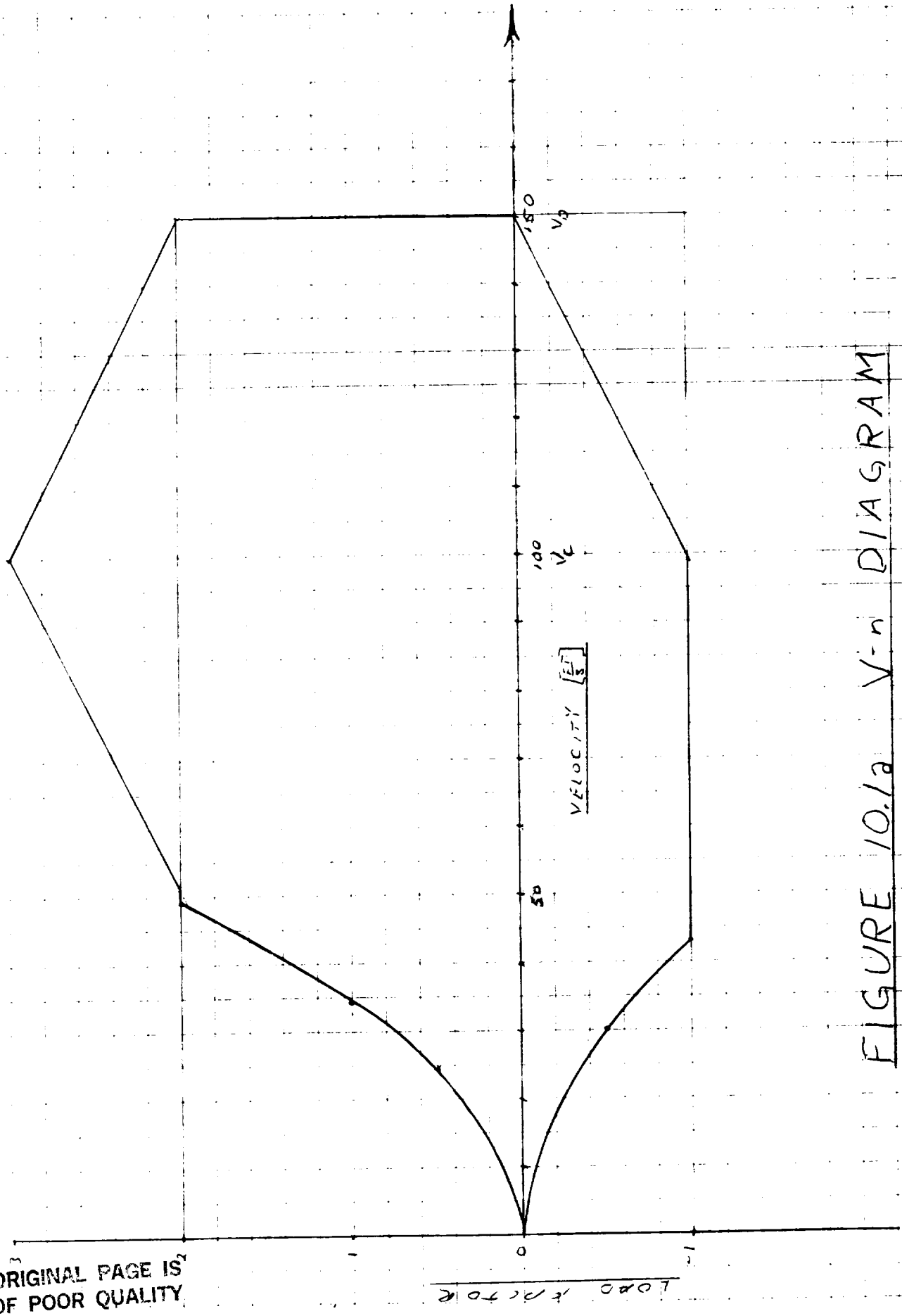

FIGURE 10.1a V-n DIAGRAM

vertical tail surface, and the fuselage were given lesser attention. Feasibility studies were performed on these sub-structures yielding favorable results allowing for construction also using spruce, balsa, and Monokote ™. However, due to the low-weight, high-strength properties of composite materials, further investigation might allow for the use of these advanced materials.

PRIMARY WING

Considerable consideration was given to the structural design of the primary wing. Using the NACA 4412 airfoil shape as the base planform on which to model the wing, several design analysis techniques were used to determine the final design of the wing. Initially a lifting line and structural analysis program was developed (Appendix 10.1) to study the effect of the modeled planform cross sectional area on the highly stressed members at the root of the wing. The information obtained from this program was utilized in obtaining a more precise model of the wing to be incorporated in the final design of the wing using Swiftos™[1], a finite element code. This finite element analysis supported the conclusions taken from Appendix 10.1 and allowed for a more detailed structural analysis of the stressed members. The worst case load configuration was supported by a wing of balsa leading and trailing edge spars, and spruce main spars located at thirty percent of the chord. The final wing design can be seen in Figure 10.1 and structural details in Table 10.1.

Table 10.1
Structural Details of the Main Wing

Structural Component	Material	Detailed Description	Root Stresses for Max Load (psi) s_{xx}	s_{yy}	s_{xy}
Main Spar	Spruce	Tappered (root to tip)	204.81	1160.33	-385.38
Leading edge	Balsa	Shaped to LE	9.81	259.16	21.53
Trailing edge	Balsa	Shaped to TE	-1.05	-229.52	-87.18
Ribs	Balsa	Shaped to Wing	-12.92	-4.00	-10.59
Sheeting	Monokote™				

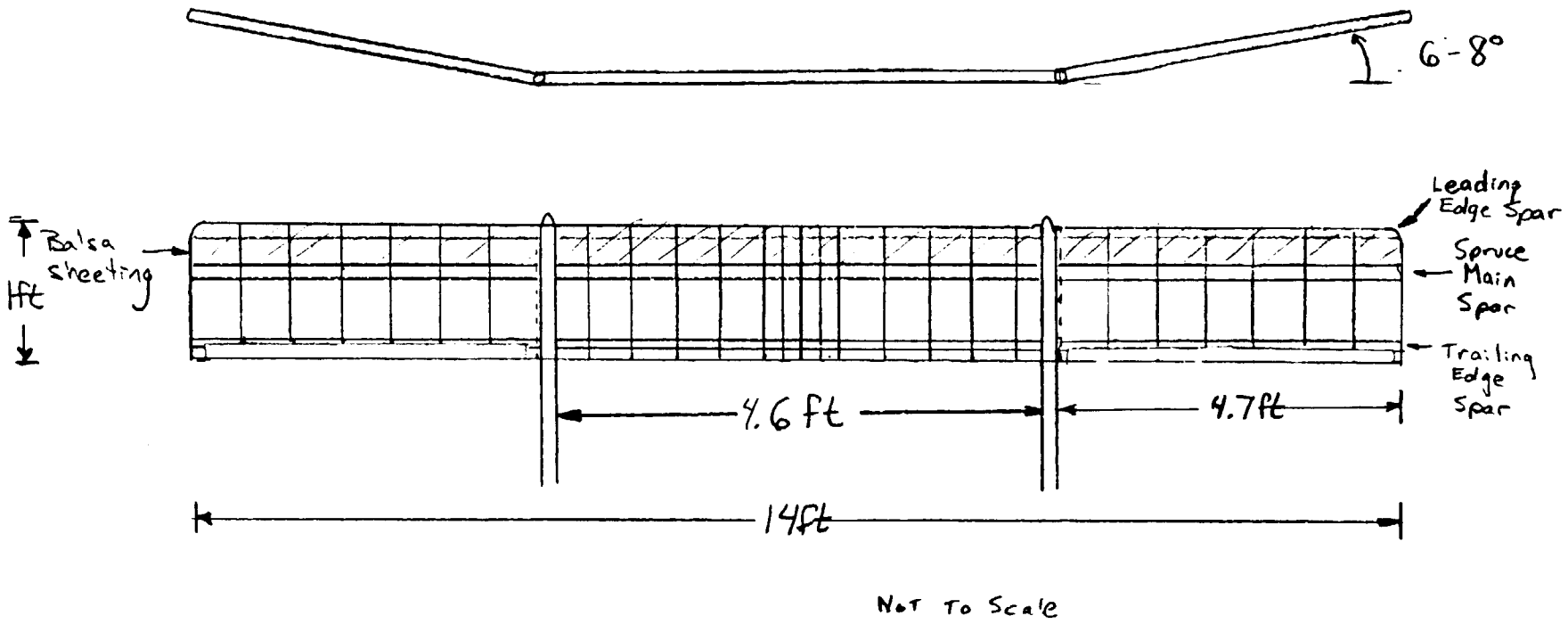

FIGURE 10.1 FINAL WING DESIGN

LIFTING LINE PROGRAM

The use of this program requires a user generated data file including the necessary information concerning the model, spar locations, areas, moduli of elasticity, and densities of the materials. Several models were tested using the aforementioned program. Although very complex models were able to be tested, the results were most reasonable with the four spar area model. Several of the models tested can be seen in Figure 10.2, while the final model used for this program can be seen in Figure 10.3.

This program generates the lift and the drag distribution for the given flight configuration and calculated the stress resultants and stresses in any of the members from the loadings. For the final test case with this program it was determined that the worst case loading would be a two **g** load (60 pounds) occuring for both the maximum velocity of the proposed Delta Monster of 150 ft/s at 2 degrees angle of attack, and at 60 ft/s at an angle of 12 degrees. Several velocities and angles of attack were tested for this model and the results are tabulated in Table 10.2 (see Figures 10A2.1-10A2.14 in Appendix 10.2 for a more complete representation of the results of the loading and stress resultants from the test case).

Table 10.2
Test Case For Appendix 10.1

Velocity (ft/s)	Angle (degrees)	Lift (lbs)	Drag (lbs)	Member Stress (psi) 1	2	3	4
50	2.0	6.72	1.45	14.7	-22.7	10.0	0.25
75	2.0	15.1	3.28	-36.8	74.3	-14.0	-17.8
100	2.0	26.9	5.83	-108.9	210.1	-47.7	-43.1
150	2.0	60.6 (2 g)	13.1	-314.9	598.1	-143.9	-115.4
60	3.0	14.5	2.11	-36.5	70.5	-15.9	-14.6
60	6.0	29.1	2.14	-137.4	248.9	-70.2	-38.7
60	9.0	43.6	2.20	-240.5	428.7	-127.2	-60.9
60	12.0	58.1 (~2 g)	2.29	-345.4	609.0	-186.8	-81.1

The load distribution was determined using Prandtl's lifting line theory[2] (Anderson: Introduction to Flight) and were verified using the Lin-air™

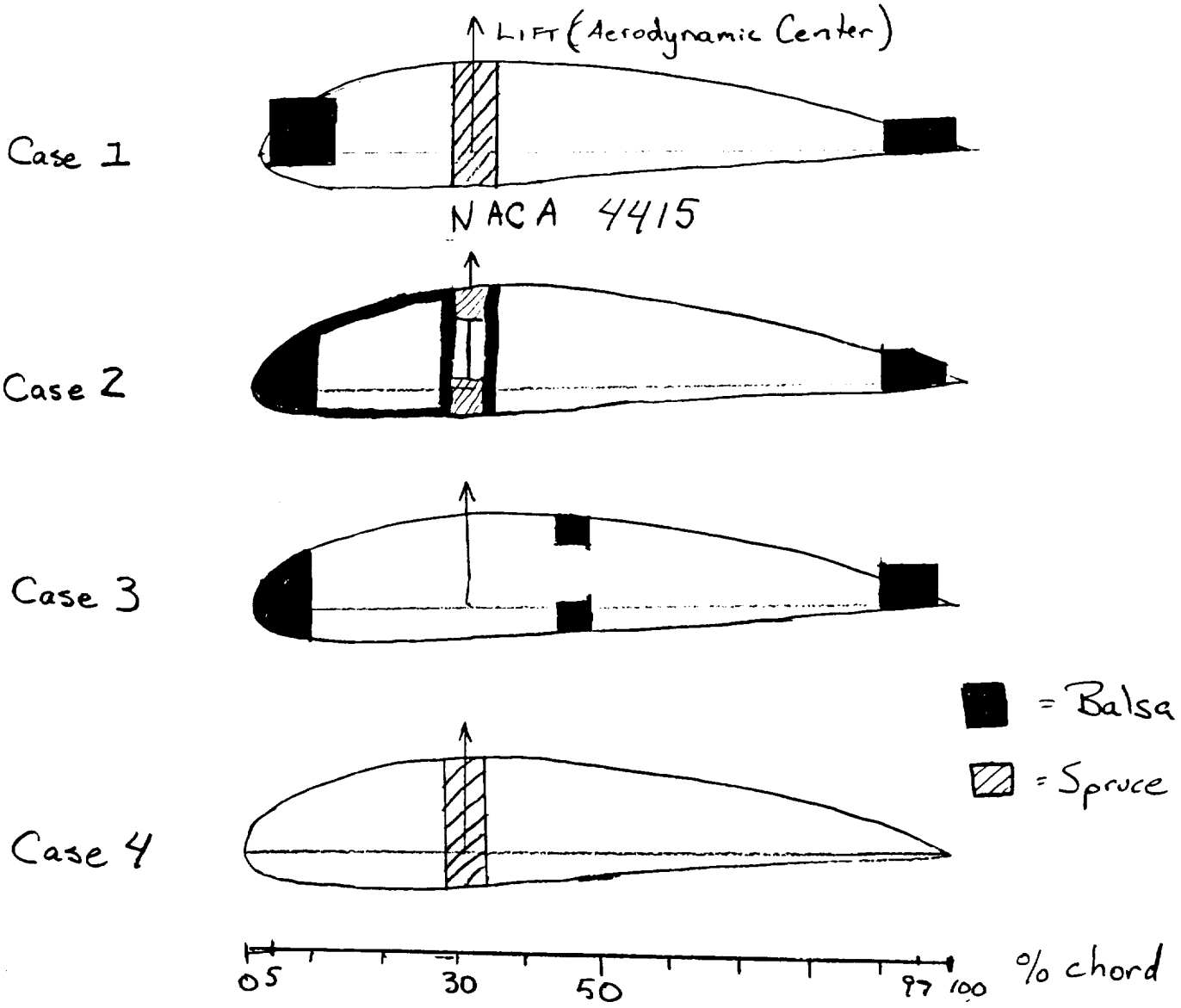

Figure 10.2 Models Tested

	Areas (in^2)
1	.0045
2	.0045
3	.0034
4	.0068

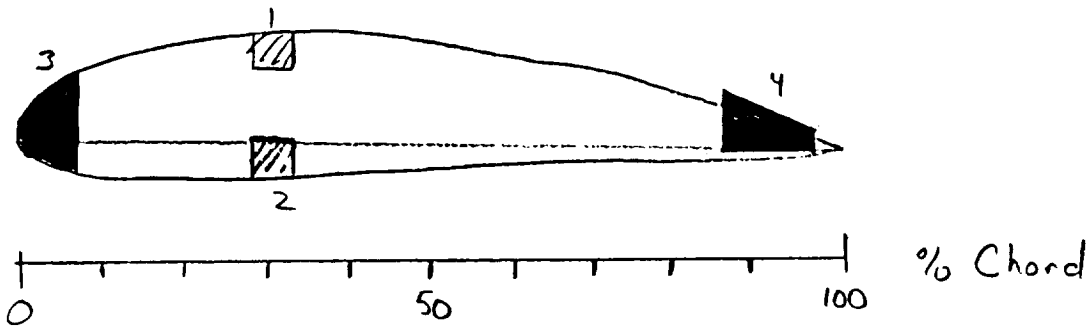

Figure 10.3
Final Test Case

lifting line program. Comparison of the results from the two lifting line programs can be seen in Table 10.3.

The loadings generated by the lifting line section of the program were the result of iterations to determine the stress resultants along this "complex beam". The methodology used for this analysis was a basic stress analysis as developed by Allen and Haisler.[3] This analysis showed high levels of stress in the main spars and lower levels of stress in the leading and trailing edge spars. It was determined from this result that the main spars were to be made of spruce and the leading and trailing edge spars were to be of balsa construction. This drastically reduced the weight of the wing while maintaining appropriate levels of stress in all

Table 10.3
Lifting Line Comparison

	Aero Lab Results	Appendix 10.1 Results
Span	14 ft.	14 ft.
Chord	2.0 ft.	1.0 ft.
Angle	6.0 degrees	6.0 degrees

Wing Position	Cl	Wing Position	Cl
0.0 (root)	.542	0.0	.607
1.095 ft.	.540	1.09 ft.	.604
2.163 ft.	.534	2.16 ft.	.593
3.178 ft.	.522	3.178 ft.	.569
4.115 ft.	.503	4.115 ft.	.518
4.950 ft.	.474	4.950 ft	.450
5.663 ft.	.431	5.663 ft.	.363
6.237 ft.	.369	6.237 ft.	.247
6.657 ft.	.278	6.657 ft.	.205
6.914 ft.	.151	6.914 ft.	.174
7.0 (tip)	0.0	7.0	.090

the members. In each case, member #2, the upper main spar had the highest stress levels. This was consistent with what was expected because this spar is the main load carrying member. A graphical representation of the effect of the loading on the stress level of the second member can be seen in Figure 10.4. The design of the wing then is concerned with maintaining structural integrity of this main spar. The stress levels in the member of the model were presented in Table 10.2. To

insure a reasonable factor of safety in the overall design and modeling technique, a more accurate representation of the wing was utilized though the Swiftos™ finite element code.

Concerns that arose from the program contained in Appendix 10.1 were analyzed and corrected as necessary. Initially, the lifting line subroutine was corrected and verified with the results from the Lin -air™ lifting line program (Table 10.3). Another concern was the modeling of the cross section of the wing. As mentioned earlier, several models were tested to determine the appropriate placement of the spars and material selection. Initially, the spars were made of the same material, spruce, however, this caused several problems in the stress distribution. It was

FIGURE 10.4: STRESS DUE TO BENDING IN MAIN SPAR #2

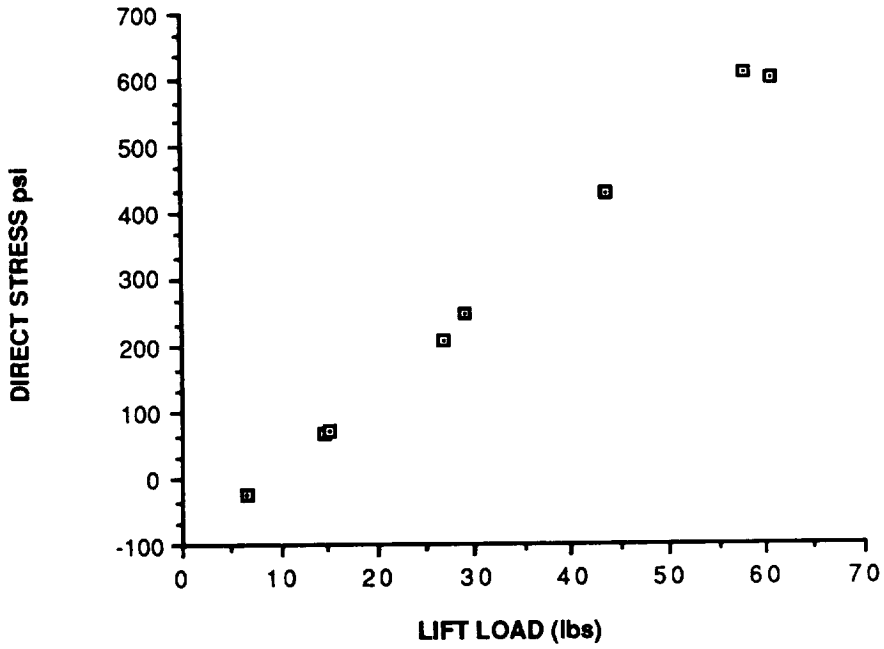

determined that only the main spars needed to be made of spruce while the leading and trailing edge spars were able to be made of balsa, a lighter material, to reduce the weight and stiffness of the beams. This forced the loads to be carried by the two main spruce spars. Optimally the placement of the main spar was determined to be at or near the aerodynamic center, (30% of the chord), so as to carry the majority of the load. The main spar

was placed exactly at the 30% chord location in the final design. This significantly reduced the stresses in the leading and trailing edge spars.

Somewhat high levels of stress were still present in all the members at this point in the design process. The loadings on the wings had been verified but the stress analysis technique had not. Therefore, a simple beam was modeled and tested. See model #4 in Figure 10.2. The results of this simple beam were verified and determined to be correct. The total load on the airplane was then analyzed and found to be high. At a velocity of 150 ft/s and an angle of 10 degrees a total lift of 125 lbs (4 g's) was produced. This loading was more than two times the expected worst load case flight configuration, thus the high stress levels made sense. Therefore, the flight configurations being tested were re-analyzed and more realistic results were obtained. For a flight velocity of 150 ft/s and an angle of attack of 2 degrees, a total lift force of 60.56 lbs was produced, or approximately the maximum load specified by the design. At a velocity of 60 ft/s and an angle of attack of 12 degrees, a lift of 58.14 lbs was produced, again the maximum load. In each of these maximum load cases the stress levels in the members were within a reasonable margin of safety for the design. The various flight velocities and angles of attack and the resulting lift forces and corresponding loads in the members can be seen in Table 10.3. Although acceptable results for the stresses in the members were now seen, these were simply the direct stresses due to bending in the wing. A more accurate model was needed for the final design of the wing and more precise loadings needed to be used. The information obtained from this four member model was carried over to the model created for the Swiftos™ finite element analysis (see Figure 10.5).

SWIFTOS™ ANALYSIS

Having done the preliminary analysis with the internally developed program and achieved some high stress values, a further refinement to the design process was considered to be in order. Therefore outside help was solicited in the form of an externally developed finite element code by Richard Swift, a Master's Degree candidate at the University of Notre Dame.

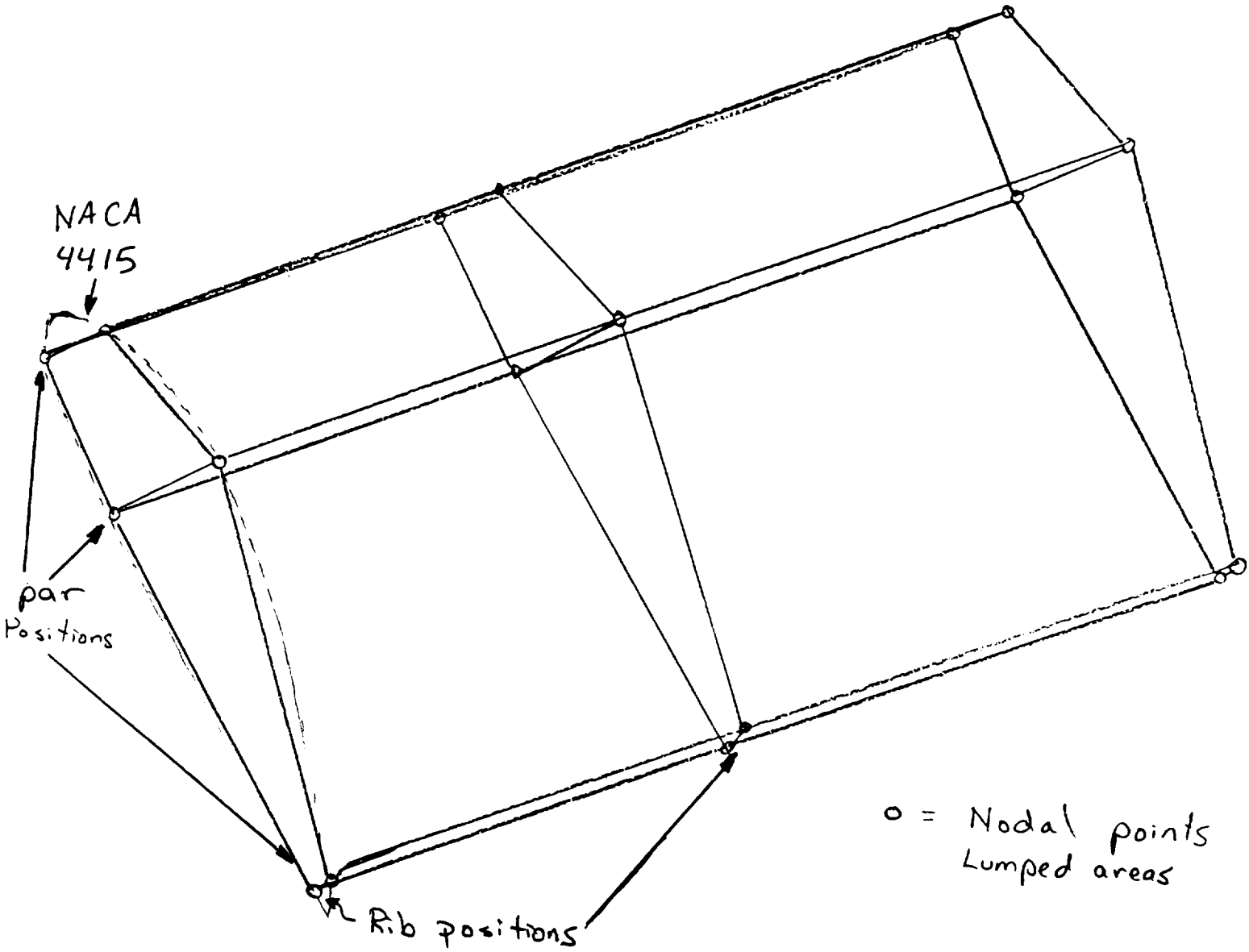

Figure 10.5 Model For Swift05

The use of this code to analyze the rough model of the wing sub-structure necessitated a drastic refinement in the model. Considerable time was spent in this endeavor and a much better approximation to the actual sub-structure was developed. However, the creation of an accurate model that physically resembled the actual sub-structure was difficult at best.

Due to the low aerodynamic loading on the aircraft and a maximum two "g" loading imposed by the design team, it was suggested that the conventional materials of balsa and spruce be used in the model for the sub-structure (ribs and spars) while a thin, plastic covering (Monokote™) was suggested for the outer covering over the sub-structure.

The basic model was very conventional. There were three spars, a leading spar made of balsa, a main spar made of spruce, and a trailing edge spar made of balsa. The model also contained 22 ribs made of balsa placed along the span of the wing. The model very accurately represented the real concept in that the wing span, wing planform, and rib placement remained intact in going from the actual concept to the model. This rib placement was conventional in that most of the ribs were evenly spaced along the span. However, to account for the interface between the tail boom and the wing, a rib was placed at that location and given a thickness of three (3) times the other ribs. Also, extra ribs were added inboard, under the fuselage. Another attempt to improve the accuracy of the model involved the addition of point loads on the wing, especially at the points where the tail booms were attached.

The major problem encountered, however, involved the modelling of the Monokote™ skin. Because no material properties or allowable stresses could be found for this material, the model was forced to deviate from the actual concept. Three ways to model this thin coating of material were attempted.

First, because it was suggested that the model should reflect the design of the sub-structure, if the sub-structure was designed without the skin it would be all that much stronger with the addition of a skin. Since the computer code required the input of skin elements, it was decided to approximate the desired condition (no skin) with a rubber-type substance. This "phantom material" was given a very low modulus of elasticity (1000 psi), a slightly high Poisson's ratio (0.5), and no mass

density. Unfortunately, this model resulted in a structure with massive twist along the span and a twist of 7.7 deg. at the tip (relative to the root). Therefore, it was determined that the model needed to be refined further.

The second attempt to accurately model the Monokote™ skin covering resulted from the suggestion that the material properties should be representative of some sort of a plastic, however, this material should carry no load in compression (thin skin). Therefore, a resin was chosen to model the material properties and the skin elements were not allowed to carry any compressive loads. This model improved the twisting problem (6.18 deg. at the tip). However, the computer code depended on the calculation of a Von Mises ratio to determine the degree of stress in each element. This was unable to be accomplished for the skin elements because of the zero allowable compressive stress input to the code. Again, it was determined that a refinement in the model would produce better results.

The final model was then developed representing the 0.004 in. Monokote™ skin as 1/16 in. thick balsa sheeting. The reasoning behind this choice was that balsa is one of the lowest strength materials readily available (especially in compression) and the difference in thickness would nearly offset the density difference to make the weight of the wing approximately the same. This model produced very good results (twist at wing tip of 2.7 deg. relative to the root) and it was decided to use this model for an optimization.

When the Swiftos™ finite element code ran an optimization, the user specified the elements to be optimized and these elements were reduced in size (cross sectional area) until they were fully stressed and the total half-span wing weight was calculated upon each iteration. One such optimization was run with the previously discussed model.

Table 10.4 shows the results of the weight reduction process by the computer code with each iteration. According to the value given for the final iteration (iteration #9) this final wing would have a weight of 2.57 lbs. A more sound weight estimate was obtained by multiplying this weight given by the computer code by a factor of safety/uncertainty of two (2). Considering the fact that the overall weight of the entire aircraft is 28 lbs., this required that the wing be approximately 18.4% of the total

aircraft weight. For this type of aircraft, where a large portion of the total aircraft weight is comprised of the instrumentation for data acquisition and transmission, this value seemed very reasonable.

TABLE 10.4 : WEIGHT HISTORY

ITERATION	WEIGHT
0	2.786
1	1.159
2	1.192
3	1.242
4	1.272
5	1.281
6	1.283
7	1.283
8	1.284
9	1.284

The final results of the optimization yielded minimum cross sectional areas for the specified optimization elements. These elements consisted of all three spars and their respective spar caps. The ribs were left at a minimum gage (1/8 in. thick) due to their low stressed state. The main spar was of primary concern. The finite element code specified a minimum of a 1/2 in. thickness at the root and tapered it to a 1/8 in. thickness at the tip. The optimization did not effect the 1/4 in. tailing edge spar and only suggested slightly increasing the area of the leading edge spar at the first two stations near the root.

Although the optimization gives the designer the cross sectional areas to meet the fully stressed condition, the resulting structure could possibly fail at the design point. Also, for this case a larger vertical deflection of the wing tip was experienced (9.4 in. at 7 ft from the root with a twist of 6.47 deg.). Therefore, all numbers obtained from the computer code should be multiplied by a factor of safety/uncertainty of 1.25-2.0 and the next largest commercially available size elements should be chosen (for economic reasons). This should yield a safe design.

TWIN TAIL BOOMS

Since the aerodynamic performance of the tail surfaces was determined to be strongly dependent upon their respective geometric angles of attack, a structure designed to support these surfaces was determined to be of extreme importance. Therefore, a detailed design study was performed on these structural elements.

The tail booms were considered to be identical. Therefore, on the basis of symmetry, it was determined that only one boom needed to be analyzed. Acting under this premise, the tail loadings were considered to act equally on each boom.

Four primary "figures of merit" were established in order to evaluate the possible combinations of variable parameters. The first goal was to keep drag to a minimum. Secondly, the weight needed to also be kept to a minimum. Thirdly, the bending of the booms in the vertical direction had to be kept to a minimum. And, finally, the twist of the aft end of the boom relative to the forward end also needed to be minimized.

The model developed for the analysis of these structures was a simple one. The booms were considered to be beams cantilevered at the wing and free to move at the aft end. The effect of the weight of the beam was considered to be negligible compared to the effect of the loadings due to the tail surfaces. Since both the horizontal and the vertical tail surfaces were flat plates (or symmetric airfoils) and the weight of the entire aircraft was only 28 lbs., for normal flight it was determined that the horizontal tail should never produce a load greater than 10 lbs. and the vertical tails should never produce loads greater than 5 lbs. each. These loads translate to a vertical load (up or down) of 5 lbs. and a torsional load about the longitudinal axis of the beam of 25 in-lbs. (in either direction) (see Figure 10.6).

Due to some realistic concerns, the range of acceptable changeable parameters was defined. These parameters include 1) cross sectional shape, 2) outside diameter, 3) length, and 4) material selection. First, since texts on solid mechanics and structural behavior indicated that circular cross sectional elements behave much better than other cross sections under conditions of torsion, and because aerodynamic drag due to smooth contours is less than that due to abrupt ones, a circular cross

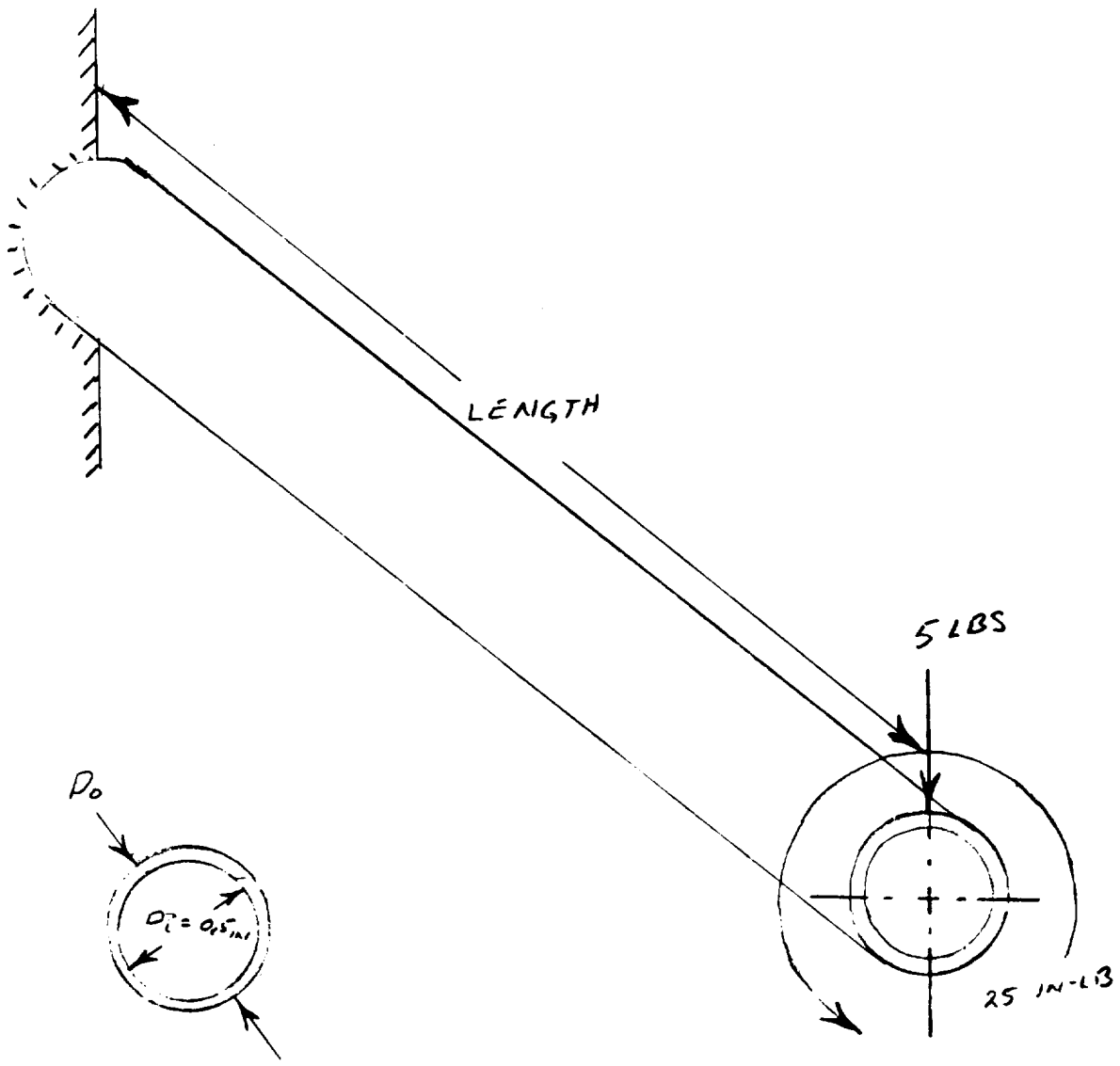

FIGURE 10.6 TAIL BOOM MODEL

section was chosen for all analyses. Second, due to drag and weight conditions, the range of acceptable outside diameters was set at 0.6-1.5 in. Third, because control rods for the rear tail control surfaces (elevator and rudders) needed to run from the servos in the wing to the tail inside of the booms, a hole 0.5 in. in diameter was needed along the entire length of the boom. Fourth, because a sufficient moment arm was needed for effective performance of the tail surfaces, the boom length needed to be between 2.5 and 3.5 feet. Finally, only certain materials were considered as candidates. In order to span a fairly wide range of material strengths and weights, the prospective materials were chosen to be balsa, spruce, aluminum, titanium, and a carbon steel.

Having constrained the variable parameters, four sensitivity studies were performed. The first study examined the effects of outside diameter and length on drag. The next study determined the effect of outside diameter, length and material selection on weight. The following study examined the effect of outside diameter, length, and material selection on beam bending, while the final study examined the effect of these same parameters on twist angle.

The first study performed was concerned with the drag produced by the tail booms. For drag calculations, due to the orientation of the boom along the direction of flow, skin friction drag was considered to be much more significant than any pressure drag that might result. Therefore, the flow was considered to be turbulent along the entire surface of the boom and the circular element was considered as an equivalent flat plate. The two variable parameters effecting the drag were the outside diameter and length of the boom. Variation of these two parameters produced some interesting results.

As the length of the boom was varied across its entire range of acceptable values while the diameter was held fixed at 1.0 in., the plot in Figure 10.7 was generated. This curve shows a linear relationship between the drag on the boom and the length of the boom.

However, looking at Figure 10.8 which is a plot of the effect of both length and diameter on the drag, it can easily seen that the effect of changes in diameter have a much more pronounced effect on drag produced by the boom than length. The increase in diameter definitely increases the drag, but also seems to increase the slope of the drag vs. length curve.

Fig. 10.7 EFFECT OF LENGTH ON DRAG

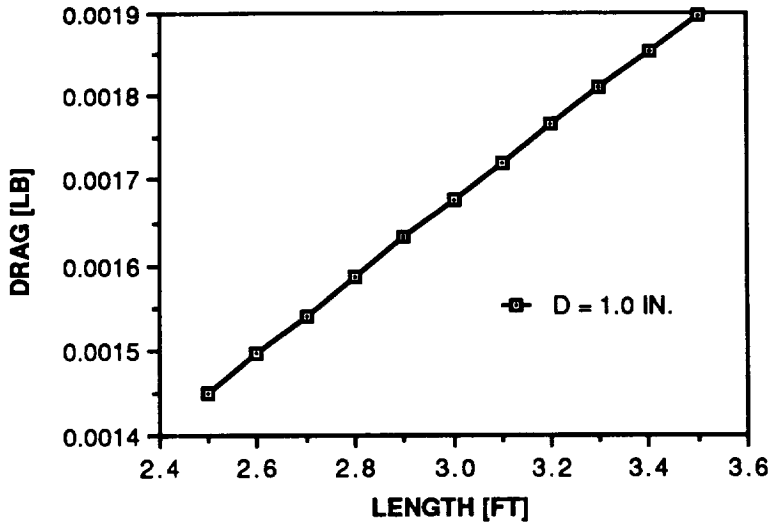

Fig. 10.8 EFFECT OF LENGTH AND DIAMETER ON DRAG

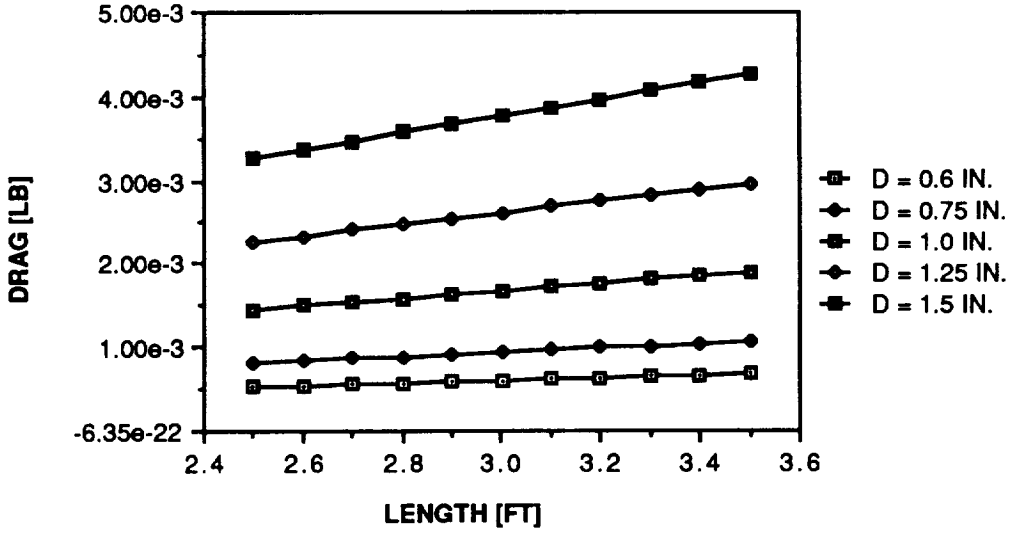

Nevertheless, all cases shown in Figure 10.8 show that the drag on the boom is extremely small and it would seem that any choice of outside diameter and length would be acceptable from a drag standpoint.

The next study that was performed concerned the sensitivity of the weight of the boom to variations in length, outside diameter, and material. Since weight is dependent upon material density and volume, all three parameters have some effect on the overall weight.

As can be seen in the plot of the effect of length and diameter on weight (Figure 10.9), the weight exhibits a dependence very similar to that of drag on these two parameters. The weight vs. length curve is linear (as expected) and variation in the outside diameter has a more pronounced effect on the weight than do variations in length.

In order to evaluate the influence of material selection on the weight, the five prospective materials were used to calculate weight vs. length curves for a constant outside diameter of 1.25 in. As can be seen in the plot in Figure 10.10, material selection plays a very definite roll in weight calculations. For example, steel with a corresponding boom weight of 8-12 lbs. (which is extremely unreasonable for this design) is much heavier than balsa with a corresponding boom weight of 0.18 - 0.25 lbs.

Having determined the sensitivity of the drag and weight of the boom to variations in the length, outside diameter and material selection, the next concern rested with acceptable levels of bending at the aft tip where the tail surfaces were to be connected. Therefore, the effect of length, outside diameter, and material selection on tip bending deflection comprised the next sensitivity study.

As can be seen in the plot of the effect of length and diameter on the bending deflection (Figure 10.11), variations in length affect the tip deflection more at smaller diameters. As might be noticed, the curve for an outside diameter of 0.6 in. does not appear on this plot. This is because the tip deflections for this case were totally unreasonable ranging from 15-43 in. This eliminated an outside diameter of 0.6 in. from further consideration.

Figure 10.12 shows a plot of the effect of the material selection on tip deflection with a constant outside diameter of 1.25 in. As can be seen from this plot, the metals behave very similarly while spruce performs slightly worse. However, the worst tip deflection for spruce was 1.22 in.

Figure 10.9
EFFECT OF LENGTH AND DIAMETER ON WEIGHT (SPRUCE)

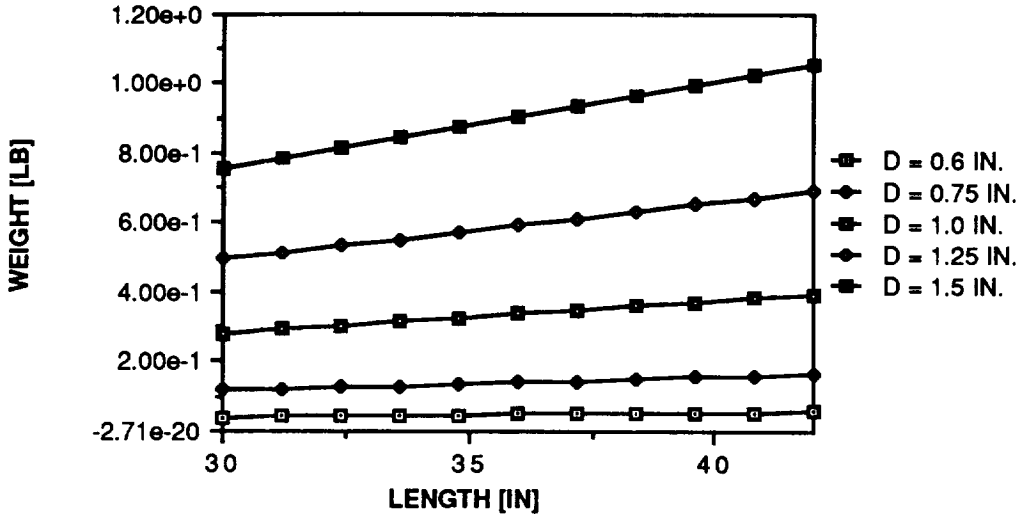

Figure 10.10
MATERIAL WEIGHT COMPARISON (D=1.25 IN.)

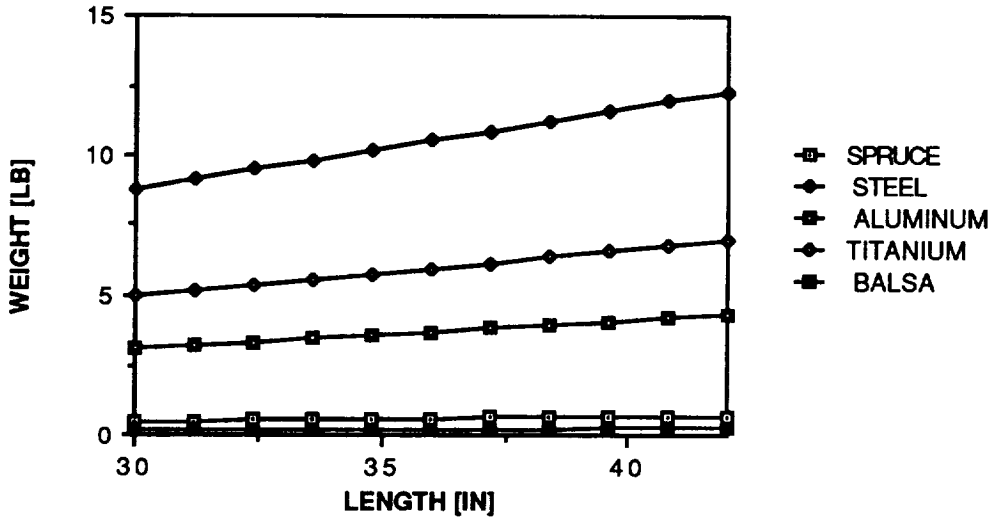

Figure 10.11
EFFECT OF LENGTH AND DIAMETER ON BENDING (SPRUCE)

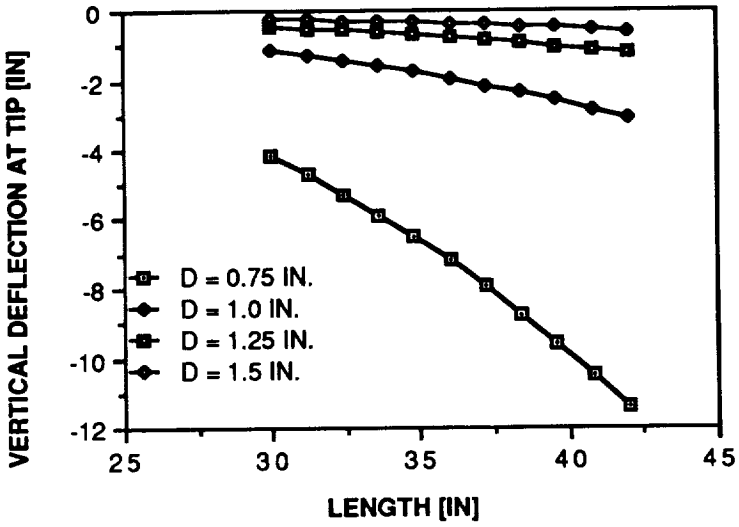

Figure 10.12
EFFECT OF MATERIAL ON BENDING (D=1.25 IN.)

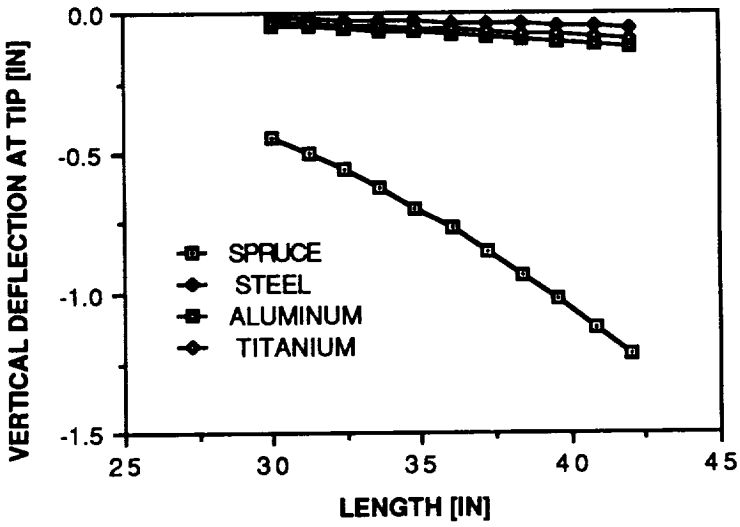

at a length of 36 in. This resulted in a change in the geometric angle of attack of the horizontal tail surface of only 1.94 deg. After consultation with the Stability and Control expert, it was determined that this was very reasonable. Note also that no curve appears in Figure 10.12 for balsa. This is because unreasonable deflections of 9-24 in. Therefore, balsa has been eliminated from further consideration.

The final sensitivity study performed in order to evaluate the effects of the variable parameters on the design involved a study of the effects of length, outside diameter, and material selection on the twist of the boom. Again, as can be seen in Figure 10.13, the relationship between the figure of merit and length is a linear function. Also, the effect of outside diameter is very small for diameters greater than 1.0 in. Diameters of 1.0, 1.25, and 1.5 all produce angles of twist of less than approximately one degree (1 deg). This would seem to be exceptional performance.

Material selection also plays an interesting role in the twist study. As can be seen in Figure 10.14, the metals (steel and aluminum) exhibit virtually no twist while spruce exhibits very little twist (0.3-0.4 deg) for a constant outside diameter of 1.25 in. Again, after consultation with the Stability and Control expert, these values were considered to be very good. Note also that no curve for titanium appears in Figure 10.14. This was for two reasons. First, extremely limited values for shear loads tolerances were available (indicating that this material was not especially good for this application). And, secondly, since titanium is usually used in high temperature applications (and is very expensive), it would seem to be inappropriate for this application.

In conclusion, after again consulting with the Stability and Control expert, a boom length to provide an optimum moment arm for the tail surfaces results in a choice of 3.3 ft. for the boom length. Also from the weight, bending and twist analyses, a diameter of 1.25 in. and a material composition of spruce were determined to produce the best all around element characteristics. Therefore, after evaluating the sensitivity of the drag, weight, bending tip deflection and twist of the circular boom, to variations in boom length, outside diameter, and material composition, a final "best case" has been determined.

Figure 10.13
EFFECT OF LENGTH AND DIAMETER ON TWIST (SPRUCE)

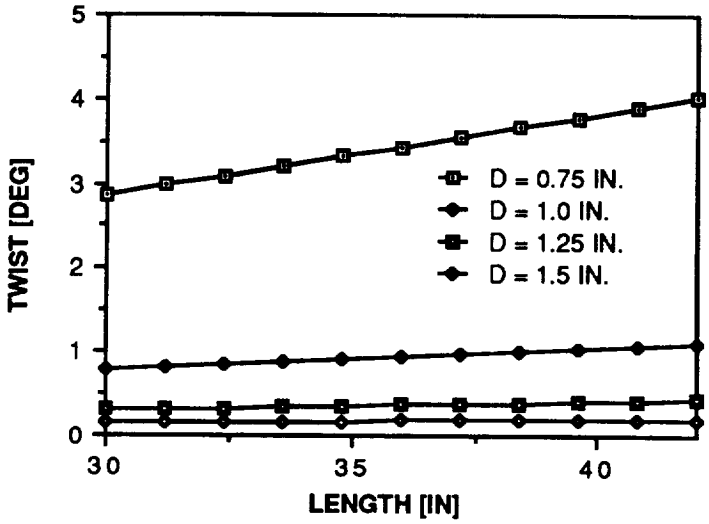

Figure 10.14
EFFECT OF MATERIAL ON TWIST (D=1.25 IN.)

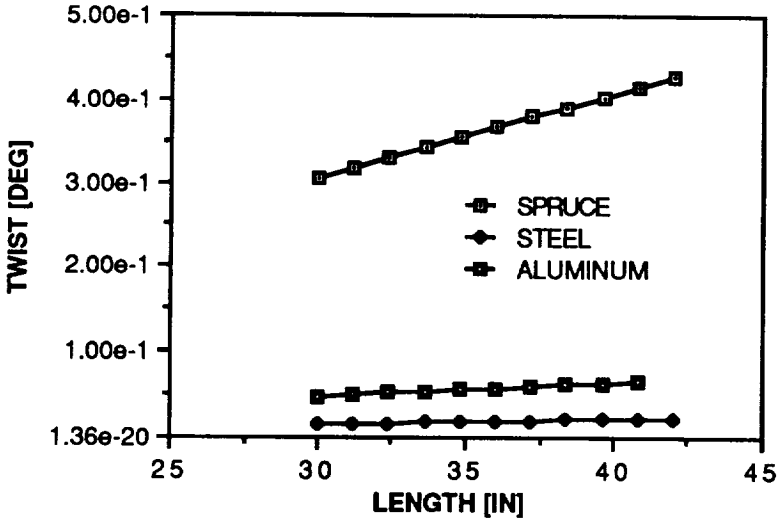

FUSELAGE

Due to the specific volume carrying requirements (data acquisition and transmission equipment) of a flying test bed aircraft, the proposed fuselage is quite large. However, because of the especially low loading of this aircraft, lightweight materials are more than sufficient to safely support the requirements.

Since this sub-structure was considered to be less critical than other structural elements, a very limited feasibility study was performed. For the feasibility study, a simplified model was developed. The fuselage was modeled as a thin-shelled (monocoque) structure (10 in. in diameter and 36 in. in length) augmented with six longitudinally positioned stringers as shown in Figure 10.15. The "shell" was made of 1/8 in. thick balsa and each stringer was made of 1/4 in. X 1/4 in. spruce.

Since the only other structural element connected to the fuselage was the main wing, this element was considered to be the major source of loading. At the interface between these two elements, a load of 28 lbs. was assumed to be transferred from the wing to the fuselage. This load corresponds to the weight of the aircraft or the lift produced during cruise. The only other loading considered was the weight of the aircraft which was assumed to be a uniform distributed load applied along the length of the fuselage.

For the purposes of loading calculations, the fuselage structure was considered to be a simple beam. Since the loading considered primarily gave rise to a pitching moment, the maximum value of this quantity was found to occur at the point of attachment of the wing. For a wing attached at a point 18 in. from the forward-most edge of the structure, a maximum pitching moment of 126 in-lbs. was calculated. This loading gave rise to a maximum direct stress due to bending of only 4.41 psi. which corresponds to an extremely high factor of safety/uncertainty.

Since the analysis performed was very simple, the extremely small final maximum load was considered to be somewhat reasonable. Although such limited analysis was performed on this structural element, the results do indicate that the fuselage will be lightly loaded and thus will be able to be constructed out of lightweight materials resulting in good

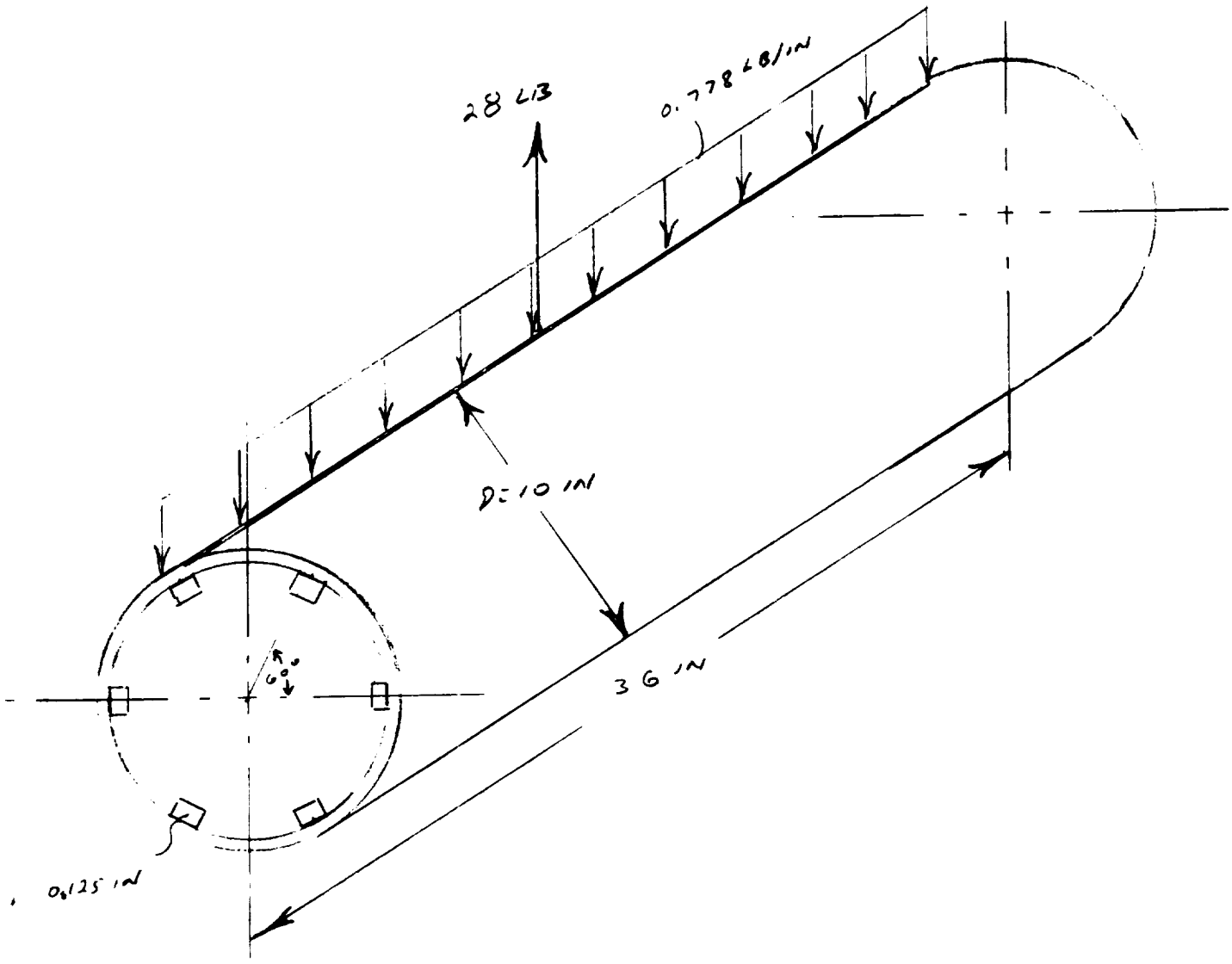

FIGURE 10.15 FUSELAGE MODEL

overall performance of the system. If anything, the model analyzed might be considered over designed. With the addition of two or three bulkheads constructed out of lightweight plywood for separating internal components and additional stiffness, it would seem that a safe and lightweight fuselage could be designed.

HORIZONTAL STABILIZER

The horizontal tail, a NACA 0012, was modeled as a simple beam supported at both ends. The lifting force from the tail would be directly supported by the spars and therefore a simple beam was used. By placing the load at the aerodynamic center of the symmetric airfoil, 75% of the load would be carried by the leading edge spar and 25% by the trailing edge spar. The cross brace members serve the purpose of supporting the drag force, but add little strength to the overall stiffness of the "beam" (See Figure 10.16). It was determined from earlier analysis on the primary wing that the loads produced could be supported by spruce and balsa spars. The worst case loading was determined with 30 degrees of elevator deflection and a Cl of 0.5. The total lift produced was 15 lbs. incorporating a factor of safety of 1.25. The maximum point of deflection for a beam supported at both ends is at the center of the beam (see Figure 10.17).

An accurate model of the horizontal tail was achieved by increasing the area of the leading edge to take into account that it has to support the main load. It was also determined that it would be made of a spruce member shaped to the leading edge of the NACA 0012. The trailing edge was to be made of balsa to reduce the weight of the tail yet carry the load. For the preliminary analysis this proved to be more than adequate. The spruce leading edge saw a maximum stress of 472 psi. and a deflection of 0.308 in. The maximum deflection occurred at the semi-span of the horizontal tail because the tail acts similarly to a beam supported at both ends. The trailing edge (balsa) stress was seen to be 355 psi. at the maximum loading. The shear stresses seen by these members was calculated and determined to be supportable (120 psi. and 90 psi. acting on the leading and trailing edges respectively) (See Table 10.5).

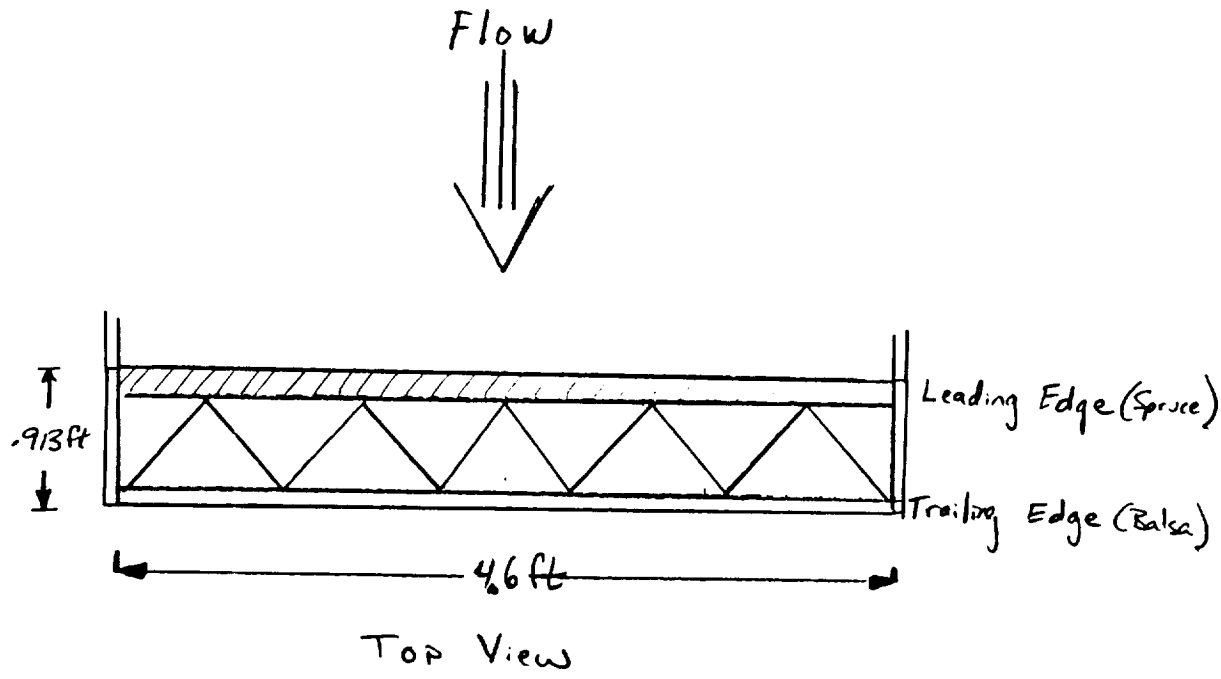

Figure 10.16 HORIZONTAL STABILIZER

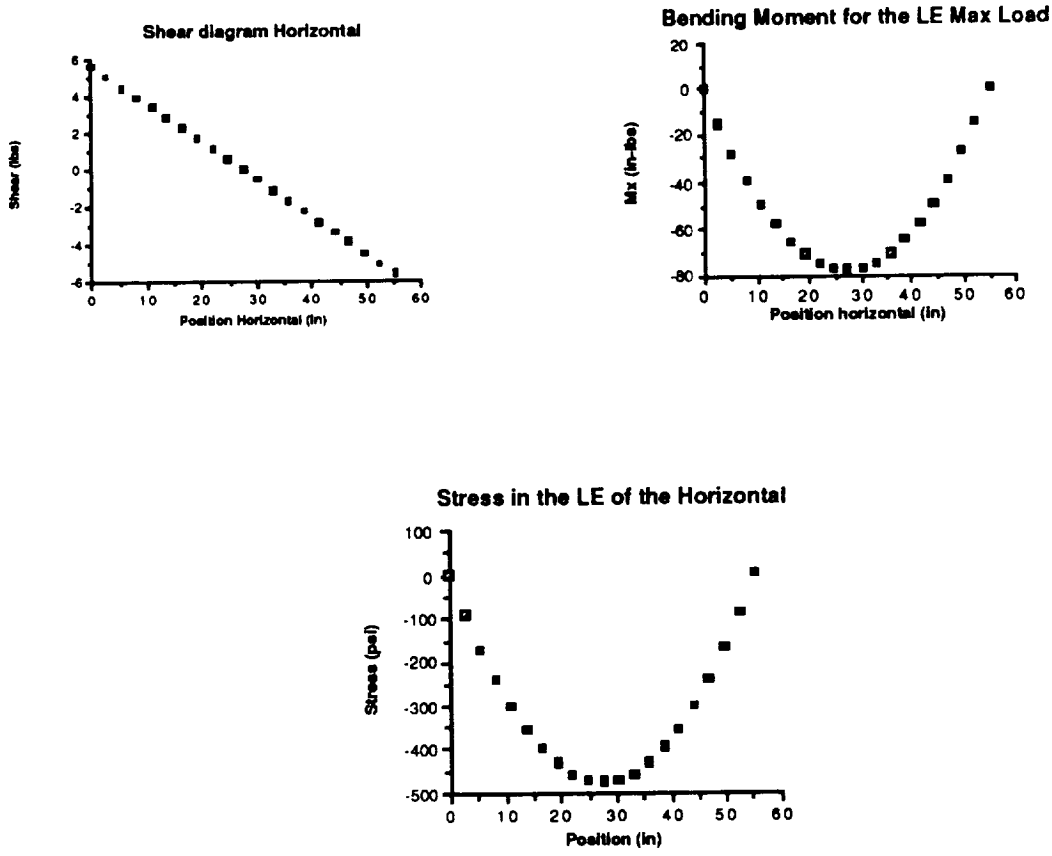

Figure 10.17
Horizontal Stabilizer Loading

The cross supports in the tail are to be made of balsa to reduce the weight. Because very small forces need to be supported by these members, they help to maintain the shape of the airfoil. The overall weight of the horizontal stabilizer was calculated to be 1.50 lbs.

Table 10.5

Stress Levels Present in the Horizontal Tail

		Area(in^2)	Stress(psi)	Max Deflection(in)
Balsa	LE	1.313	472.7	6.17
	TE	0.875	355.0	2.05
Spruce	LE	1.313	472.7	.308
	TE	0.875	355.0	.103
Birch	LE	1.313	472.7	.199
	TE	0.875	355.0	.066

VERTICAL STABILIZER

In consideration of the twin vertical tail configuration, the tails needed to be identical and perfectly aligned. Because there were two vertical tail surfaces, each tail needed to carry only half of the load necessary for directional stability. In the worst case a maximum loading of fourteen pounds would be needed to maintain stability. Each tail would then see a maximum force of seven pounds. This loading is based on a rudder deflection of 25 degrees and a factor of safety of 1.4. The small cross sectional area (maximum thickness) of the NACA 0012 airfoil to be used on the proposed Delta Monster was the main constraint on the area of the spars. The structural analysis assumed a simple beam supported at the base of the vertical stabilizer. The load was assumed to be distributed as follows: 75% of the load acting on the leading edge spar and the remaining load (25%) on the trailing edge spar. The design of the leading edge spar incorporated the fact that it needed to support the majority of the load, therefore a spruce leading edge and a balsa trailing edge were selected (See Figure 10.18). The maximum design loads and the resulting shear and bending moment diagrams can be seen in Figure 10.19.

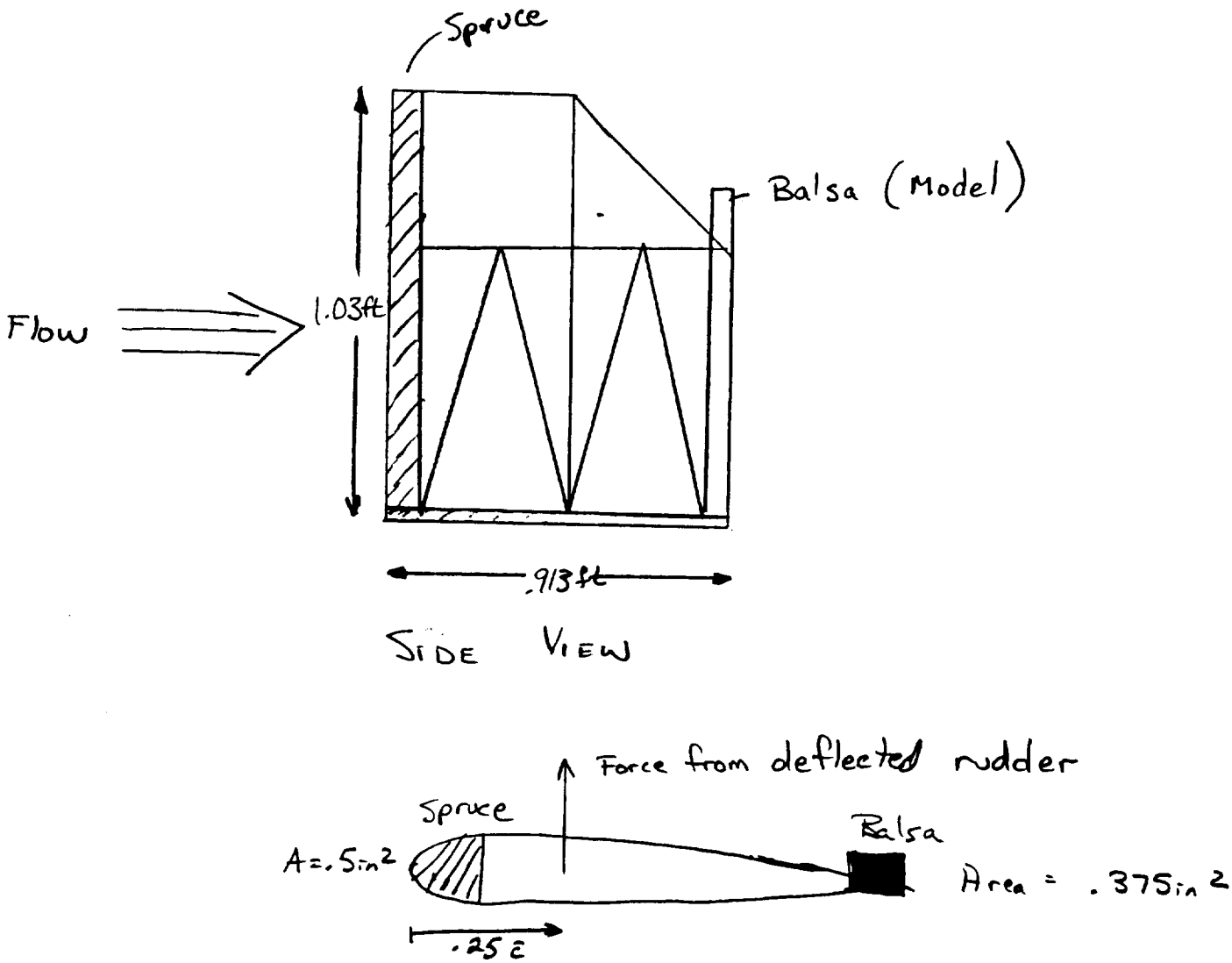

Figure 10.18 Vertical Stabilizer

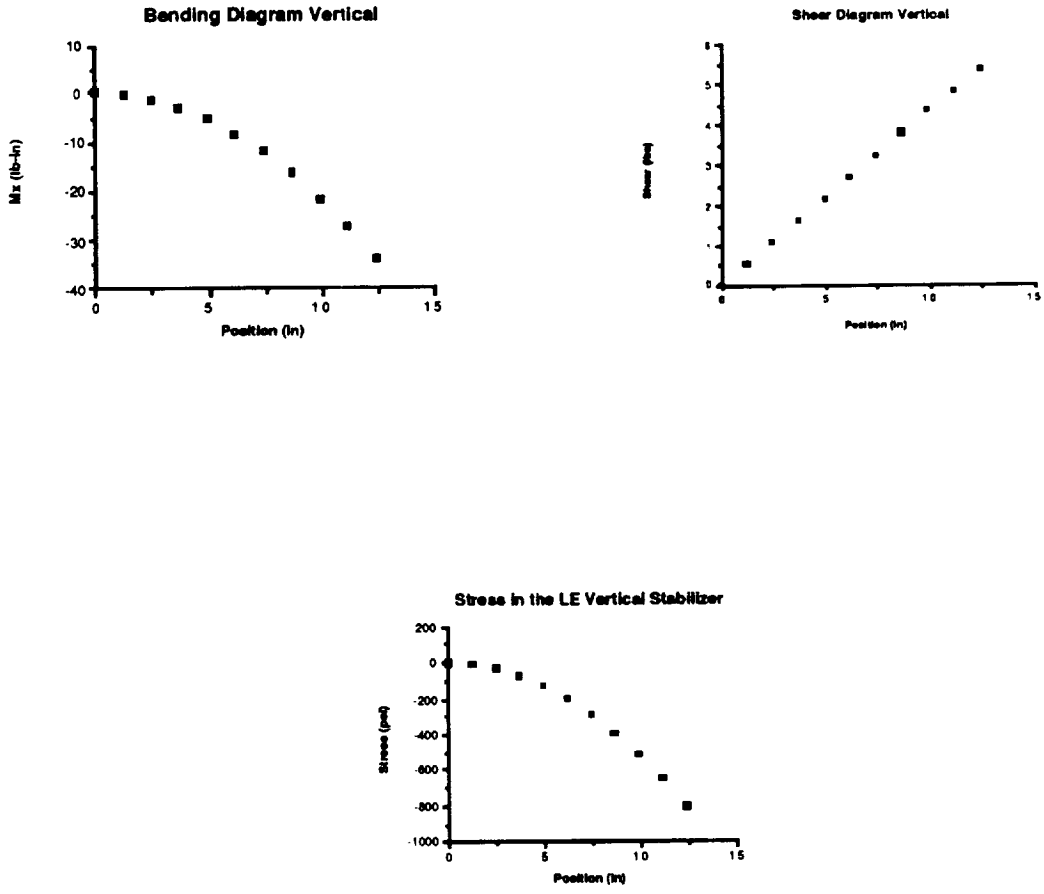

Figure 10.19
Loading in the Vertical Stabilizer

In analyzing the loading, a maximum stress level in the spruce spar was seen to be 757.6 psi while the stress in the trailing edge balsa spar was 449.0 psi. It was determined that the loads could easily be supported by such a design. The cross members would more than adequately support the load due to the drag on the tail (See Table 10.6). As was the case with the horizontal stabilizer, the members were to be made of balsa to minimize the weight. The overall weight of the vertical stabilizer was found to be 0.35 pounds.

Table 10.6

Stress Levels Present in the Vertical Tail

		Area(in^2)	Stress(psi)	Max Deflection(in)
Balsa	LE	0.500	757.6	4.00
	TE	0.375	449.2	1.34
Spruce	LE	0.500	757.6	.020
	TE	0.375	449.2	.067
Birch	LE	0.500	757.6	.013
	TE	0.375	449.2	.043

Although it has been shown that tail surfaces constructed of balsa and spruce should easily support the required loads, further refinements of both the loading model and the sub-structure model is necessary for further design.

APPENDIX 10.1

```
-OPD UNIVERSITY FTN77 VER. 228S     <USER3>S213900561>STUDENT>WING.F77        14:11:41
'I' ER OPTIONS:   LISTING INTL NOMAP CHECK NOBIG LOGL DYNM NOOFFSET LGO NOANSI NODEBU
                  FPN NOLUNFREC NOSILENT NO_OPTIMISE NOIMPURE

)0 1                PROGRAM WING
)0 2          C     BRIAN MCDONALD
)0 3          C     PRELIMINARY DESIGN OF THE WING BY DETERMINING THE ROOT BENDING
)004
)0 5          C     This program determines the direct stress due to bending
)0 6          C     on an airfoil section.  Prandtl's lifting line theory for a
)0 7          C     finite wing is used to find the lift generated by the
)008          C     airfoil.
)009          C     The program determines the section properties
)0 0          C     of the data input through  the data file.  The loadings found
)0 1          C     from the lifting line theory are then applied to find the stress
)012          C     resultants.  For a given aspect ratio the root stresses are found
)013          C     and ploted.  EITHER THE VELOCITY OR THE ANGLE OF ATTACK CAN VARY
)014
)0 5                REAL A1(52,53),C(52),AIN(52),G(52),CL(52),CDI(52),Y(14),Z(14)
)0 6                REAL A2(14),E(14),IYY(14),IZZ(14),IYZ(14),PY(26),PZ(26),MXL(26)
)017                REAL VY(26),VZ(26),MX(26),MY(26),MZ(26),X(52),PS(26),ANG(52)
)018                REAL PLO(26,4),PL01(26,4),PL02(26,4),PL03(26,4),PL04(26,4)
)0 9                REAL PS1(52),PMAT(14),WCHUNK(14),POCL(52,4),POCD(52,4)
)0 0                REAL Z1(14),Y1(14),SIG(4),VEL(4),ANGLE(4)
)0 1                INTEGER LOC(52)
)022
)023                OPEN(UNIT=66,FILE='AIRFOIL.DATA',STATUS='UNKNOWN')
)0 4                TEST= 0.
)0 5                WTOTS= 0.
)026          C     ********   DATA INPUT  ***********
)027                READ(66,*)K
)0 8                DO 14 J = 1,K
)0 9.01             READ(66,*)S,Z1(J),Y1(J),A2(J),E(J),IZZ(J),IYY(J),IYZ(J),PMAT(J)
)030.01             WCHUNK(J) = A2(J)*PMAT(J)
)031.01             WTOTS= WTOTS+ WCHUNK(J)
)032.01          14 CONTINUE
)0 3                WRITE(1,*)'IWR?'
)0 4                READ(1,*)IWR
)035             95 CONTINUE
)036                TEST = 0.
)0 7                TH = 0.
)0 8                WRITE(1,*)'ENTER THE NUMBER OF WINGS TO BE TESTED (1-4)'
)039                READ(1,*)IM
)040                DO 100 MLOOP = 1,IM
)041.01             CDO =  .035
)0 2.01             CHORD = 1.0
)0 3.01             B = 14.0
)044.01             WTOT = WTOTS*B
)045.01             WRITE(1,*)'WEIGHT = ',WTOT
)0 6.01             CENP = .3
)0 7.01             CENP =-CENP * CHORD
)048.01             WRITE(1,*)'ENTER THE AIRSPEED IN FT/SEC'
)049.01             READ(1,*) V
)0 0.01             N = 52
)0 1.01             WRITE(1,*)'ENTER THE ANGLE OF ATTACK'
)0 2.01             READ(1,*)A
)053.01             A = A*4*ATAN(1.)/180.
)054.01             DA = 0.0
)0 5.01             RHO  = .0023769
)0 6.01             DO 3 I = 1,N
)057.02             PS1(I) = -B/2.+REAL(I)*B/REAL(N)
)058.02           3 CONTINUE
)0 9.01             DO 4 I = 1,K
)0 0.02             Z(I) = Z1(I)
)0 1.02             Y(I) = Y1(I)
)062.02           4 CONTINUE
)063.01             CALL ALPHA(N,DA,A,A1,C,CHORD,B,ANG)
)0 4.01
)0 5.01             CALL SIM(N,A1,B,V,CHORD,AIN,G,CL,CDI,BCL,CLTOT,CDTOT,TEST,X
)066.01            .,LOC,TH,C,ANG,CDO)
)067.01             WRITE(IWR,*)
)0 8.01             WRITE(IWR,*)'*************************************************'
)0 9.01             WRITE(IWR,*)' VELOCITY = ',V,'ft/s    ANGLE = ',A*180/(4*ATAN(1.))
)0 0.01             WRITE(IWR,*)
)071.01
)072.01             WRITE(IWR,*)'THE TOTAL LIFT PRODUCED IS ',CLTOT,'(lbs)'
)0 3.01             WRITE(IWR,*)'THE TOTAL DRAG IS ',CDTOT,'(lbs)'
)0 4.01             DO 18 I= 1,N
)0 5.02             POCL(I,MLOOP) = CL(I)
```

ORIGINAL PAGE IS
OF POOR QUALITY

```
)076.02          POCD(I,MLOOP) = CDI(I)
)077.02     18   CONTINUE
)078.02
)079.01          CALL SECT(N,TEST,TH,CL,CDI,C,AIN,RHO,PY,PZ,MXL,V,VY,VZ,MX,B,MY
)080.01         . ,MZ,IWR,Y,Z,A2,E,IYY,IZZ,IYZ,CENP,WTOTS,K,SIG,VEL,ANGLE)
)081.01
)082.01          WRITE(IWR,*)'LIFT AND DRAG DISTRIBUTION ALONG WING'
)083.01          WRITE(IWR,*)
)084.01          WRITE(IWR,*)'       STATION      CL                CD            ANGLE'
)085.01
)086.01          DO 8 I = 1,N
)087.02          WRITE(IWR,*)I,CL(I),CDI(I),AIN(I)*180./(4.*ATAN(1.))
)088.02     8    CONTINUE
)089.02
)090.01          DO 9 I = 1,N/2
)091.02          PS(I) = B/2.-REAL(I)*B/REAL(N)
)092.02          PLO(I,MLOOP)=VY(I)
)093.02          PLO1(I,MLOOP)= VZ(I)
)094.02          PLO2(I,MLOOP) = MX(I)
)095.02          PLO3(I,MLOOP) = MY(I)
)096.02          PLO4(I,MLOOP) = MZ(I)
)097.02     9    CONTINUE
)098.02
)099.01     100  CONTINUE
)100.01     c    Plots of the lift and drag for no flap
)101.01
)102             CALL TPLOT(-11,PS1,POCL,N,52,4)
)103             CALL TITLE('CL FOR TEST WING')
)104             CALL TLABEL('POSITION FROM CENTERLINE [ft]','Cl ')
)105             READ(1,*)S
)106             CALL TPLOT(-11,PS1,POCD,N,52,4)
)107             CALL TITLE('CD FOR TEST WING')
)108             CALL TLABEL('POSITION FROM CENTERLINE [ft]','Cd')
)109             READ(1,*)S
)110
)111        C    Plots of the internal stress resultants comparing flap and no flap
)112
)113             CALL TPLOT(-11,PS,PLO,25,26,4)
)114             CALL TITLE('STRESS RESULTANTS Vy')
)115             CALL TLABEL('POSITION FROM CENTERLINE [ft]','Vy [lbs]')
)116             READ(1,*)S
)117             CALL TPLOT(-11,PS,PLO1,25,26,4)
)118             CALL TITLE('STRESS RESULTANTS Vz')
)119             CALL TLABEL('POSITION FROM CENTERLINE [ft]','Vz [lbs]')
)120             READ(1,*)S
)121             CALL TPLOT(-11,PS,PLO2,25,26,4)
)122             CALL TITLE('STRESS RESULTANT Mx')
)123             CALL TLABEL('POSITION FROM CENTERLINE [ft]','Mx [ft-lbs]')
)124             READ(1,*)S
)125             CALL TPLOT(-11,PS,PLO3,25,26,4)
)126             CALL TITLE('STRESS RESULTANT My')
)127             CALL TLABEL('POSITION FROM CENTERLINE [ft]','My [ft-lbs]')
)128             READ(1,*)S
)129             CALL TPLOT(-11,PS,PLO4,25,26,4)
)130             CALL TITLE('STRESS RESULTANT Mz')
)131             CALL TLABEL('POSITION FROM CENTERLINE [ft]','Mz [ft-lbs]')
)132             WRITE(1,*)'INPUT 1, AND THEN A THREE FOR ANGLES'
)133             READ(1,*)S
)134             IF (S .LT. 2) THEN
)135.01              CALL TPLOT(-11,VEL,SIG,4,4,1)
)136.01              CALL TITLE('BENDING STRESS AT ROOT AT MAX STRESSED MEMBER')
)137.01              CALL TLABEL('VELOCITY ft/s','STRESS psi')
)138.01          ELSE
)139.01              call TPLOT(-11,ANGLE,SIG,4,4,1)
)140.01              CALL TITLE('BENDING STRESS AT ROOT AT MAX STRESSED MEMBER')
)141.01              Call TLABEL('ANGLE degs','STRESS psi')
)142.01          ENDIF
)143             WRITE(1,*)'WOULD YOU CARE TO START OVER FOR A NEW WING AT A NEW
)144            .ANGLE OF ATTACK? (1 FOR YES)'
)145             READ(1,*)I
)146             IF(I.EQ.1) GOTO 95
)147
)148             WRITE(1,*)'THANK YOU FOR CHOSING McDONALD SOFTWARE SYSTEMS'
)149
)150             CLOSE(UNIT = 66)
)151             STOP
)152             END
```

```
0153
 154
 155       C      *** SUBROUTINE TO DETERMINE THE COEFFICIENTS OF THE LIFTING LINE
0156
0157                SUBROUTINE ALPHA(N, DA, A, A1, C, CHORD, B, ANG)
 158
 159                REAL A1(N, N+1), C(N), ANG(N)
 160
0161                PI = 4. *ATAN(1. )
0162                THETA = REAL(PI/N)
 163                DA = 2. *REAL(DA/N)
 164
0165       C        DETERMINE THE ANGLE OF ATTACK AND THE CHORD AT EACH SECTION
0166
 167                DO 10 I  = 1, 26
 168
 169       c        Detemine the RHS of the equations for the lifting line
0170. 01           A1(I, N+1) = A-DA*REAL(I)
0171. 01           A1(N-I+1, N+1)=A1(I, N+1)
 172. 01           ANG(I) = A1(I, N+1)
 173. 01           ANG(N-I+1) = A1(I, N+1)
0174. 01   C       Symmetric airfoil alpha lift = 0 is 0
0175. 01
 176. 01   c       Determine the chord at each position
 177. 01
 178. 01           C(I)= CHORD
0179. 01           C(N-I+1) = C(I)
0180. 01
 181. 01     10    CONTINUE
 182                T =0.
0183                DO 20 J = 1, N
0184. 01           T = T + REAL(PI/N)
 185. 01           DO 30 I = 1, N
 186. 01   C       The specific point that is being looked at
 187. 01
0188. 01   c       The coefficients of the point being examined.
0189. 01
 190. 02           A1(J, I)=2. *B/(PI*C(J))*SIN(REAL(I*T))+REAL(I*SIN(REAL(I*T)))/SIN(T
 191. 02          . )
0192. 02
0193. 02     30    CONTINUE
 194. 01     20    CONTINUE
 195. 01
 196. 01
0197                RETURN
0198                END


0199
 200       C      SUBROUTINE TO FIND THE SOLUTIONS TO THE SIMULTANEOUS EQUATIONS
 201
 202
0203                SUBROUTINE SIM(N, A1, B, V, CHORD, AIN, G, CL, CDI, BCL, CLTOT, CDTOT
0204               . , TEST, X, LOC, TH, C, ANG, CDO)
 205
 206
0207                REAL A1(N, N+1), X(N), G(N), CL(N), CDI(N), AIN(N), C(N), ANG(N)
0208                INTEGER LOC(52)
 209                CLTOT= 0.
 210                RHO = .0023769
 211                AIND = 0.
0212                H = 0.
0213                DO 10 I = 1, N
 214. 01           X(I) = A1(I, N+1)
 215. 01     10    CONTINUE
0216                PI = 4. *ATAN(1. )
0217
 218                CALL SIMEQ(A1, X, N, N, LOC)
 219                T = 0.
 220                CDTOT = 0.
0221                CLTOT = 0.
0222                DO 40 I = 1, N
 223. 01           T = T + PI/REAL(N)
 224. 01           AIND = 0.
0225. 01           H = 0.
0226. 01           DO 50 J = 1, N
 227. 02           H = H +X(J)*SIN(REAL(J*T))
 228. 02           AIND = AIND + REAL(J)*(X(J))*SIN(REAL(J*T))/SIN(T)
 229. 02
```

```
0230.02      50  CONTINUE
 231.02  C       ANGLE OF ATTACK OF EACH SECTION
 232.01          AIN(I) = ANG(I)-AIND
0233.01  C       CIRCULATION AT EACH SECTION
0234.01          G(I) = 2.*B*V*H
 235.01          CL(I) = 2*G(I)/(V*C(I))
 236.01          CDI(I) =CDO+ 2./(V*B*CHORD)*AIN(I)*G(I)*B/REAL(N)
0237.01          CLTOT = CLTOT + CL(I)*.5*RHO*V**2*B*CHORD/N
0238.01          CDTOT = CDTOT + CDI(I)*.5*RHO*V**2*B*CHORD/N
 239.01      40  CONTINUE
 240.01
 241              E = 0.
0242              DO 60 I = 2,N
0243.01           E = E+REAL(I)*(X(I)/X(1))**2
 244.01
 245.01      60  CONTINUE
0246              RETURN
0247              END



0248
0249
 250      C       Subroutine to determine section properties and the direct stress
 251
0252              SUBROUTINE SECT(N,TEST,TH,CL,CDI,C,AIN,RHO,PY,PZ,MXL,V,VY,VZ,
0253             .MX,B,MY,MZ,IWR,Y,Z,A2,E,IYY,IZZ,IYZ,CENP,WTOTS,K,SIG,VEL,ANGLE)
 254
 255              REAL CL(N),CDI(N),C(N),AIN(N),PY(N/2),PZ(N/2),MXL(N/2),VY(N/2)
 256              REAL VZ(N/2),MX(N/2),MY(N/2),MZ(N/2),Y(14),Z(14),A2(14),E(14)
0257              REAL IYY(14),IZZ(14),IYZ(14),MXOLD,MYOLD,MZOLD,SIG(4),VEL(4)
0258              REAL ANGLE(4)
 259              INTEGER P6,POS
 260
0261
0262      C       CALCULATE THE SECTION PROPERTIES
 263      C       Weighted centroid
 264              Eref= 6.5E6*144.
 265              ASTAR = 0.
0266              YB = 0.
0267              ZB = 0.
 268              YYT = 0.
 269              ZZT = 0.
0270              YZT = 0.
0271
 272              DO 20 M = 1,K
 273.01           ASTAR = ASTAR + A2(M)*E(M)/EREF
 274.01           YB = YB+Y(M)*E(M)/EREF*A2(M)
0275.01           ZB = ZB+Z(M)*E(M)/EREF*A2(M)
0276.01
 277.01      20  CONTINUE
 278              YB = YB/ASTAR
0279              ZB = ZB/ASTAR
0280              DIST = ZB - CENP
 281      C       Calculate the section properties relative to the centroid
 282              WRITE(1,*)'ZBAR =',ZB
 283               WRITE(1,*)'YBAR = ',YB
0284
0285              DO 25 I = 1,K
 286.01           YYT = YYT+E(I)/EREF*A2(I)*(Z(I)-ZB)**2+IYY(I)
 287.01           ZZT = ZZT+E(I)/EREF*A2(I)*(Y(I)-YB)**2+IZZ(I)
0288.01           YZT = YZT+E(I)/EREF*A2(I)*(Y(I)-YB)*(Z(I)-ZB)+IYZ(I)
0289.01
 290.01       25 CONTINUE
 291.01  C       Calculate bending moments due to the loading
 292              Q = .5*RHO*V**2
0293      C       WEIGHT PER SPAN (lbs/ft) = WTOTS
0294              DO 30 I = 1,N/2
 295.01           PY(I) = Q*C(I)*CL(I)*COS(AIN(I))+Q*C(I)*CDI(I)*SIN(AIN(I))
 296.01          .-WTOTS*COS(AIN(I))
0297.01           PZ(I) =  Q*C(I)*CL(I)*SIN(AIN(I))-Q*C(I)*CDI(I)*COS(AIN(I))
0298.01          .-WTOTS*SIN(AIN(I))
 299.01           FORCEY= Q*C(I)*CL(I)*COS(AIN(I))+Q*C(I)*CDI(I)*SIN(AIN(I))
 300.01           FORCEZ=  Q*C(I)*CL(I)*SIN(AIN(I))-Q*C(I)*CDI(I)*COS(AIN(I))
 301.01
0302.01           ACMX = 0.1*Q*C(I)**2
0303.01           MXL(I)=FORCEZ*(DIST)-FORCEY*(YB)+ACMX
 304.01
 305.01       30 CONTINUE
0306.01
```

```
0307.01   C      Determine internal stress resultants
0308.01
 309             DX = B/N
 310             DO 35 I = 1,N/2-1
0311
0312.01          IF(I .NE. 1) THEN
 313.02             VYOLD = VY(I-1)
 314.02             VZOLD = VZ(I-1)
0315.02             MXOLD = MX(I-1)
0316.02          ELSE
0317.02             VYOLD = 0.
 318.02             VZOLD = 0.
 319.02             MXOLD = 0.
0320.02          ENDIF
0321.01          WRITE(1,*)'MXOLD',MXOLD
 322.01          VY(I) = VYOLD + (PY(I+1)+PY(I))/2.*DX
 323.01          VZ(I) = VZOLD + (PZ(I+1)+PZ(I))/2.*DX
0324.01          MX(I) = MXOLD + (MXL(I+1)+MXL(I))/2.*DX
0325.01          WRITE(IWR,*)'VY',I,'=',VY(I),'VZ=',VZ(I),'MX=',MX(I)
0326.01     35   CONTINUE
 327             WRITE(IWR,*)
 328             DO 40 I =1,N/2-1
0329.01          IF (I.EQ.1) THEN
0330.02             MZOLD = 0.
 331.02             MYOLD = 0.
 332.02          ELSE
0333.02             MZOLD = MZ(I-1)
0334.02             MYOLD = MY(I-1)
0335.02          ENDIF
 336.01          MZ(I) = MZOLD + (VY(I+1)+VY(I))/2.*DX
 337.01          MY(I) = MYOLD - (VZ(I+1)+VZ(I))/2.*DX
0338.01
0339.01     40   CONTINUE
 340.01
 341.01   C      Stress resultants have now been calculated along the "beam"
0342             WRITE(IWR,*)
0343             WRITE(IWR,*)' WING POSITION  CROSS SECTION MEMBER     Y              Z
0344                        DIRECT STRESS'
 345         C   DETERMINE STRESS AT A SELECTED POINT ALONG THE WING
 346             WRITE(1,*)'ENTER A NUMBER FROM 1 TO ',N/2-1,' ALONG THE WING'
0347             READ(1,*) POS
0348
 349         C   WRITE(1,*)'AT SECTION',POS,'WHAT INDIVIDUAL MEMBER IN THE STRUCTUR
 350         C   E IS TO BE ANALYZED?'
0351         C   WRITE(1,*)'ENTER A NUMBER FROM 1 TO ',K,' FOR A SPECIFIC MEMBER,
0352         C   OR ENTER 50 FOR ALL.'
0353         C   READ(1,*)P6
 354             P6 = 55
 355             IF(P6 .GT. 49) THEN
0356.01             N1 = 1
0357.01             N2 = K
 358.01          ELSE
 359.01             N1 = P6
0360.01             N2 = P6
0361.01          ENDIF
0362.01
 363             DO 60 I = N1,N2
0364.01          EASE1 = (MZ(POS)*YYT+MY(POS)*YZT)/(YYT*ZZT-YZT**2)
0365.01          EASE2 = (MY(POS)*ZZT+MZ(POS)*YZT)/(YYT*ZZT-YZT**2)
0366.01
 367.01          SIGMA = -EASE1*E(I)/EREF*(Y(I)-YB)+EASE2*E(I)/EREF*(Z(I)-ZB)
 368.01          SIGMA = SIGMA/144.
0369.01          IF (I .EQ. 2) SIG(I) = SIGMA
0370.01   C
0371.01          WRITE(IWR,*)POS,I,'       ',Y(I),Z(I),SIGMA
 372.01
 373.01     60   CONTINUE
0374             WRITE(IWR,*)
0375             VEL(1) = 50.
 376             VEL(2) = 75.
 377             VEL(3) = 100.
0378             VEL(4)  = 150.
0379             ANGLE(1) = 3.
0380             ANGLE(2) = 6.
 381             ANGLE(3) = 10.
 382             ANGLE(4) = 12.
0383
0384             RETURN
 385             END
```

```
*: ********************************************
 ( ELOCITY =       50.0000     ft/s    ANGLE =       2.00000

THE TOTAL LIFT PRODUCED IS       6.72936     (lbs)
TI E TOTAL DRAG IS       1.45953     (lbs)
V          1=    -0.109181    VZ=    -2.874651E-02MX=    7.972394E-02
V          2=    -0.197349    VZ=    -5.772563E-02MX=    0.157236
VY         3=    -0.267263    VZ=    -8.676833E-02MX=    0.232810
VV         4=    -0.321656    VZ=    -0.115763     MX=    0.306724
V          5=    -0.363042    VZ=    -0.144646     MX=    0.379237
V          6=    -0.393629    VZ=    -0.173386     MX=    0.450582
VY         7=    -0.415305    VZ=    -0.201974     MX=    0.520959
VY         8=    -0.429649    VZ=    -0.230413     MX=    0.590536
V          9=    -0.437971    VZ=    -0.258714     MX=    0.659454
V         10=    -0.441344    VZ=    -0.286891     MX=    0.727830
V         11=    -0.440647    VZ=    -0.314959     MX=    0.795759
VY        12=    -0.436596    VZ=    -0.342932     MX=    0.863319
VY        13=    -0.429775    VZ=    -0.370824     MX=    0.930573
V         14=    -0.420664    VZ=    -0.398646     MX=    0.997575
V         15=    -0.409657    VZ=    -0.426409     MX=     1.06437
VY        16=    -0.397078    VZ=    -0.454122     MX=     1.13099
VY        17=    -0.383200    VZ=    -0.481792     MX=     1.19746
V         18=    -0.368251    VZ=    -0.509427     MX=     1.26382
V         19=    -0.352426    VZ=    -0.537033     MX=     1.33008
V         20=    -0.335891    VZ=    -0.564615     MX=     1.39626
VY        21=    -0.318794    VZ=    -0.592178     MX=     1.46238
VY        22=    -0.301263    VZ=    -0.619726     MX=     1.52845
V         23=    -0.283418    VZ=    -0.647264     MX=     1.59449
V         24=    -0.265368    VZ=    -0.674794     MX=     1.66050
VY        25=    -0.247216    VZ=    -0.702321     MX=     1.72650

 I ING POSITION  CROSS SECTION MEMBER      Y              Z          DIRECT STRESS
          25            1          9.520000E-02   -0.245000          14.7497
          25            2         -2.380000E-02   -0.245000         -22.6973
          25            3          1.190000E-02   -2.380000E-02      10.0193
          25            4          0.238000       -0.857000          0.249879

LIFT AND DRAG DISTRIBUTION ALONG WING

     STATION       CL             CD          ANGLE
           1    3.030080E-02   3.500281E-02    0.276317
           2    5.810238E-02   3.501032E-02    0.529839
           3    8.254056E-02   3.502084E-02    0.752689
           4    0.103484       3.503277E-02    0.943669
           5    0.121127       3.504490E-02     1.10456
           6    0.135825       3.505646E-02     1.23858
           7    0.147979       3.506701E-02     1.34941
           8    0.157986       3.507639E-02     1.44067
           9    0.166210       3.508455E-02     1.51566
          10    0.172964       3.509156E-02     1.57725
          11    0.178517       3.509753E-02     1.62789
          12    0.183089       3.510259E-02     1.66958
          13    0.186860       3.510686E-02     1.70397
          14    0.189977       3.511046E-02     1.73239
          15    0.192558       3.511348E-02     1.75592
          16    0.194695       3.511601E-02     1.77542
          17    0.196466       3.511813E-02     1.79156
          18    0.197928       3.511990E-02     1.80489
          19    0.199130       3.512136E-02     1.81585
          20    0.200109       3.512255E-02     1.82478
          21    0.200894       3.512352E-02     1.83194
          22    0.201509       3.512427E-02     1.83755
          23    0.201971       3.512485E-02     1.84176
          24    0.202292       3.512524E-02     1.84469
          25    0.202481       3.512548E-02     1.84642
          26    0.202544       3.512555E-02     1.84699
          27    0.202481       3.512548E-02     1.84642
          28    0.202292       3.512524E-02     1.84469
          29    0.201971       3.512485E-02     1.84176
          30    0.201509       3.512427E-02     1.83755
          31    0.200894       3.512352E-02     1.83194
          32    0.200109       3.512255E-02     1.82478
          33    0.199130       3.512136E-02     1.81585
          34    0.197928       3.511990E-02     1.80489
          35    0.196466       3.511813E-02     1.79156
          36    0.194696       3.511601E-02     1.77542
          37    0.192558       3.511348E-02     1.75593
          38    0.189978       3.511046E-02     1.73240
```

39	0.186861	3.510686E-02	1.70397
40	0.183089	3.510259E-02	1.66958
41	0.178518	3.509753E-02	1.62790
42	0.172965	3.509156E-02	1.57726
43	0.166211	3.508455E-02	1.51567
44	0.157988	3.507639E-02	1.44069
45	0.147981	3.506701E-02	1.34943
46	0.135827	3.505646E-02	1.23861
47	0.121130	3.504490E-02	1.10459
48	0.103488	3.503277E-02	0.943703
49	8.254497E-02	3.502085E-02	0.752728
50	5.810761E-02	3.501033E-02	0.529886
51	3.030701E-02	3.500281E-02	0.276373
52	6.680464E-06	3.500000E-02	6.830189E-05

++ **********
VELOCITY = 75.0000 ft/s ANGLE = 2.00000

TOTAL LIFT PRODUCED IS 15.1411 (lbs)
TOTAL DRAG IS 3.28395 (lbs)

1=	-6.473903E-02	VZ=	-6.340687E-02	MX=	0.179379
2=	-8.220570E-02	VZ=	-0.126585	MX=	0.353781
3=	-5.860879E-02	VZ=	-0.189253	MX=	0.523823
4=	-9.991424E-05	VZ=	-0.251258	MX=	0.690128
5=	8.766666E-02	VZ=	-0.312546	MX=	0.853284
6=	0.199722	VZ=	-0.373125	MX=	1.01381
7=	0.331822	VZ=	-0.433042	MX=	1.17216
8=	0.480410	VZ=	-0.492362	MX=	1.32871
9=	0.642543	VZ=	-0.551157	MX=	1.48377
10=	0.815804	VZ=	-0.609496	MX=	1.63762
11=	0.998221	VZ=	-0.667444	MX=	1.79046
12=	1.18818	VZ=	-0.725058	MX=	1.94247
13=	1.38437	VZ=	-0.782390	MX=	2.09379
14=	1.58571	VZ=	-0.839483	MX=	2.24454
15=	1.79131	VZ=	-0.896375	MX=	2.39483
16=	2.00045	VZ=	-0.953097	MX=	2.54472
17=	2.21251	VZ=	-1.00968	MX=	2.69429
18=	2.42698	VZ=	-1.06614	MX=	2.84359
19=	2.64341	VZ=	-1.12251	MX=	2.99268
20=	2.86145	VZ=	-1.17880	MX=	3.14159
21=	3.08075	VZ=	-1.23502	MX=	3.29036
22=	3.30102	VZ=	-1.29120	MX=	3.43902
23=	3.52200	VZ=	-1.34734	MX=	3.58760
24=	3.74344	VZ=	-1.40345	MX=	3.73613
25=	3.96512	VZ=	-1.45956	MX=	3.88464

WING POSITION	CROSS SECTION MEMBER	Y	Z	DIRECT STRESS
25	1	9.520000E-02	-0.245000	-36.7645
25	2	-2.380000E-02	-0.245000	74.3051
25	3	1.190000E-02	-2.380000E-02	-14.0347
25	4	0.238000	-0.857000	-17.8257

LIFT AND DRAG DISTRIBUTION ALONG WING

STATION	CL	CD	ANGLE
1	3.030079E-02	3.500281E-02	0.276317
2	5.810238E-02	3.501032E-02	0.529839
3	8.254056E-02	3.502084E-02	0.752689
4	0.103484	3.503277E-02	0.943669
5	0.121127	3.504490E-02	1.10456
6	0.135825	3.505646E-02	1.23858
7	0.147979	3.506701E-02	1.34941
8	0.157986	3.507639E-02	1.44067
9	0.166210	3.508455E-02	1.51566
10	0.172964	3.509156E-02	1.57725
11	0.178517	3.509753E-02	1.62789
12	0.183089	3.510259E-02	1.66958
13	0.186860	3.510686E-02	1.70397
14	0.189977	3.511046E-02	1.73239
15	0.192558	3.511348E-02	1.75392
16	0.194695	3.511601E-02	1.77542
17	0.196466	3.511813E-02	1.79156
18	0.197928	3.511990E-02	1.80489
19	0.199130	3.512136E-02	1.81585
20	0.200109	3.512255E-02	1.82478
21	0.200894	3.512352E-02	1.83194
22	0.201509	3.512427E-02	1.83755
23	0.201971	3.512485E-02	1.84176
24	0.202292	3.512524E-02	1.84469

25	0.202481	3.512548E-02	1.84642
26	0.202544	3.512555E-02	1.84699
27	0.202482	3.512548E-02	1.84642
28	0.202292	3.512524E-02	1.84469
29	0.201971	3.512485E-02	1.84176
30	0.201509	3.512427E-02	1.83755
31	0.200894	3.512352E-02	1.83194
32	0.200109	3.512255E-02	1.82478
33	0.199130	3.512136E-02	1.81585
34	0.197928	3.511990E-02	1.80489
35	0.196466	3.511813E-02	1.79156
36	0.194696	3.511601E-02	1.77542
37	0.192558	3.511348E-02	1.75593
38	0.189978	3.511046E-02	1.73240
39	0.186861	3.510686E-02	1.70397
40	0.183089	3.510259E-02	1.66958
41	0.178518	3.509753E-02	1.62790
42	0.172965	3.509156E-02	1.57726
43	0.166211	3.508455E-02	1.51567
44	0.157988	3.507639E-02	1.44069
45	0.147981	3.506701E-02	1.34943
46	0.135827	3.505646E-02	1.23861
47	0.121130	3.504490E-02	1.10459
48	0.103488	3.503277E-02	0.943703
49	8.254498E-02	3.502085E-02	0.752728
50	5.810761E-02	3.501033E-02	0.529886
51	3.030701E-02	3.500281E-02	0.276373
52	6.680463E-06	3.500000E-02	6.830189E-05

****

VELOCITY = 100.000 ft/s ANGLE = 2.00000

THE TOTAL LIFT PRODUCED IS 26.9174 (lbs)

THE TOTAL DRAG IS 5.83813 (lbs)

1=	-2.520377E-03	VZ=	-0.111931	MX=	0.318896
2=	7.899480E-02	VZ=	-0.222988	MX=	0.628944
3=	0.233507	VZ=	-0.332731	MX=	0.931240
4=	0.450078	VZ=	-0.440951	MX=	1.22689
5=	0.718659	VZ=	-0.547605	MX=	1.51695
6=	1.03041	VZ=	-0.652759	MX=	1.80233
7=	1.37780	VZ=	-0.756537	MX=	2.08383
8=	1.75449	VZ=	-0.859092	MX=	2.36214
9=	2.15526	VZ=	-0.960577	MX=	2.63782
10=	2.57581	VZ=	-1.06114	MX=	2.91132
11=	3.01264	VZ=	-1.16092	MX=	3.18304
12=	3.46287	VZ=	-1.26003	MX=	3.45327
13=	3.92417	VZ=	-1.35858	MX=	3.72229
14=	4.39463	VZ=	-1.45665	MX=	3.99030
15=	4.87267	VZ=	-1.55433	MX=	4.25747
16=	5.35699	VZ=	-1.65166	MX=	4.52395
17=	5.84650	VZ=	-1.74872	MX=	4.78985
18=	6.34029	VZ=	-1.84554	MX=	5.05528
19=	6.83759	VZ=	-1.94217	MX=	5.32032
20=	7.33772	VZ=	-2.03865	MX=	5.58505
21=	7.84010	VZ=	-2.13500	MX=	5.84952
22=	8.34422	VZ=	-2.23125	MX=	6.11381
23=	8.84959	VZ=	-2.32743	MX=	6.37795
24=	9.35578	VZ=	-2.42357	MX=	6.64201
25=	9.86237	VZ=	-2.51969	MX=	6.90602

WING POSITION	CROSS SECTION MEMBER	Y	Z	DIRECT STRESS
25	1	9.520000E-02	-0.245000	-108.884
25	2	-2.380000E-02	-0.245000	210.108
25	3	1.190000E-02	-2.380000E-02	-47.7103
25	4	0.238000	-0.857000	-43.1315

LIFT AND DRAG DISTRIBUTION ALONG WING

STATION	CL	CD	ANGLE
1	3.030080E-02	3.500281E-02	0.276317
2	5.810238E-02	3.501032E-02	0.529839
3	8.254056E-02	3.502084E-02	0.752689
4	0.103484	3.503277E-02	0.943669
5	0.121127	3.504490E-02	1.10456
6	0.135825	3.505646E-02	1.23858
7	0.147979	3.506701E-02	1.34941
8	0.157986	3.507639E-02	1.44067
9	0.166210	3.508455E-02	1.51566
10	0.172964	3.509156E-02	1.57725

11	0.178517	3.509753E-02	1.62789
12	0.183089	3.510259E-02	1.66958
13	0.186860	3.510686E-02	1.70397
14	0.189977	3.511046E-02	1.73239
15	0.192558	3.511348E-02	1.75592
16	0.194695	3.511601E-02	1.77542
17	0.196466	3.511813E-02	1.79156
18	0.197928	3.511990E-02	1.80489
19	0.199130	3.512136E-02	1.81585
20	0.200109	3.512255E-02	1.82478
21	0.200894	3.512352E-02	1.83194
22	0.201509	3.512427E-02	1.83755
23	0.201971	3.512485E-02	1.84176
24	0.202292	3.512524E-02	1.84469
25	0.202481	3.512548E-02	1.84642
26	0.202544	3.512555E-02	1.84699
27	0.202481	3.512548E-02	1.84642
28	0.202292	3.512524E-02	1.84469
29	0.201971	3.512485E-02	1.84176
30	0.201509	3.512427E-02	1.83755
31	0.200894	3.512352E-02	1.83194
32	0.200109	3.512255E-02	1.82478
33	0.199130	3.512136E-02	1.81585
34	0.197928	3.511990E-02	1.80489
35	0.196466	3.511813E-02	1.79156
36	0.194696	3.511601E-02	1.77542
37	0.192558	3.511348E-02	1.75593
38	0.189978	3.511046E-02	1.73240
39	0.186861	3.510686E-02	1.70397
40	0.183089	3.510259E-02	1.66958
41	0.178518	3.509753E-02	1.62790
42	0.172965	3.509156E-02	1.57726
43	0.166211	3.508455E-02	1.51567
44	0.157988	3.507639E-02	1.44069
45	0.147981	3.506701E-02	1.34943
46	0.135827	3.505646E-02	1.23861
47	0.121130	3.504490E-02	1.10459
48	0.103488	3.503277E-02	0.943703
49	8.254497E-02	3.502085E-02	0.752728
50	5.810761E-02	3.501033E-02	0.529886
51	3.030701E-02	3.500281E-02	0.276373
52	6.680464E-06	3.500000E-02	6.830189E-05

****

VELOCITY = 150.000 ft/s ANGLE = 2.00000

ORIGINAL PAGE IS
OF POOR QUALITY

HE TOTAL LIFT PRODUCED IS 60.5643 (lbs)

HE TOTAL DRAG IS 13.1358 (lbs)

VY	1=	0.175247	VZ=	-0.250573	MX=	0.717516
VY	2=	0.539568	VZ=	-0.498426	MX=	1.41512
VY	3=	1.06812	VZ=	-0.742670	MX=	2.09529
VY	4=	1.73630	VZ=	-0.982930	MX=	2.76051
VY	5=	2.52149	VZ=	-1.21920	MX=	3.41314
VY	6=	3.40382	VZ=	-1.45171	MX=	4.05524
VY	7=	4.36630	VZ=	-1.68081	MX=	4.68863
VY	8=	5.39472	VZ=	-1.90689	MX=	5.31482
VY	9=	6.47731	VZ=	-2.13035	MX=	5.93509
VY	10=	7.60440	VZ=	-2.35156	MX=	6.55047
VY	11=	8.76810	VZ=	-2.57086	MX=	7.16183
VY	12=	9.96197	VZ=	-2.78854	MX=	7.76987
VY	13=	11.1807	VZ=	-3.00484	MX=	8.37516
VY	14=	12.4201	VZ=	-3.22000	MX=	8.97818
VY	15=	13.6765	VZ=	-3.43419	MX=	9.57931
VY	16=	14.9471	VZ=	-3.64757	MX=	10.1789
VY	17=	16.2293	VZ=	-3.86026	MX=	10.7772
VY	18=	17.5212	VZ=	-4.07240	MX=	11.3744
VY	19=	18.8209	VZ=	-4.28407	MX=	11.9707
VY	20=	20.1271	VZ=	-4.49537	MX=	12.5664
VY	21=	21.4383	VZ=	-4.70636	MX=	13.1614
VY	22=	22.7533	VZ=	-4.91713	MX=	13.7561
VY	23=	24.0713	VZ=	-5.12772	MX=	14.3504
VY	24=	25.3910	VZ=	-5.33820	MX=	14.9445
VY	25=	26.7117	VZ=	-5.54863	MX=	15.5385

WING POSITION	CROSS SECTION MEMBER	Y	Z	DIRECT STRESS
25	1	9.520000E-02	-0.245000	-314.941
25	2	-2.380000E-02	-0.245000	598.117
25	3	1.190000E-02	-2.380000E-02	-143.926
25	4	0.238000	-0.857000	-115.434

LIFT AND DRAG DISTRIBUTION ALONG WING

STATION	CL	CD	ANGLE
1	3.030079E-02	3.500281E-02	0.276317
2	5.810238E-02	3.501032E-02	0.529839
3	8.254056E-02	3.502084E-02	0.752689
4	0.103484	3.503277E-02	0.943669
5	0.121127	3.504490E-02	1.10456
6	0.135825	3.505646E-02	1.23858
7	0.147979	3.506701E-02	1.34941
8	0.157986	3.507639E-02	1.44067
9	0.166210	3.508455E-02	1.51566
10	0.172964	3.509156E-02	1.57725
11	0.178517	3.509753E-02	1.62789
12	0.183089	3.510259E-02	1.66958
13	0.186860	3.510686E-02	1.70397
14	0.189977	3.511046E-02	1.73239
15	0.192558	3.511348E-02	1.75592
16	0.194695	3.511601E-02	1.77542
17	0.196466	3.511813E-02	1.79156
18	0.197928	3.511990E-02	1.80489
19	0.199130	3.512136E-02	1.81585
20	0.200109	3.512255E-02	1.82478
21	0.200894	3.512352E-02	1.83194
22	0.201509	3.512427E-02	1.83755
23	0.201971	3.512485E-02	1.84176
24	0.202292	3.512524E-02	1.84469
25	0.202481	3.512548E-02	1.84642
26	0.202544	3.512555E-02	1.84699
27	0.202482	3.512548E-02	1.84642
28	0.202292	3.512524E-02	1.84469
29	0.201971	3.512485E-02	1.84176
30	0.201509	3.512427E-02	1.83755
31	0.200894	3.512352E-02	1.83194
32	0.200109	3.512255E-02	1.82478
33	0.199130	3.512136E-02	1.81585
34	0.197928	3.511990E-02	1.80489
35	0.196466	3.511813E-02	1.79156
36	0.194696	3.511601E-02	1.77542
37	0.192558	3.511348E-02	1.75593
38	0.189978	3.511046E-02	1.73240
39	0.186861	3.510686E-02	1.70397
40	0.183089	3.510259E-02	1.66958
41	0.178518	3.509753E-02	1.62790
42	0.172965	3.509156E-02	1.57726
43	0.166211	3.508455E-02	1.51567
44	0.157988	3.507639E-02	1.44069
45	0.147981	3.506701E-02	1.34943
46	0.135827	3.505646E-02	1.23861
47	0.121130	3.504490E-02	1.10459
48	0.103488	3.503277E-02	0.943703
49	8.254498E-02	3.502085E-02	0.752728
50	5.810761E-02	3.501033E-02	0.529886
51	3.030701E-02	3.500281E-02	0.276373
52	6.680463E-06	3.500000E-02	6.830189E-05

****

VELOCITY = 60.0000 ft/s ANGLE = 3.00000

THE TOTAL LIFT PRODUCED IS 14.5354 (lbs)
THE TOTAL DRAG IS 2.10836 (lbs)

VY	1=	-6.793669E-02	VZ=	-4.097214E-02	MX=	0.112103
VY	2=	-9.049205E-02	VZ=	-8.165105E-02	MX=	0.219381
VY	3=	-7.362996E-02	VZ=	-0.121627	MX=	0.322413
VY	4=	-2.325891E-02	VZ=	-0.160675	MX=	0.421795
VY	5=	5.519058E-02	VZ=	-0.198712	MX=	0.518090
VY	6=	0.156946	VZ=	-0.235747	MX=	0.611804
VY	7=	0.277933	VZ=	-0.271845	MX=	0.703374
VY	8=	0.414738	VZ=	-0.307096	MX=	0.793172
VY	9=	0.564535	VZ=	-0.341600	MX=	0.881507
VY	10=	0.725006	VZ=	-0.375457	MX=	0.968637
VY	11=	0.894258	VZ=	-0.408758	MX=	1.05477
VY	12=	1.07074	VZ=	-0.441585	MX=	1.14009
VY	13=	1.25320	VZ=	-0.474010	MX=	1.22472
VY	14=	1.44060	VZ=	-0.506095	MX=	1.30879
VY	15=	1.63209	VZ=	-0.537893	MX=	1.39240
VY	16=	1.82696	VZ=	-0.569451	MX=	1.47562
VY	17=	2.02464	VZ=	-0.600807	MX=	1.55852
VY	18=	2.22462	VZ=	-0.631995	MX=	1.64115

VY	19=	2.42650	VZ=	-0.663046	MX=	1.72357
VY	20=	2.62991	VZ=	-0.693983	MX=	1.80581
VY	21=	2.83452	VZ=	-0.724831	MX=	1.88792
VY	22=	3.04008	VZ=	-0.755610	MX=	1.96992
VY	23=	3.24631	VZ=	-0.786337	MX=	2.05184
VY	24=	3.45298	VZ=	-0.817032	MX=	2.13370
VY	25=	3.65987	VZ=	-0.847711	MX=	2.21555

WING POSITION	CROSS SECTION MEMBER	Y	Z	DIRECT STRESS
25	1	9.520000E-02	-0.245000	-36.4504
25	2	-2.380000E-02	-0.245000	70.4807
25	3	1.190000E-02	-2.380000E-02	-15.8825
25	4	0.238000	-0.857000	-14.5790

LIFT AND DRAG DISTRIBUTION ALONG WING

STATION	CL	CD	ANGLE
1	4.545134E-02	3.500631E-02	0.414478
2	8.715376E-02	3.502324E-02	0.794759
3	0.123811	3.504691E-02	1.12903
4	0.155226	3.507374E-02	1.41550
5	0.181692	3.510103E-02	1.65684
6	0.203738	3.512704E-02	1.85788
7	0.221968	3.515080E-02	2.02412
8	0.236979	3.517188E-02	2.16101
9	0.249315	3.519024E-02	2.27349
10	0.259446	3.520601E-02	2.36588
11	0.267776	3.521945E-02	2.44183
12	0.274633	3.523084E-02	2.50437
13	0.280290	3.524045E-02	2.55595
14	0.284966	3.524854E-02	2.59859
15	0.288836	3.525534E-02	2.63388
16	0.292043	3.526103E-02	2.66313
17	0.294698	3.526580E-02	2.68734
18	0.296891	3.526977E-02	2.70734
19	0.298694	3.527306E-02	2.72378
20	0.300163	3.527575E-02	2.73717
21	0.301341	3.527793E-02	2.74791
22	0.302263	3.527962E-02	2.75633
23	0.302956	3.528091E-02	2.76264
24	0.303438	3.528181E-02	2.76703
25	0.303722	3.528233E-02	2.76963
26	0.303816	3.528251E-02	2.77048
27	0.303722	3.528233E-02	2.76963
28	0.303438	3.528181E-02	2.76704
29	0.302956	3.528091E-02	2.76264
30	0.302263	3.527962E-02	2.75633
31	0.301341	3.527793E-02	2.74791
32	0.300163	3.527576E-02	2.73717
33	0.298695	3.527306E-02	2.72378
34	0.296892	3.526977E-02	2.70734
35	0.294698	3.526580E-02	2.68734
36	0.292043	3.526103E-02	2.66313
37	0.288837	3.525534E-02	2.63389
38	0.284966	3.524854E-02	2.59859
39	0.280291	3.524045E-02	2.55596
40	0.274634	3.523085E-02	2.50437
41	0.267777	3.521946E-02	2.44184
42	0.259448	3.520602E-02	2.36589
43	0.249316	3.519024E-02	2.27350
44	0.236981	3.517188E-02	2.16103
45	0.221971	3.515080E-02	2.02415
46	0.203741	3.512704E-02	1.85791
47	0.181696	3.510103E-02	1.65688
48	0.155231	3.507374E-02	1.41555
49	0.123817	3.504691E-02	1.12909
50	8.716157E-02	3.502324E-02	0.794830
51	4.546056E-02	3.500631E-02	0.414560
52	1.002069E-05	3.500000E-02	1.011722E-04

****

VELOCITY = 60.0000 ft/s ANGLE = 6.00000

THE TOTAL LIFT PRODUCED IS 29.0708 (lbs)
THE TOTAL DRAG IS 2.14417 (lbs)

VY	1=	8.850852E-03	VZ=	-3.988638E-02	MX=	0.103866
VY	2=	0.108413	VZ=	-7.679535E-02	MX=	0.197797
VY	3=	0.286710	VZ=	-0.109324	MX=	0.282884
VY	4=	0.531884	VZ=	-0.136813	MX=	0.360299

VY	5=	0.833049	VZ=	-0.159144	MX=	0.431177
VY	6=	1.18065	VZ=	-0.176546	MX=	0.496555
VY	7=	1.56653	VZ=	-0.189436	MX=	0.557344
VY	8=	1.98388	VZ=	-0.198316	MX=	0.614323
VY	9=	2.42706	VZ=	-0.203697	MX=	0.668151
VY	10=	2.89145	VZ=	-0.206067	MX=	0.719374
VY	11=	3.37328	VZ=	-0.205868	MX=	0.768443
VY	12=	3.86947	VZ=	-0.203488	MX=	0.815732
VY	13=	4.37752	VZ=	-0.199265	MX=	0.861545
VY	14=	4.89536	VZ=	-0.193489	MX=	0.906135
VY	15=	5.42132	VZ=	-0.186407	MX=	0.949709
VY	16=	5.95400	VZ=	-0.178229	MX=	0.992442
VY	17=	6.49223	VZ=	-0.169135	MX=	1.03448
VY	18=	7.03504	VZ=	-0.159280	MX=	1.07593
VY	19=	7.58159	VZ=	-0.148798	MX=	1.11692
VY	20=	8.13118	VZ=	-0.137806	MX=	1.15753
VY	21=	8.68317	VZ=	-0.126407	MX=	1.19783
VY	22=	9.23701	VZ=	-0.114693	MX=	1.23790
VY	23=	9.79220	VZ=	-0.102751	MX=	1.27779
VY	24=	10.3483	VZ=	-9.065971E-02	MX=	1.31758
VY	25=	10.9048	VZ=	-7.849430E-02	MX=	1.35732

WING POSITION	CROSS SECTION MEMBER	Y	Z	DIRECT STRESS
25	1	9.520000E-02	-0.245000	-137.368
25	2	-2.380000E-02	-0.245000	248.913
25	3	1.190000E-02	-2.380000E-02	-70.1605
25	4	0.238000	-0.857000	-38.7369

LIFT AND DRAG DISTRIBUTION ALONG WING

STATION	CL	CD	ANGLE
1	9.090269E-02	3.502528E-02	0.828955
2	0.174308	3.509299E-02	1.58952
3	0.247622	3.518766E-02	2.25807
4	0.310452	3.529499E-02	2.83100
5	0.363383	3.540415E-02	3.31368
6	0.407476	3.550818E-02	3.71576
7	0.443936	3.560320E-02	4.04824
8	0.473959	3.568754E-02	4.32201
9	0.498629	3.576098E-02	4.54697
10	0.518893	3.582408E-02	4.73176
11	0.535551	3.587785E-02	4.88367
12	0.549266	3.592338E-02	5.00874
13	0.560581	3.596181E-02	5.11191
14	0.569932	3.599417E-02	5.19718
15	0.577673	3.602136E-02	5.26777
16	0.584086	3.604417E-02	5.32625
17	0.589396	3.606324E-02	5.37467
18	0.593783	3.607912E-02	5.41468
19	0.597388	3.609227E-02	5.44755
20	0.600325	3.610303E-02	5.47434
21	0.602682	3.611171E-02	5.49583
22	0.604527	3.611853E-02	5.51265
23	0.605912	3.612366E-02	5.52528
24	0.606876	3.612724E-02	5.53407
25	0.607444	3.612935E-02	5.53925
26	0.607631	3.613005E-02	5.54096
27	0.607444	3.612935E-02	5.53925
28	0.606876	3.612724E-02	5.53407
29	0.605912	3.612366E-02	5.52528
30	0.604527	3.611853E-02	5.51265
31	0.602682	3.611171E-02	5.49583
32	0.600326	3.610304E-02	5.47434
33	0.597389	3.609227E-02	5.44756
34	0.593783	3.607912E-02	5.41468
35	0.589396	3.606324E-02	5.37468
36	0.584086	3.604417E-02	5.32626
37	0.577674	3.602137E-02	5.26778
38	0.569933	3.599417E-02	5.19719
39	0.560582	3.596182E-02	5.11192
40	0.549268	3.592339E-02	5.00875
41	0.535553	3.587785E-02	4.88369
42	0.518896	3.582409E-02	4.73179
43	0.498632	3.576098E-02	4.54701
44	0.473963	3.568755E-02	4.32205
45	0.443942	3.560321E-02	4.04829
46	0.407483	3.550819E-02	3.71582
47	0.363392	3.540417E-02	3.31376
48	0.310463	3.529500E-02	2.83110

49	0.247635	3.518768E-02	2.25819
50	0.174323	3.509300E-02	1.58966
51	9.092112E-02	3.502529E-02	0.829121
52	2.004139E-05	3.500000E-02	2.023444E-04

****
VELOCITY = 60.0000 ft/s ANGLE = 9.00000

THE TOTAL LIFT PRODUCED IS 43.6062 (lbs)
HE TOTAL DRAG IS 2.20385 (lbs)

VY	1=	8.559194E-02	VZ=	-3.705918E-02	MX=	9.542280E-02
VY	2=	0.307097	VZ=	-6.606840E-02	MX=	0.175521
VY	3=	0.646426	VZ=	-8.405343E-02	MX=	0.241843
VY	4=	1.08569	VZ=	-8.971044E-02	MX=	0.296118
VY	5=	1.60849	VZ=	-8.294143E-02	MX=	0.340064
VY	6=	2.20046	VZ=	-6.440517E-02	MX=	0.375278
VY	7=	2.84939	VZ=	-3.516605E-02	MX=	0.403177
VY	8=	3.54508	VZ=	3.549031E-03	MX=	0.424989
VY	9=	4.27911	VZ=	5.050237E-02	MX=	0.441752
VY	10=	5.04459	VZ=	0.104531	MX=	0.454335
VY	11=	5.83591	VZ=	0.164586	MX=	0.463457
VY	12=	6.64849	VZ=	0.229747	MX=	0.469713
VY	13=	7.47862	VZ=	0.299219	MX=	0.473593
VY	14=	8.32324	VZ=	0.372322	MX=	0.475501
VY	15=	9.17985	VZ=	0.448476	MX=	0.475773
VY	16=	10.0464	VZ=	0.527187	MX=	0.474685
VY	17=	10.9211	VZ=	0.608034	MX=	0.472470
VY	18=	11.8027	VZ=	0.690657	MX=	0.469326
VY	19=	12.6897	VZ=	0.774742	MX=	0.465420
VY	20=	13.5812	VZ=	0.860017	MX=	0.460897
VY	21=	14.4763	VZ=	0.946240	MX=	0.455883
VY	22=	15.3741	VZ=	1.03319	MX=	0.450492
VY	23=	16.2739	VZ=	1.12068	MX=	0.444827
VY	24=	17.1750	VZ=	1.20852	MX=	0.438983
VY	25=	18.0767	VZ=	1.29653	MX=	0.433050

WING POSITION	CROSS SECTION MEMBER	Y	Z	DIRECT STRESS
25	1	9.520000E-02	-0.245000	-240.500
25	2	-2.380000E-02	-0.245000	428.706
25	3	1.190000E-02	-2.380000E-02	-127.205
25	4	0.238000	-0.857000	-60.9462

LIFT AND DRAG DISTRIBUTION ALONG WING

STATION	CL	CD	ANGLE
1	0.136354	3.505690E-02	1.24344
2	0.261461	3.520923E-02	2.38427
3	0.371433	3.542226E-02	3.38709
4	0.465678	3.566372E-02	4.24651
5	0.545074	3.590935E-02	4.97052
6	0.611213	3.614341E-02	5.57363
7	0.665905	3.635719E-02	6.07236
8	0.710939	3.654697E-02	6.48302
9	0.747944	3.671221E-02	6.82047
10	0.778340	3.685420E-02	7.09765
11	0.803328	3.697516E-02	7.32550
12	0.823902	3.707763E-02	7.51310
13	0.840872	3.716410E-02	7.66786
14	0.854899	3.723690E-02	7.79577
15	0.866510	3.729808E-02	7.90166
16	0.876128	3.734938E-02	7.98938
17	0.884094	3.739230E-02	8.06201
18	0.890672	3.742803E-02	8.12201
19	0.896081	3.745761E-02	8.17133
20	0.900487	3.748184E-02	8.21150
21	0.904022	3.750136E-02	8.24374
22	0.906789	3.751670E-02	8.26897
23	0.908867	3.752825E-02	8.28792
24	0.910313	3.753629E-02	8.30110
25	0.911165	3.754104E-02	8.30887
26	0.911446	3.754261E-02	8.31144
27	0.911165	3.754104E-02	8.30887
28	0.910313	3.753629E-02	8.30110
29	0.908867	3.752825E-02	8.28792
30	0.906789	3.751670E-02	8.26897
31	0.904022	3.750136E-02	8.24374
32	0.900488	3.748184E-02	8.21151
33	0.896083	3.745762E-02	8.17133
34	0.890673	3.742804E-02	8.12202

35	0.884093	3.739230E-02	8.06202
36	0.876129	3.734939E-02	7.98939
37	0.866512	3.729808E-02	7.90167
38	0.854901	3.723691E-02	7.79579
39	0.840874	3.716411E-02	7.66788
40	0.823903	3.707764E-02	7.51312
41	0.803331	3.697518E-02	7.32553
42	0.778344	3.685421E-02	7.09768
43	0.747949	3.671223E-02	6.82051
44	0.710946	3.654700E-02	6.48308
45	0.665913	3.635722E-02	6.07244
46	0.611224	3.614345E-02	5.57372
47	0.545087	3.590938E-02	4.97064
48	0.465693	3.566377E-02	4.24666
49	0.371453	3.542230E-02	3.38727
50	0.261484	3.520927E-02	2.38448
51	0.136382	3.505693E-02	1.24369
52	3.006203E-05	3.500000E-02	3.005283E-04

****
VELOCITY = 60.0000 ft/s ANGLE = 12.0000

THE TOTAL LIFT PRODUCED IS 58.1417 (lbs)
THE TOTAL DRAG IS 2.28740 (lbs)

/Y	1=	0.162256	VZ=	-3.249162E-02	MX=	8.677563E-02
/Y	2=	0.505423	VZ=	-4.947683E-02	MX=	0.152571
VY	3=	1.00514	VZ=	-4.583711E-02	MX=	0.199333
VY	4=	1.63737	VZ=	-1.942376E-02	MX=	0.229340
/Y	5=	2.38011	VZ=	2.978240E-02	MX=	0.244909
/Y	6=	3.21418	VZ=	0.100476	MX=	0.248224
VY	7=	4.12330	VZ=	0.190652	MX=	0.241248
VY	8=	5.09391	VZ=	0.298039	MX=	0.225686
/Y	9=	6.11486	VZ=	0.420365	MX=	0.202993
/Y	10=	7.17707	VZ=	0.555502	MX=	0.174386
/Y	11=	8.27311	VZ=	0.701541	MX=	0.140880
VY	12=	9.39699	VZ=	0.856811	MX=	0.103314
VY	13=	10.5438	VZ=	1.01987	MX=	6.237894E-02
/Y	14=	11.7095	VZ=	1.18948	MX=	1.864692E-02
/Y	15=	12.8910	VZ=	1.36460	MX=	-2.740859E-02
VY	16=	14.0853	VZ=	1.54433	MX=	-7.539360E-02
VY	17=	15.2904	VZ=	1.72792	MX=	-0.124978
/Y	18=	16.5043	VZ=	1.91471	MX=	-0.175883
/Y	19=	17.7254	VZ=	2.10413	MX=	-0.227870
/Y	20=	18.9524	VZ=	2.29570	MX=	-0.280735
VY	21=	20.1839	VZ=	2.48898	MX=	-0.334296
VY	22=	21.4191	VZ=	2.68358	MX=	-0.388393
/Y	23=	22.6568	VZ=	2.87913	MX=	-0.442880
/Y	24=	23.8962	VZ=	3.07532	MX=	-0.497621
VY	25=	25.1364	VZ=	3.27181	MX=	-0.552488

WING POSITION	CROSS SECTION MEMBER	Y	Z	DIRECT STRESS
25	1	9.520000E-02	-0.245000	-345.374
25	2	-2.380000E-02	-0.245000	609.030
25	3	1.190000E-02	-2.380000E-02	-186.760
25	4	0.238000	-0.857000	-81.0994

LIFT AND DRAG DISTRIBUTION ALONG WING

STATION	CL	CD	ANGLE
1	0.181805	3.510116E-02	1.65791
2	0.348615	3.537197E-02	3.17903
3	0.495243	3.575068E-02	4.51613
4	0.620904	3.617996E-02	5.66201
5	0.726766	3.661662E-02	6.62736
6	0.814952	3.703274E-02	7.43151
7	0.887872	3.741279E-02	8.09649
8	0.947918	3.775017E-02	8.64403
9	0.997258	3.804392E-02	9.09395
10	1.03779	3.829636E-02	9.46353
11	1.07110	3.851140E-02	9.76733
12	1.09853	3.869355E-02	10.0175
13	1.12116	3.884728E-02	10.2238
14	1.13986	3.897671E-02	10.3944
15	1.15535	3.908547E-02	10.5355
16	1.16817	3.917669E-02	10.6525
17	1.17879	3.925297E-02	10.7493
18	1.18757	3.931651E-02	10.8294
19	1.19478	3.936909E-02	10.8951
20	1.20065	3.941216E-02	10.9487

21	1.20536	3.944687E-02	10.9917
22	1.20905	3.947414E-02	11.0253
23	1.21182	3.949466E-02	11.0506
24	1.21375	3.950898E-02	11.0681
25	1.21489	3.951742E-02	11.0785
26	1.21526	3.952021E-02	11.0819
27	1.21489	3.951742E-02	11.0785
28	1.21375	3.950898E-02	11.0681
29	1.21182	3.949466E-02	11.0506
30	1.20905	3.947414E-02	11.0253
31	1.20536	3.944688E-02	10.9917
32	1.20065	3.941217E-02	10.9487
33	1.19478	3.936911E-02	10.8951
34	1.18757	3.931652E-02	10.8294
35	1.17879	3.925297E-02	10.7494
36	1.16817	3.917670E-02	10.6525
37	1.15535	3.908549E-02	10.5356
38	1.13987	3.897672E-02	10.3944
39	1.12116	3.884730E-02	10.2238
40	1.09854	3.869358E-02	10.0175
41	1.07111	3.851143E-02	9.76737
42	1.03779	3.829639E-02	9.46357
43	0.997264	3.804396E-02	9.09401
44	0.947926	3.775022E-02	8.64411
45	0.887884	3.741285E-02	8.09658
46	0.814966	3.703281E-02	7.43164
47	0.726784	3.661670E-02	6.62752
48	0.620925	3.618004E-02	5.66221
49	0.495269	3.575076E-02	4.51638
50	0.348646	3.537203E-02	3.17932
51	0.181842	3.510120E-02	1.65824
52	4.008277E-05	3.500000E-02	4.046887E-04

APPENDIX 10.2

FIGURE 10A2.1

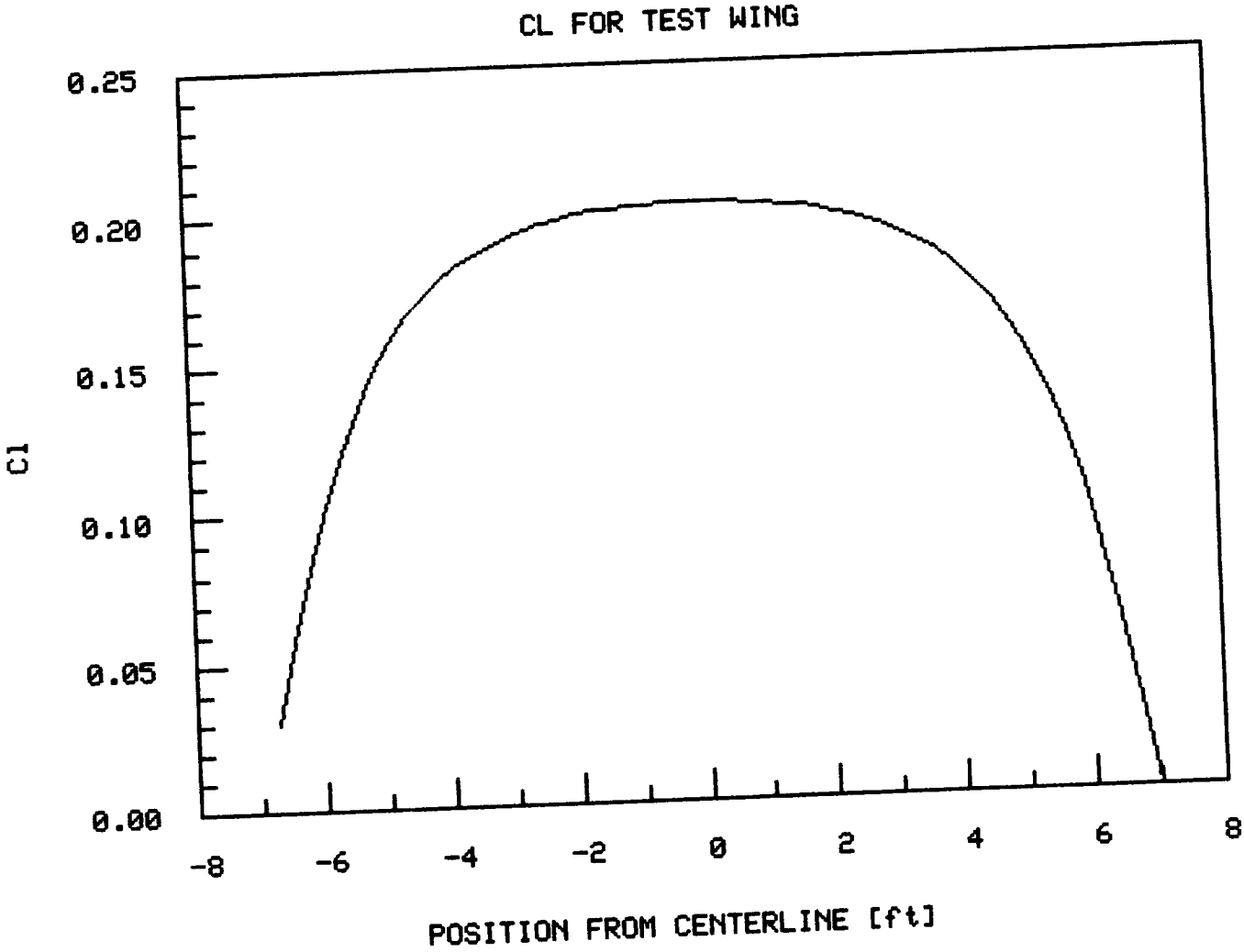

FIGURE 10A2.2

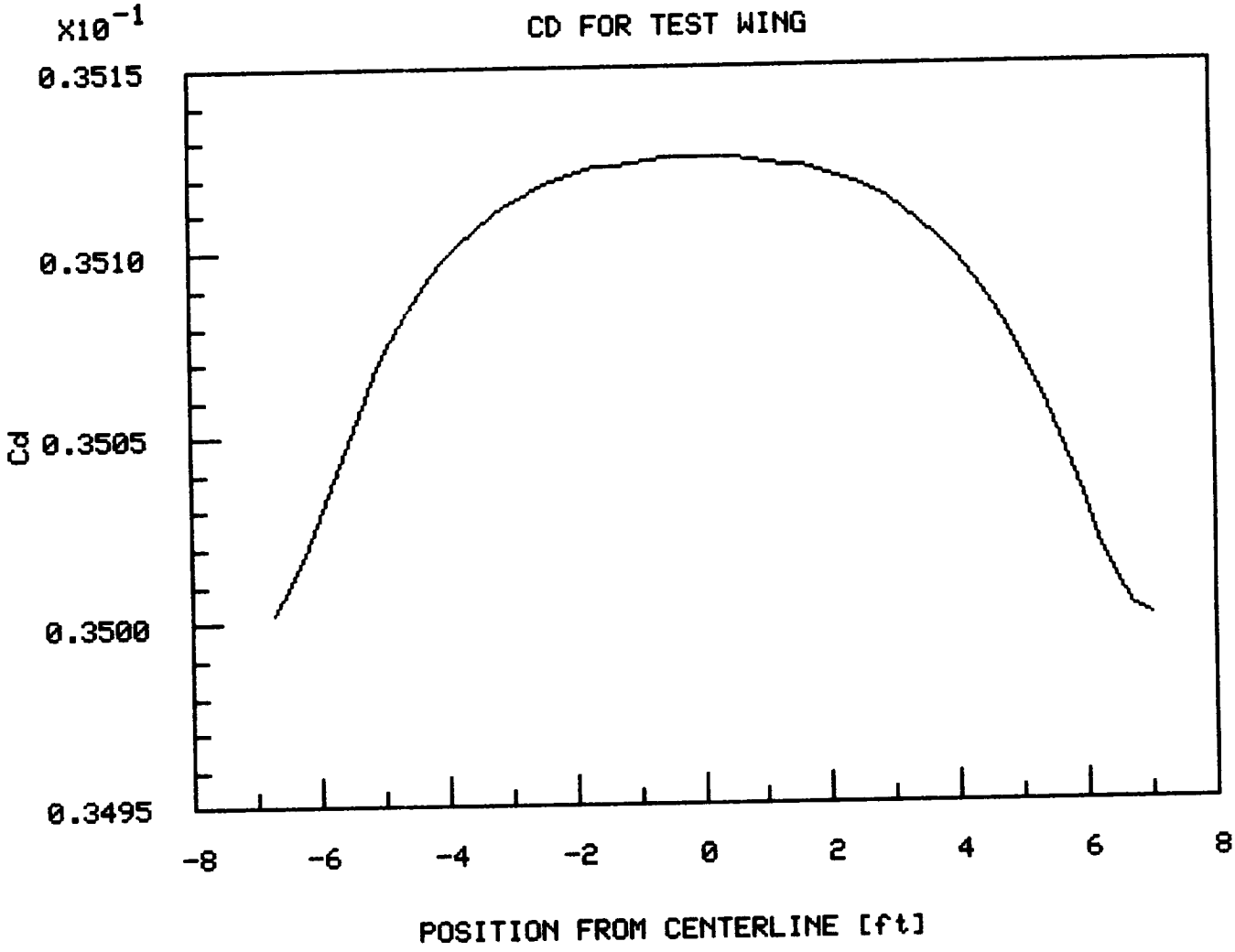

FIGURE 10A2.3

ALPHA=2 deg.

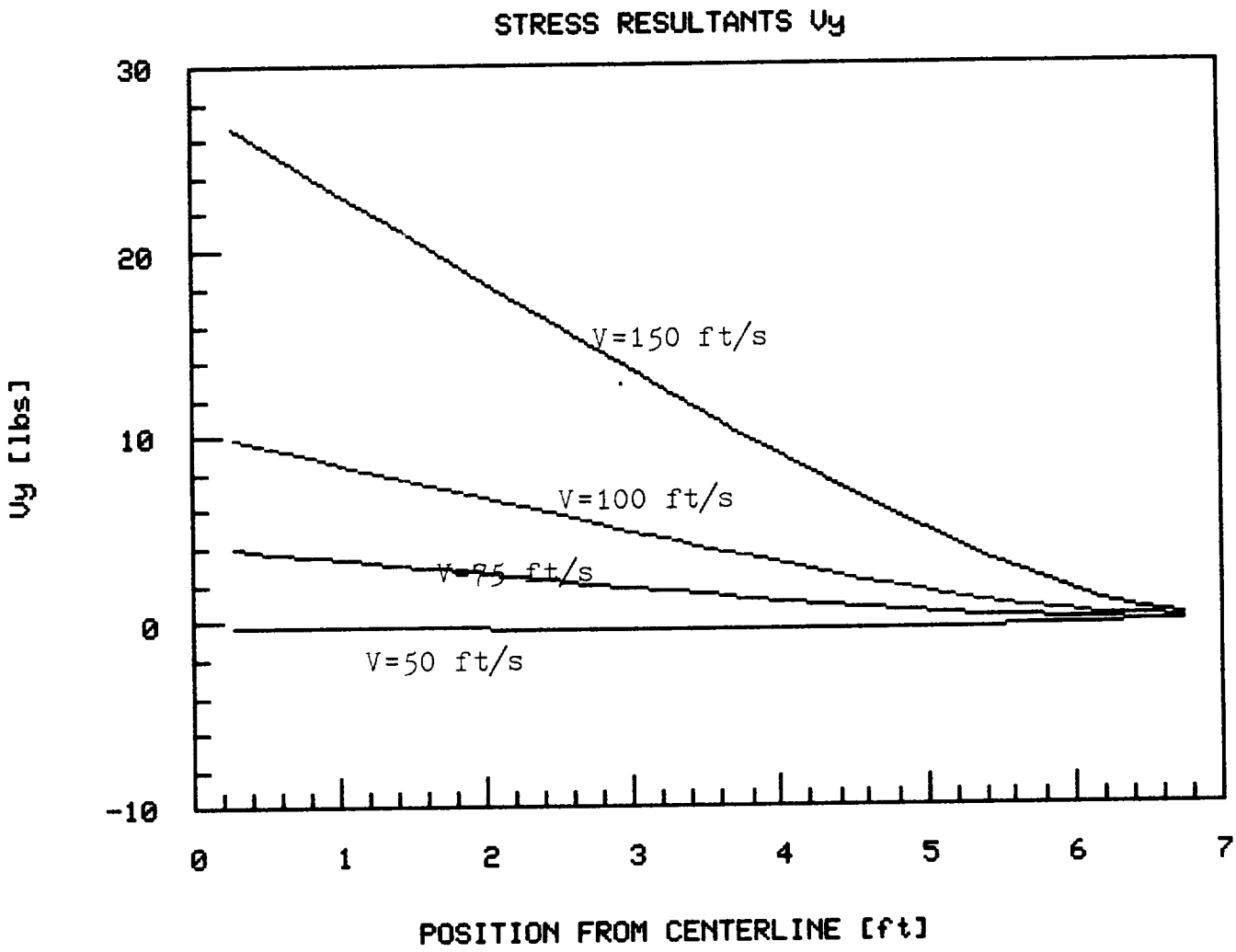

FIGURE 10A2.4

ALPHA=2 deg.

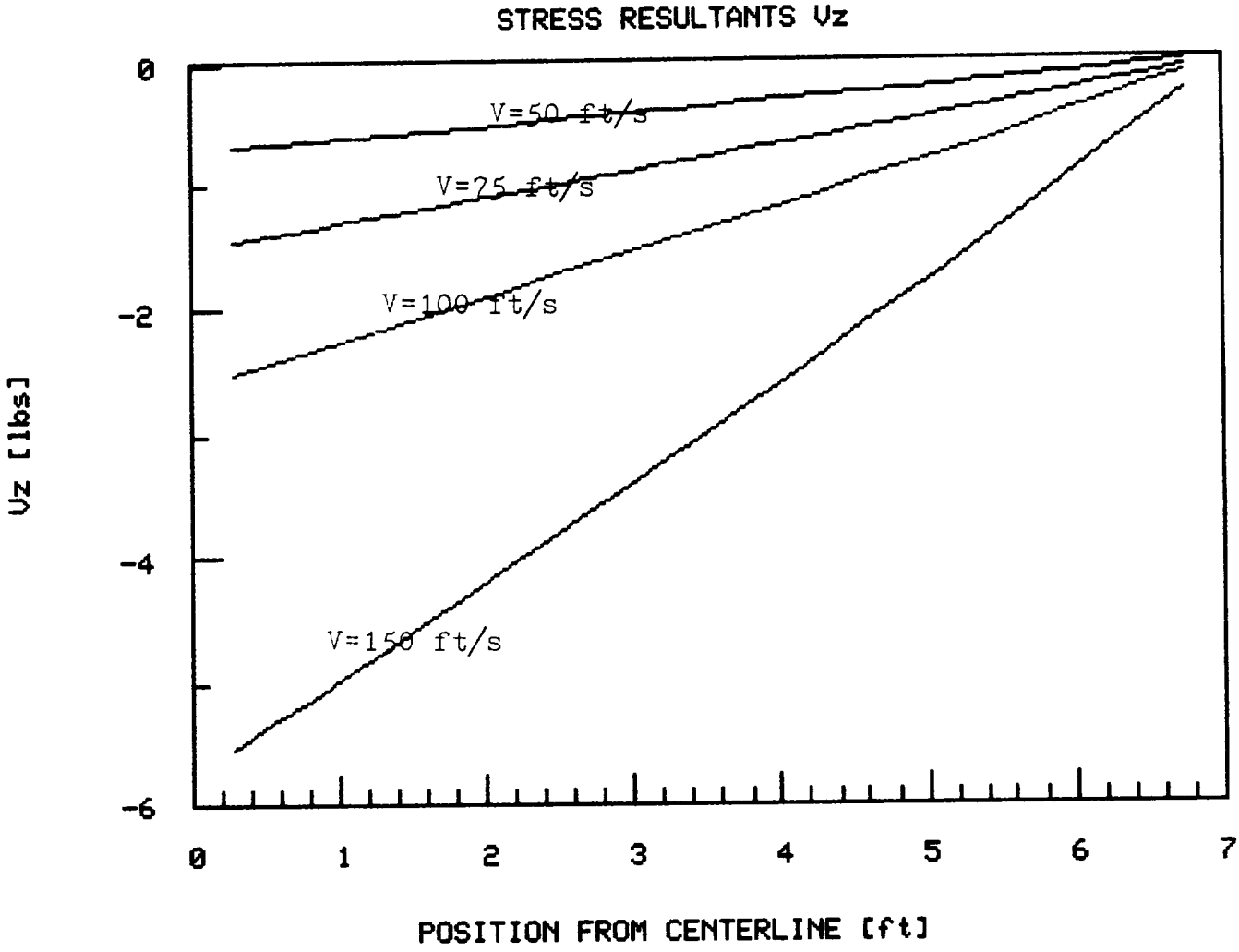

FIGURE 10A2.5

ALPHA=2 deg.

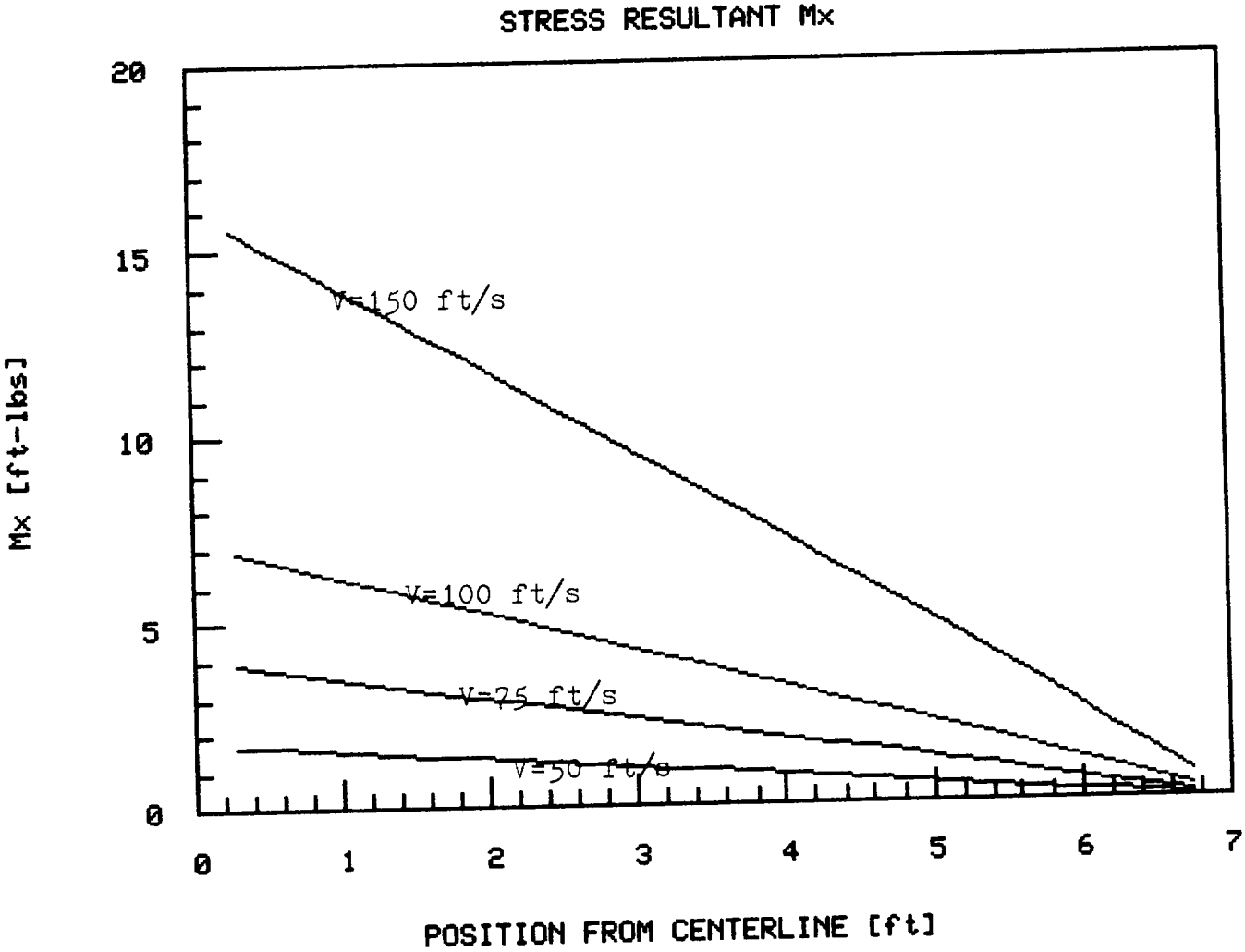

FIGURE 10A2.6

ALPHA=2 deg.

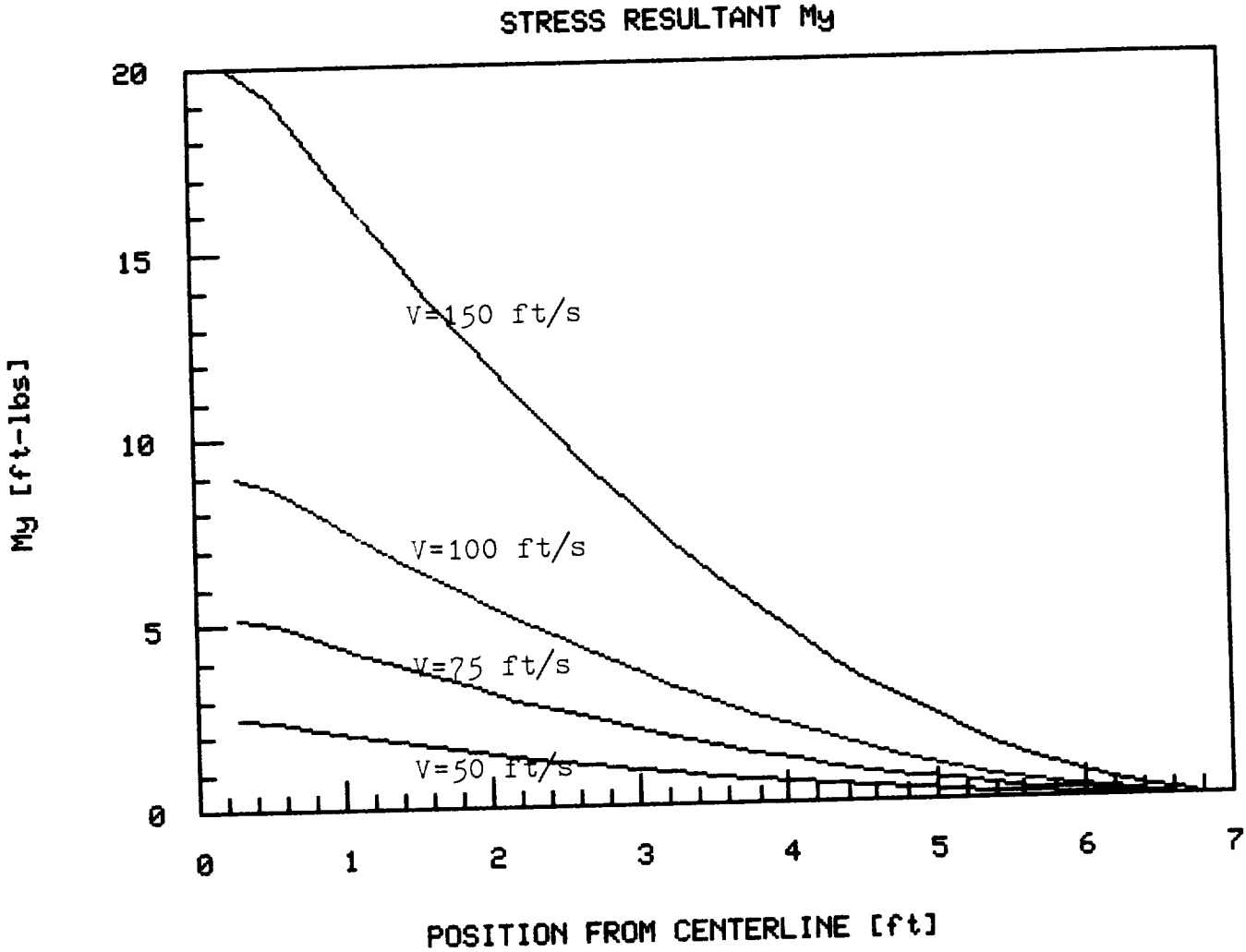

FIGURE 1CA2.7

ALPHA=2 deg.

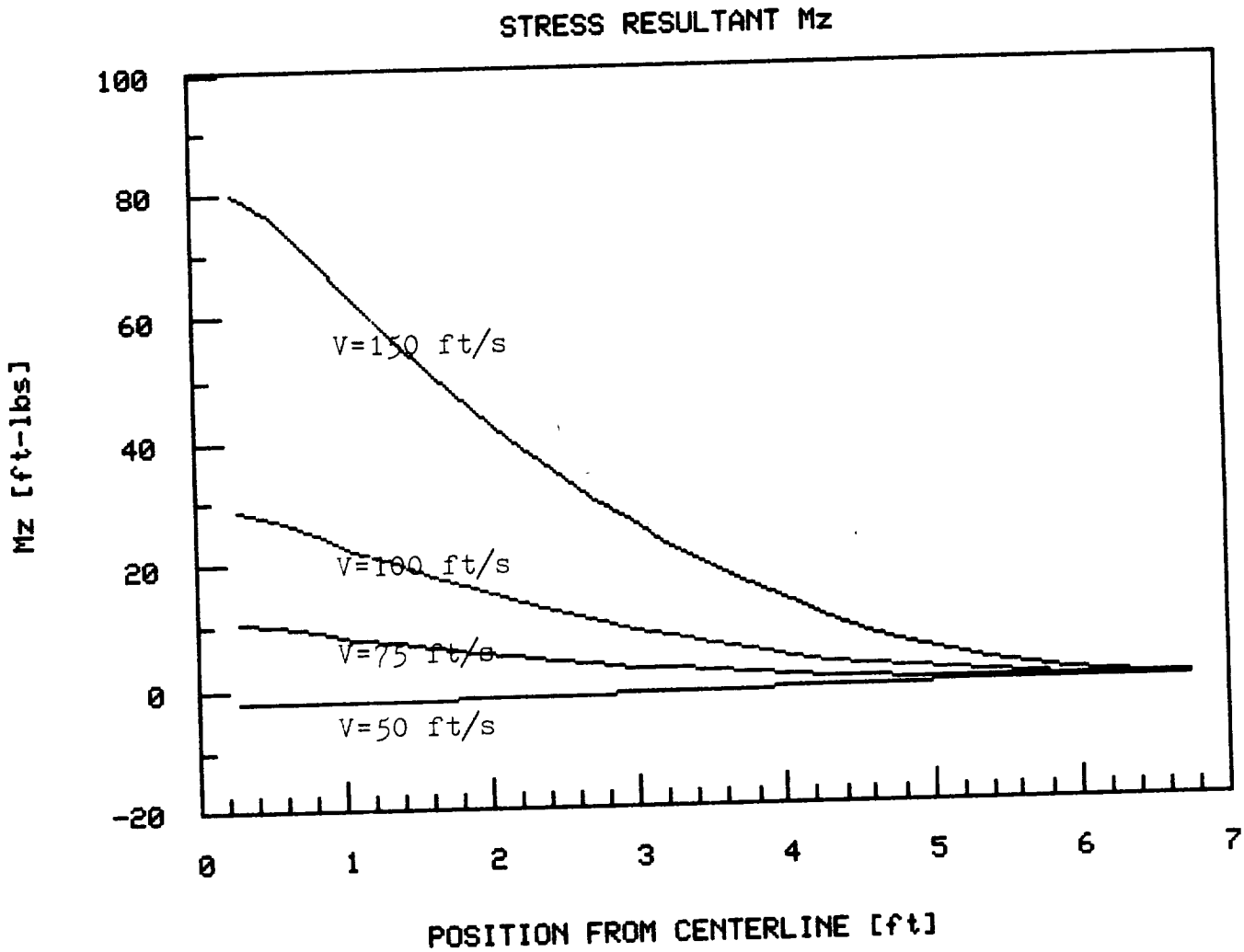

FIGURE 10A2.8

V=60 ft/s

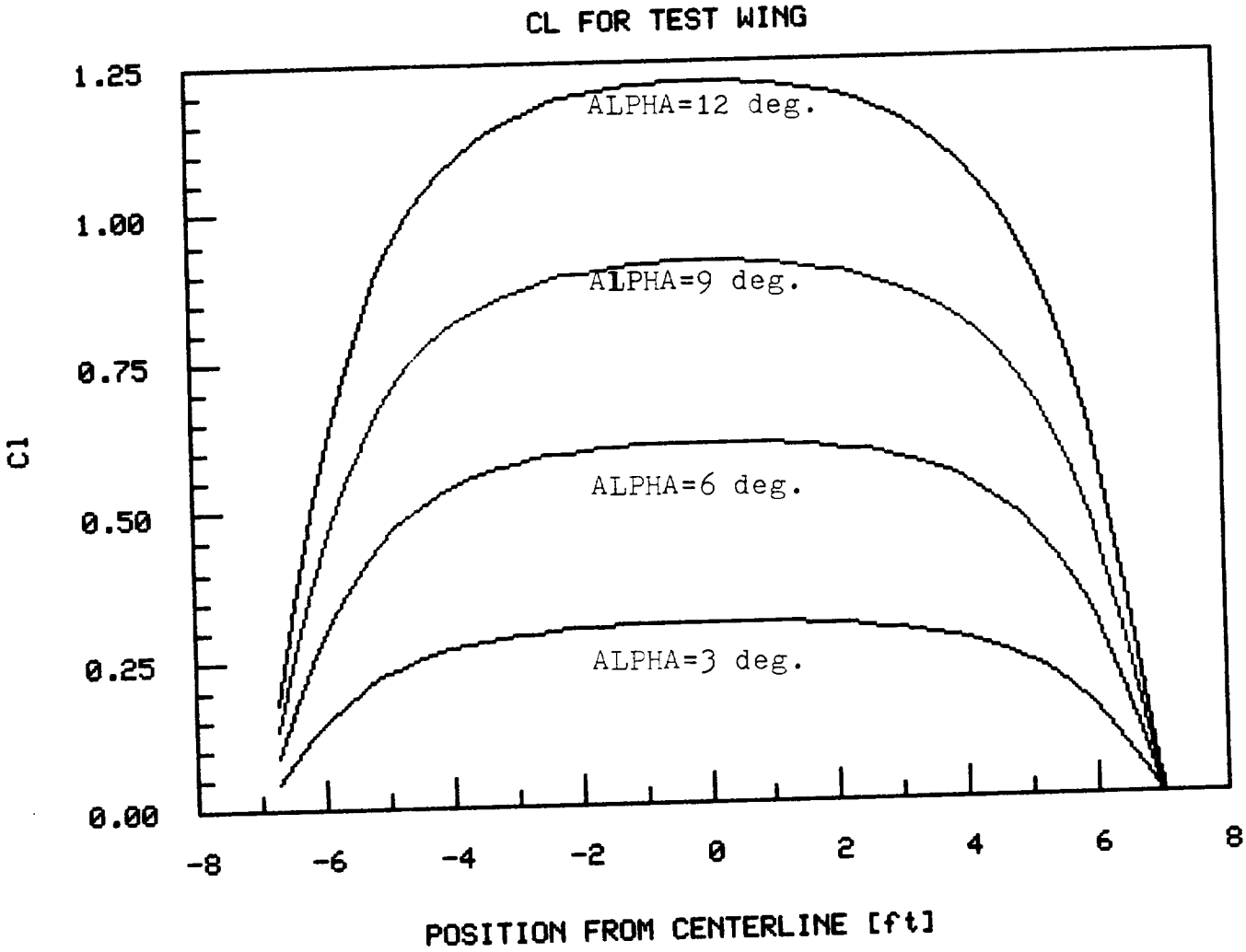

FIGURE 10A2.9

V=60 ft/s

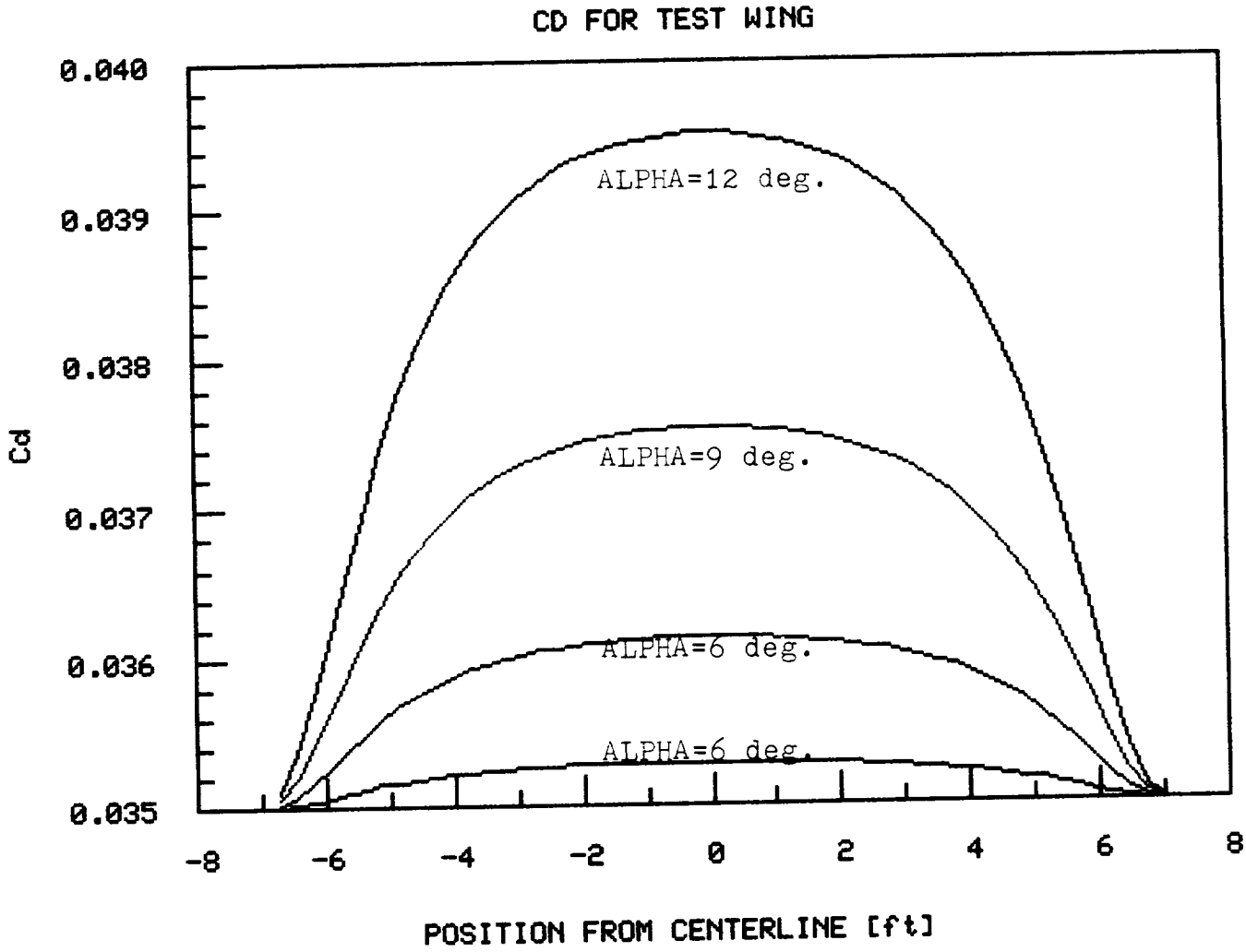

FIGURE 10A2.10

V=60 ft/s

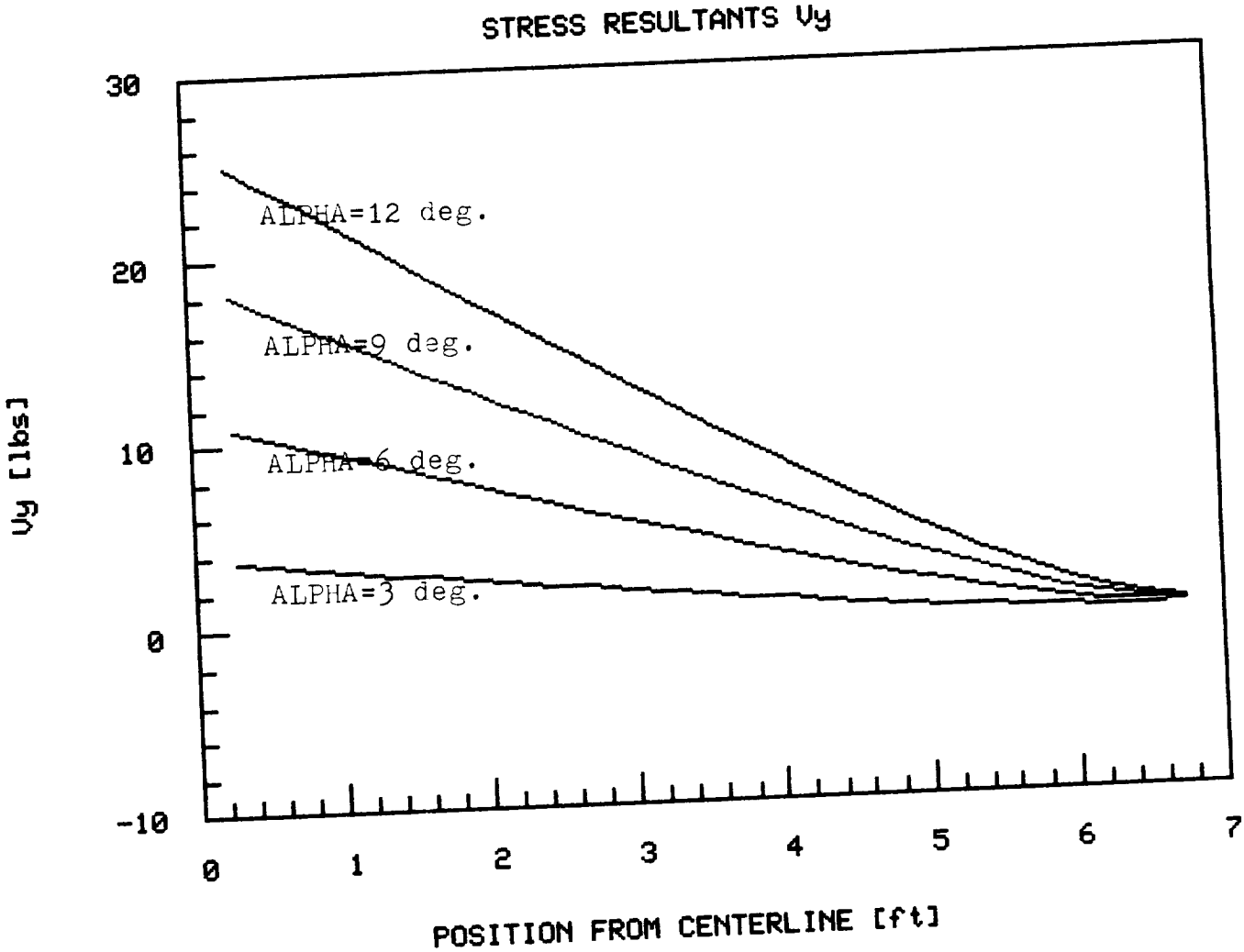

FIGURE 10A2.11

V=60 ft/s

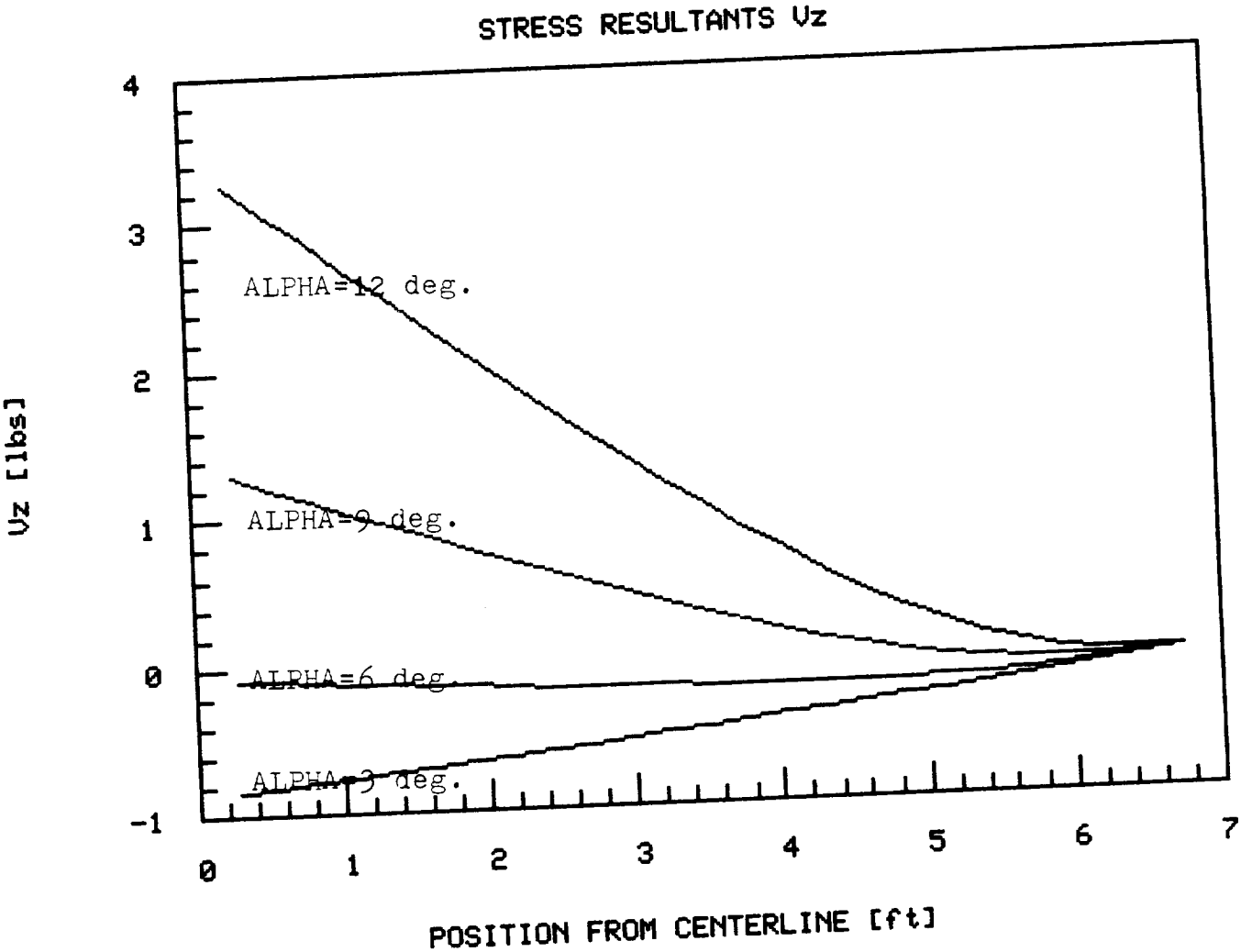

FIGURE 10A2.12

V=60 ft/s

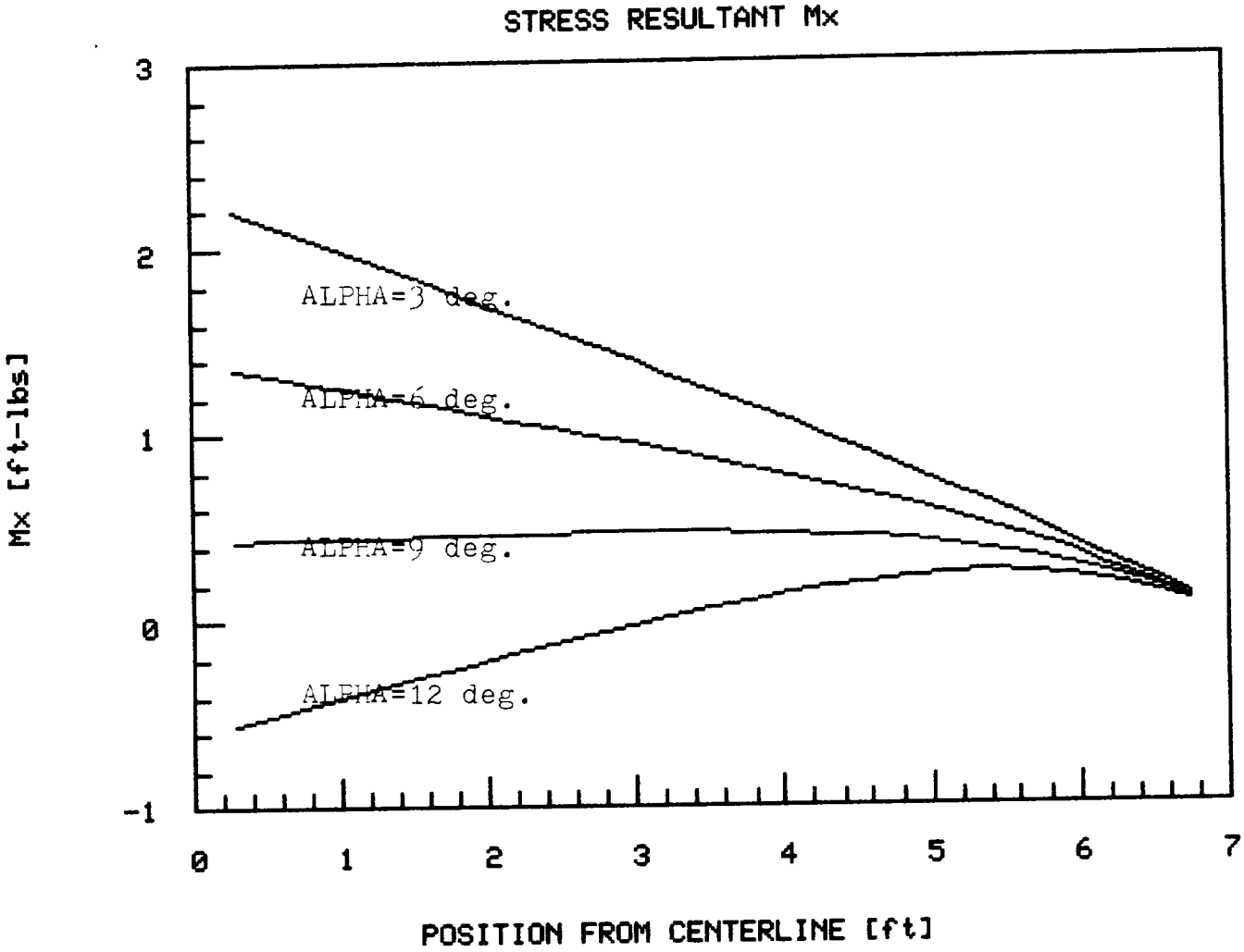

FIGURE 10A2.13

V=60 ft/s

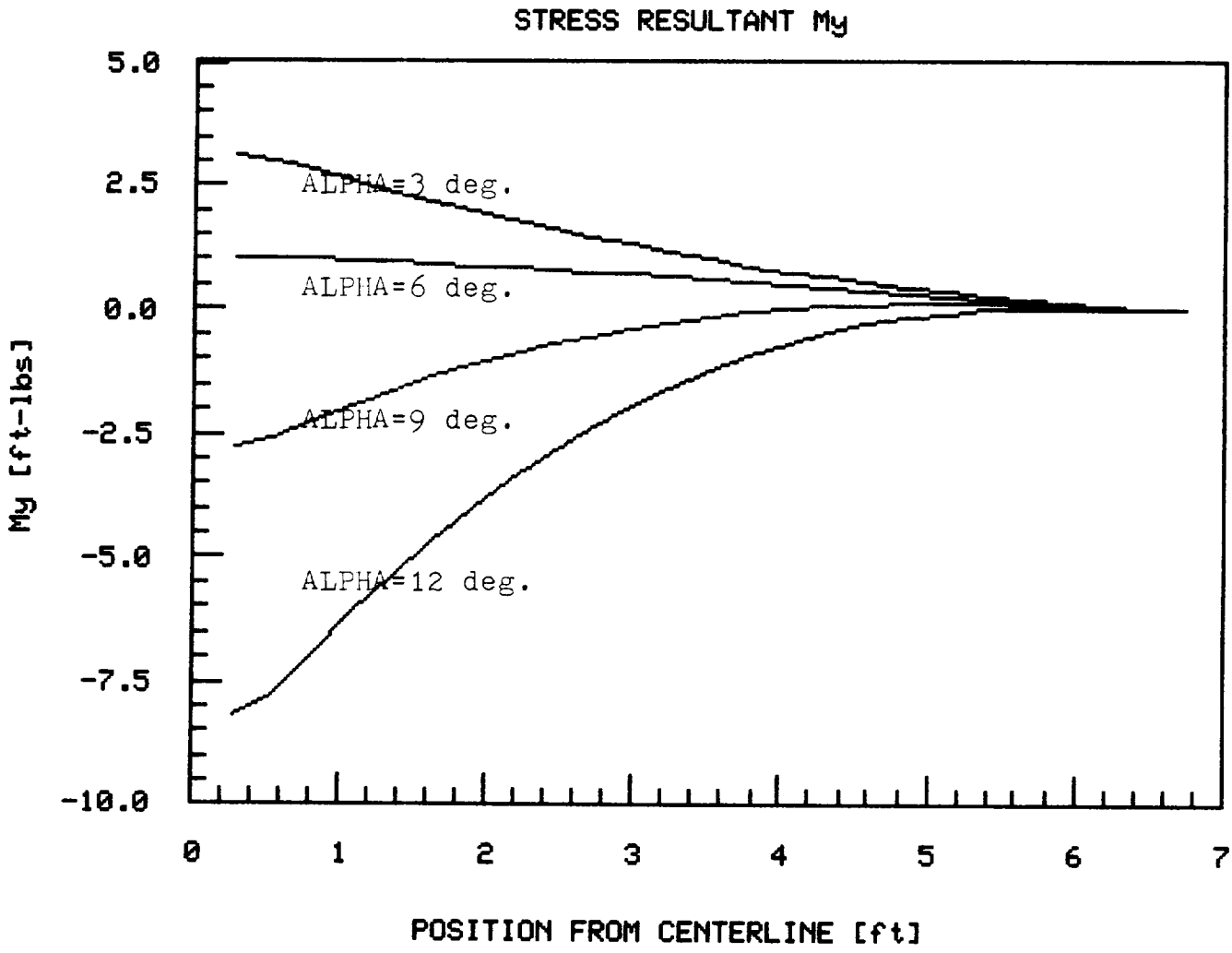

FIGURE 10A2.14

V=60 ft/s

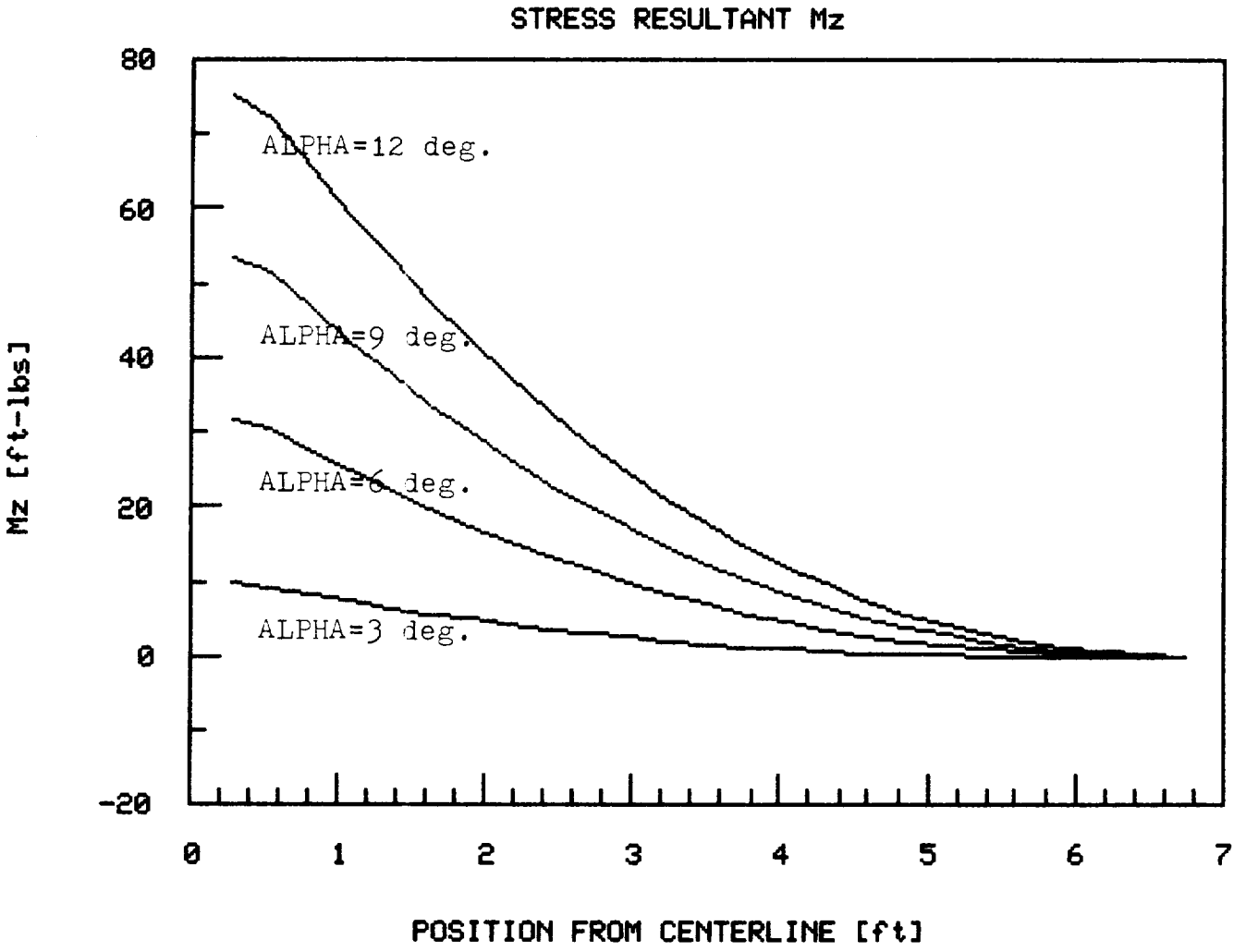

CHAPTER 11

AERODYNAMIC INTERFERENCE

INTERFERENCE

A requirement of this design is valid interpretation of collected data. Thus it is necessary to understand the flow seen by the test section and to ensure that the test section is out of the boundary layer.

The fixed parameters were density, viscosity, and flow condition (that is, turbulent). The horizontal distance varied from 1 to 3 ft, the freestream velocity from 50 to 160 ft/s, and the vertical distance from zero (at the fuselage surface) to infinity. The density and viscosity could have been varied with altitude if desired, but sea-level properties were used.

It was determined that the test section will be affected most strongly by the boundary layer over the fuselage surface. Obviously, the test section must never be in the boundary layer. From a theoretical approach, the approximate (two-dimensional, flat plate) height of the turbulent boundary layer was not difficult to find: $d = 0.37 * x / Re_x^{0.2}$ where $Re_x = r\ n\ x / m$ (see Appendix 11). The resulting Reynold's number was a local property (Re_x), and would not fall within the 4E4->1E6 Re range based on wing root chord. Therefore, the test section would safely see Re rather than the Re_x seen by the boundary layer directly below the test section.

Calculation of d requires knowing whether the flow is turbulent or laminar. Although the plane will be as clean as possible, the flow will still be turbulent. The Delta Monster will see its largest boundary layer, δ = 0.85 in, at the rear of the fuselage (3 feet) and freestream velocity of 50 ft/s (see Figure 11.1).

For completeness, a temperature boundary layer also exists, not coincident with the velocity boundary layer. According to White (p. 325), the assumption of incompressibility removes any interdependence of velocity and temperature. Note that there will also be extremely thin boundary layers on the upper and lower surfaces of the test section. In addition, the tripod supports will disturb the flow.

The top surface of the fuselage section is flat forward of and underneath the test section, so flow acceleration will be minimal (boundary layer growth slows as flow moves aft on a flat surface).

Fig. 11.1: Boundary Layer Thickness

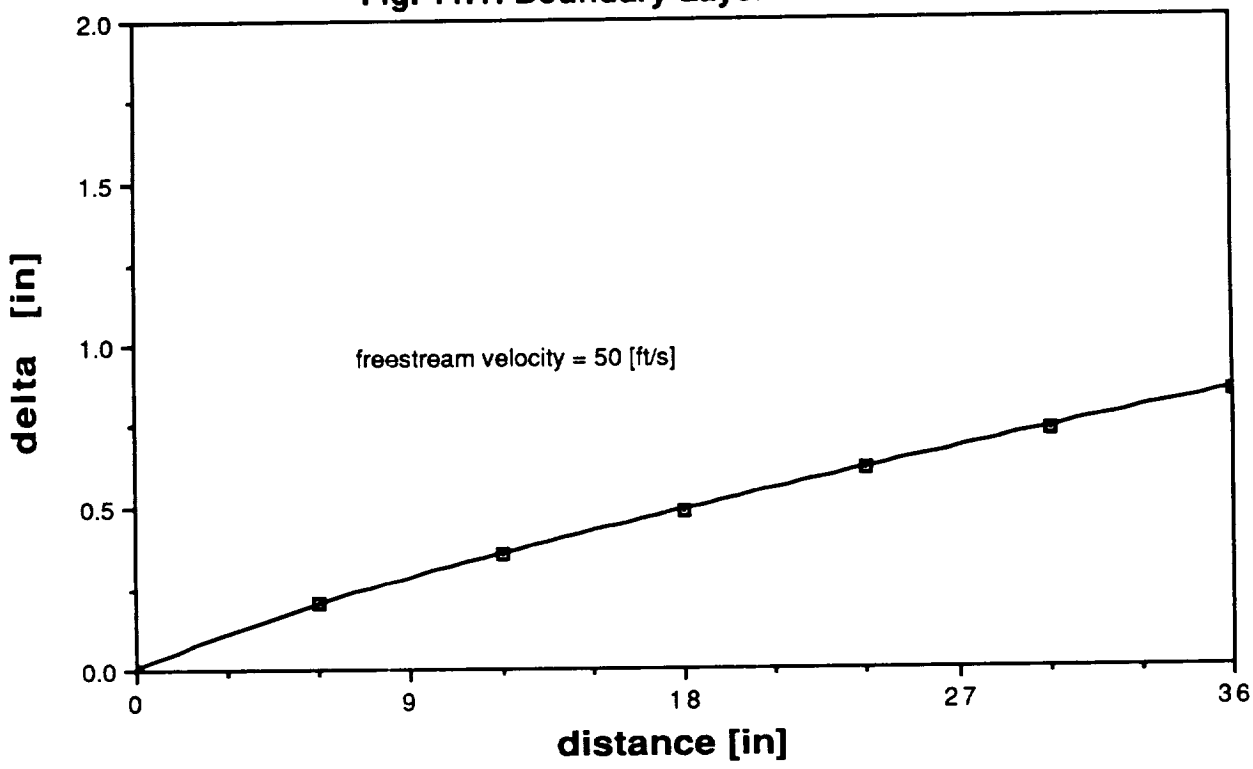

Consideration was given to a wide fuselage to maximize flow consistency, possibly even attaching a plate to the top of the fuselage to widen and lengthen the fuselage section below the delta wing. Two alternate, but related ideas were either to instrument the top surface of the fuselage or to mount a wake rake vertically from the fuselage when the test section is not present. The proposed Delta Monster uses this wake rake. The goal is to understand the flow both with and without the delta wing. The fuselage was designed with serious consideration given to the test section. Notably, the fuselage will not be lifting while the system is gathering data.

Because the delta wing was above the fuselage while the wing was below, much of the lift distribution and downwash was blocked. The wake rake was necessary to show flow behavior, since there was no reliable three-dimensional flow prediction method.

Serious prediction problems arise out of the three-dimensional flow agitated by the wing / fuselage combination. The result is "wedge shaped separations over the top of the wing" (Stokely, p. 78) and fuselage, near the wing root. Also, a strong field of downwash exists behind the wing, with a similar upwash field ahead of the wing.

The relationship between boundary layer thickness, location, and Reynold's number is the same whether the surface is flat, inclined, or curved -- the proportionality constant, however, is different (Schlichting, pp. 111-112). Use of 0.37 as the proportionality constant should yield results very close to reality, since x and Re_x are at least one order of magnitude larger than the constant.

A serious control discontinuity occurs when the test section moves into or out of separated flow, notably on takeoff or landing. The test section is effectively stalled when in the separated flow, but will lift and drag when outside this region. Transition may be difficult, as the test section may want to porpoise in and out of the separated zone. The test section is located where its lift and drag vectors oppose each other when added into the pitching moment.

REFERENCES

Abell, "Turbulation," Soartech 1, pp.12-21.

Anderson, J., Fundamentals of Aerodynamics, pp. 142-144, 235, 264,517-542.

Fox and McDonald, Introduction to Fluid Mechanics, pp. 425-482.

Kuethe and Chow, Foundations of Aerodynamics, pp. 71-177.

Schlichting, Boundary Layer Theory, pp.107-112, (1960).

Simons, Model Aircraft Aerodynamics, pp. 31-38.

Stokely, H., "Some Ideas on the Aerodynamics of Fuselage Design," Soartech 4, pp. 78-80.

White, Viscous Fluid Flow, pp. 325-471.

APPENDIX 11.1

```
: \LFORD UNIVERSITY FTN77 VER. 2289     <USER3>S0385078&8>STUDENT>DSGN1.F77        10

COMPILER OPTIONS:  LISTING INTL DCLVAR NOMAP CHECK NOBIG LOGL DYNM NOOFFSET LGO N
                   NOFRN FPN NOLUNFREC NOSILENT NO_OPTIMISE NOIMPURE

    0001      C MICHAEL J. FLYNN
    0002      C AERO 441 -- GREEN MISSION
    0003      C DELTA MONSTER
    0004      C HEIGHT OF BOUNDARY LAYER
    0005      C = F(RE)
    0006      C = F(VEL,RHO,VIS,DIS)
    0007      C
    0008      C RE  = REYNOLD'S NUMBER AT POINT
    0009      C VEL = FREESTREAM VELOCITY, [FT/SEC]
    0010      C DIS = DISTANCE FROM TIP OF FUSELAGE TO POINT, [FT]
    0011      C RHO = DENSITY (CONSTANT), [SL/(FT**3)]
    0012      C VIS = VISCOSITY (CONSTANT), [SL/(FT*SEC)]
    0013      C
    0014            REAL DIS(20),VEL(20,20),RE(20,20),DT(20,20)
    0015
    0016            IWR=6
    0017            RHO=0.0023769
    0018            VIS=3.73E-07
    0019            WRITE(IWR,*) 'VISCOSITY =',VIS,'[SL/(FT*SEC)]'
    0020            WRITE(IWR,*) 'DENSITY =',RHO,'[SL/(FT**3)]'
    0021            DO 10 I=1,3
  0022.01           DIS(I)=REAL(I)
  0023.01           WRITE(IWR,*) 'DISTANCE =',DIS(I),'[FT]'
  0024.01           WRITE(IWR,*) '      VEL                    RE                TURB'
  0025.01           WRITE(IWR,*) '    [FT/SEC]                 []                [IN]'
  0026.01           DO 20 J=1,16
  0027.02           VEL(I,J)=10.*REAL(J)
  0028.02           RE(I,J)=RHO*VEL(I,J)*DIS(I)/VIS
  0029.02   C TURBULENT
  0030.02           DT(I,J)=12.*0.37*DIS(I)/(RE(I,J)**0.2)
  0031.02           WRITE(IWR,*) VEL(I,J),RE(I,J),DT(I,J)
  0032.02    20     CONTINUE
  0033.01    10     CONTINUE
  0034.01
    0035            STOP
    0036            END



END OF COMPILATION CLOCKED      .436 SECONDS
```

[SCOSITY = 3.730000E-07[SL/(FT*SEC)]
ENSITY = 2.376900E-03[SL/(FT**3)]

DISTANCE = 1.00000 [FT]

VEL [FT/SEC]	RE []	TURB [IN]
10.0000	63723.9	0.485873
20.0000	127448.	0.422977
30.0000	191172.	0.390030
40.0000	254895.	0.368223
50.0000	318619.	0.352151
60.0000	382343.	0.339541
70.0000	446067.	0.329233
80.0000	509791.	0.320556
90.0000	573515.	0.313093
100.000	637239.	0.306565
110.000	700963.	0.300777
120.000	764686.	0.295588
130.000	828410.	0.290893
140.000	892134.	0.286614
150.000	955858.	0.282686
160.000	1.019582E+06	0.279061

DISTANCE = 2.00000 [FT]

VEL [FT/SEC]	RE []	TURB [IN]
10.0000	127448.	0.845954
20.0000	254895.	0.736445
30.0000	382343.	0.679082
40.0000	509791.	0.641113
50.0000	637239.	0.613130
60.0000	764686.	0.591175
70.0000	892134.	0.573227
80.0000	1.019582E+06	0.558121
90.0000	1.147030E+06	0.545128
100.000	1.274477E+06	0.533761
110.000	1.401925E+06	0.523683
120.000	1.529373E+06	0.514648
130.000	1.656820E+06	0.506475
140.000	1.784268E+06	0.499024
150.000	1.911716E+06	0.492185
160.000	2.039163E+06	0.485873

DISTANCE = 3.00000 [FT]

VEL [FT/SEC]	RE []	TURB [IN]
10.0000	191172.	1.17009
20.0000	382343.	1.01862
30.0000	573515.	0.939281
40.0000	764686.	0.886763
50.0000	955858.	0.848058
60.0000	1.147030E+06	0.817691
70.0000	1.338201E+06	0.792867
80.0000	1.529373E+06	0.771972
90.0000	1.720544E+06	0.754000
100.000	1.911716E+06	0.738278
110.000	2.102888E+06	0.724338
120.000	2.294059E+06	0.711842
130.000	2.485230E+06	0.700537
140.000	2.676402E+06	0.690230
150.000	2.867573E+06	0.680771
160.000	3.058745E+06	0.672041

CHAPTER 12

DELTA WING

DELTA WING

Since the purpose of this vehicle is to compliment wind tunnel tests it was decided that the vehicle should be designed such that it can accommodate a wide range of test wings for the given flight regime. From the work done in stability it was found that testing many different wings was a feasible option, thus giving the RPV concept some validity.

The goal of obtaining in-flight data on the delta wing is going to be accomplished through the use of pressure ports on the top surface of the wing. Each test wing is expected to contain approximately 100 pressure taps. These taps will be spaced differently on each half of the wing to allow for pressure measurement at a large number of data points (see Figure 12.1). This also serves to reduce the total number of channels required in the data acquisition system.

Another conclusion concerning instrumentation of the delta wing was that it needs only to be instrumented on the top surface. To obtain lower surface pressure readings the wing can be flipped over and the tests performed again. This too serves to allow for the inclusion of a large number of data points without putting a high demand on the data acquisition system.

One major concern in dealing with a flying test-bed is determining possible flow field interference from the fuselage or other aircraft components. In order to determine the existence and quantify such interference it will be necessary to make trial flights without the test wing mounted on the aircraft. For this reason it is essential that the aircraft be stable both with and without the delta wing.

Because the delta wing and its associated flows are still a developing topic it would be beneficial to incorporate some form of flow visualization system on the test vehicle. Because of difficulties associated with in-flight smoke visualization systems an alternate system is suggested. Although no work has been done in this area a system such as dyed monofilament fishing line coupled with a strobe light and operated at night is a possible solution.

MAP OF PRESSURE PORTS ON A 60° SWEEP DELTA WING

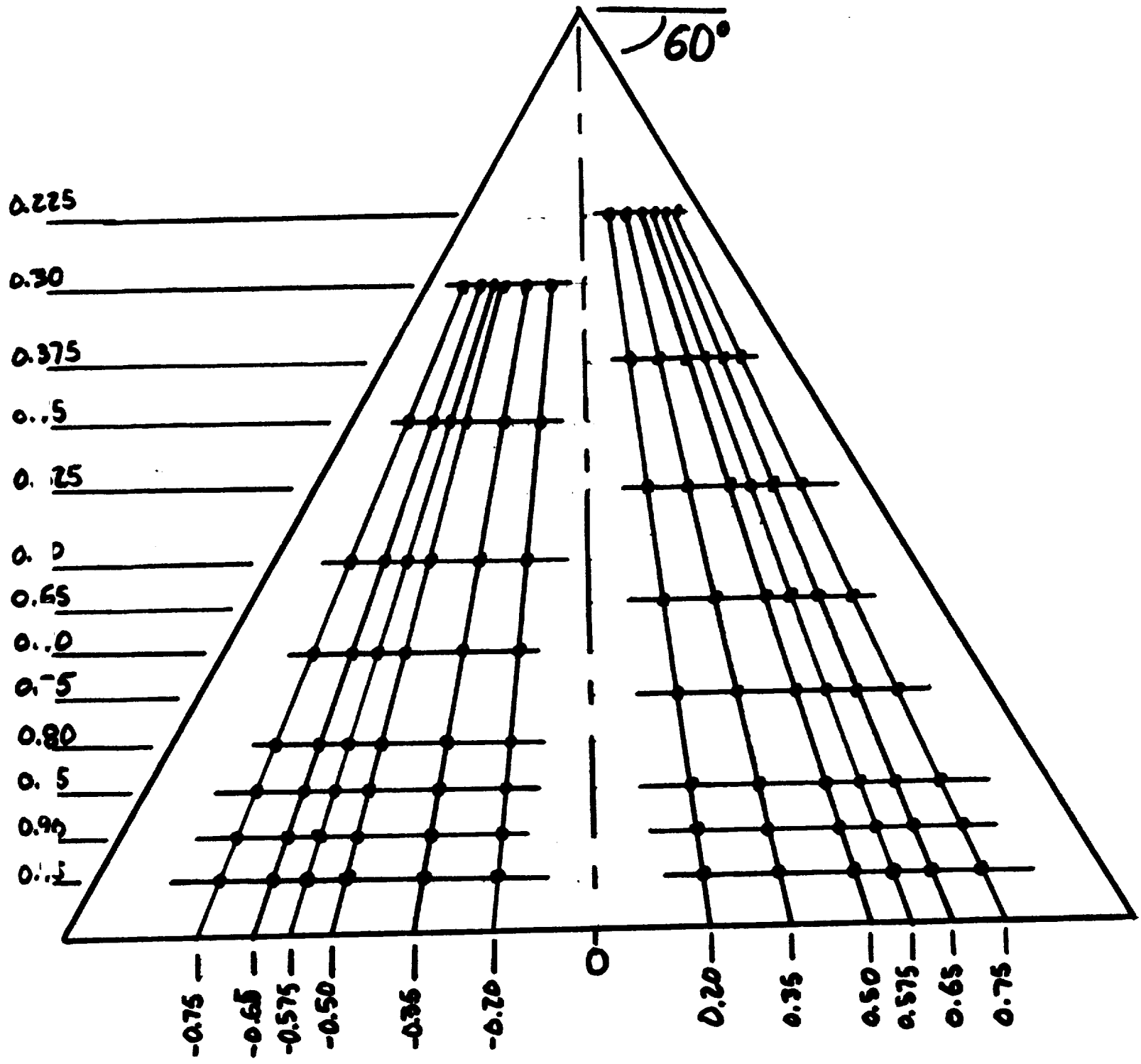

FIGURE 12.1

CHAPTER 13

MANUFACTURING REQUIREMENTS

MANUFACTURE

Manufacture of the proposed RPV is of major concern because its effectiveness could determine the practicality of the concept. Small-scale production could be accomplished with the proper equipment and a somewhat substantial expenditure of time. Fabrication in this manner would entail the development of templates and patterns for all phases of construction. The actual vehicle could then be constructed by hand - fabricating each component of the aircraft. Additional time must be spent assembling these components into the complete structure. Although this method assures the high quality of the finished product it is very time consuming, hence very costly.

Perhaps a more viable option for producing the aircraft would be to utilize current full-scale, automated production systems. This means that the aircraft components would all be machine fabricated (die-cut) and marketed as a ready-to-assemble kit. This has the advantage of reducing the overall production cost (assuming there would be a sufficient market for the vehicle) while boosting production rate significantly. This is also an attractive proposition from the consumer's point of view because it eliminates the time requirements of fabricating an entire vehicle.

An even more desirable option for the consumer would be to have the vehicle furnished completely assembled and ready to fly. This would eliminate all construction time and cost liabilities and, if inexpensive enough, would provide a distinct advantage over the previous options. Producing such a vehicle would require the expansion of the automation system to include operations to align and bond the structural components. It was thought that such a system might not be cost effective and thus from a production perspective might not be a feasible task.

CHAPTER 14

SYSTEM SAFETY CONSIDERATIONS

SYSTEM SAFETY CONSIDERATIONS

The proposed Delta Monster is very safety conscious, with four main areas of concern. First, the structural design of the aircraft must be sound so that it does not come apart, especially during the catapault launch. Second, the plane must be launched in a large enough area in case it goes out of control. Third, weather conditions must be very good during flight. And fourth, a pilot must be standing by to take manual control of the design if there is a malfunction in the preprogrammed system flying the design.

The Delta Monster was designed to handle 2g loads and will not be subjected to greater loads. This should ensure the craft will not break, resulting in loss of time and money and debris hazard. The most critical structural envelope is launch, with ground impact during retrieval of secondary consideration. Breakage on impact will not pose a serious physical hazard. Since the design will be able to handle launch and retrieval the rest of the flight will not be a problem, as the flight mission is data collection, which is accomplished during steady level flight in good weather conditions.

The plane will be launched only away from people. Thus, during the launch phase, if the plane cannot be controlled to avoid crashing, people will not be injured.

Weather conditions must be very good for flight to take place. Valid data collection requires good, constant, known conditions. Consequently, little consideration was given to gust loads. Gusts would invalidate the data. Also, the plane must be kept in visual range during the entire flight which requires good weather.

During data collection, the proposed Delta Monster will be controlled by a computer. In the event that this system fails, the pilot will be able to override the computer and resume manual control of the aircraft. This system, therefore, allows for the acquisition of aerodynamic data using a remotely piloted vehicle without the need for concern over personal safety.

CHAPTER 15

PRODUCTION PLANS AND COST ESTIMATE

PRODUCTION PLANS AND COST ANALYSIS

The design of this RPV is of little use unless it can be constructed and operated as prescribed. A primary concern in the production of this aircraft was the overall cost. It was necessary that the RPV be designed such that the data obtained was of the same quality as that obtained in wind tunnel tests and the cost associated with the RPV comparable to that of wind tunnel testing. Hence a breakdown of the aircraft's cost was deemed necessary. The cost breakdown was as follows:

1. Structural materials.....$200
2. Propulsion system
   a. Engine.....$100
   b. Ducted Fan.....$150
3. Data Acquisition System
   a. 100 pressure transducers (@ $100 each).....$10,000
   b. 2 inclinometers (@ $250 each).....$500
   c. Signal Processing System.....$600
      1 RCT-3 transmitter
      1 RCRI-1C receiver
      1 RTEI encoder
      1 RTDI decoder
      1 RTI1 telemetry interface
   d. 10 Tattletale Model 5
      data acquisition systems (@ $325 each).....$3,250
   e. 120 pressure tubes.....$10
   f. 1 yaw indicator.....$50
   g. 1 heading indicator.....$400

TOTAL $15,260

CHAPTER 16

SOCIAL AND ENVIRONMENTAL IMPACT

SOCIAL & ENVIRONMENTAL IMPACT

The use of the remotely piloted vehicle as a test bed for data acquisition presents a number of environmental and social challenges. All of these can be met through creative planning and regulation. To avoid crashing into homes, commercial airliners, and adversely affecting radio and television communications, special zones for testing these vehicles should be established. The zones should lie outside of commercial aviation routes and should be placed on non-populated and non-residential land. In addition, the zones should be established on land that will permit sighting of the vehicle through all phases of the flight. Forested areas, especially those with dry seasons, are to be avoided. Parts of the ocean and remote lakes are preferred.

In the short run, the use of remotely piloted vehicles will most likely be confined to a relatively small number of businesses and research facilities. The cumulative noise and pollution will have a relatively small impact on the environment. Because this concept accelerates the rate of research, it will ideally maximize existing technologies and minimize their larger effects on the environment. In practice, however, there is very little to prevent the abuse of this research or its extension to high altitude flight. For this reason, remotely piloted vehicles for the specific purpose of data acquisition should be licensed. All vehicles beyond a certain weight , with a particularly noisy or powerful propulsion system, or with telemetry beyond a certain power level should require a permit to be flown and must be flown in the special zones. Extension to flight beyond line of sight should not be granted in these zones, unless adequate means to survey the flight of the vehicle can be established. Although primarily designed for low level altitude tests, the Delta Monster has the capability of achieving much higher altitudes and falls within this category.

In the long term, the use of remotely piloted vehicles for data acquisition will increase precision technology in the construction of these craft. These technologies will permeate the toy industry and educational system, increasing the problem of regulation while also increasing the general population's knowledge of flight and aerodynamics. Because the

skys and airways are continually being carved up as the population increases, special testing zones must eventually subordinate themselves to the demands of travel and communication. A small number of permanent zones might therefore be established at the national level. Finally, the number of unidentified flying objects will remain constant as the education of the general population increases with the increase of flying objects.

CHAPTER 17

TECHNOLOGY DEMONSTRATOR

TECHNOLOGY DEMONSTRATOR

The technology demonstrator was constructed primarily as a scaled model to test the feasibility of the basic aerodynamic configuration. This scale was based on the desire to have the technology demonstrator wing span equal to one half of the actual design wing span. The ability of certain design decisions to produce a stable, controllable environment in which data acquisition is meaningful, was of critical and immediate importance. The actual construction of the demonstrator provided insights into the structural integrity of the design, and in the case of the horizontal tailplane, exposed problems that might arise during the construction of the actual RPV. Launch was to be achieved by a high speed hand launch to avoid the low Reynold's numbers and stall associated with the scale model. The flight test path was chosen to maximize endurance during the cruise phase.

The critical differences between the actual RPV and the demonstrator are the different power plants and weights. The Reynold's number of the scale model was not directly matched with the RPV design because the velocity and chord combinations produced flight conditions not able to be achieved by the Astro-15 propulsion unit. The weight was specifically reduced from the 28.6 lbs of the RPV design to 5 lbs to meet the capabilities of the Astro-15.

The scaling to the scale model at a disproportionate weight and for far lower Reynold's numbers necessitated a change in the selection of the airfoil. In choosing the airfoil, the wing chord, and corresponding aspect ratio, a tradeoff between approximating the aerodynamic configuration of the RPV and producing a technology demonstrator with enough lift and low enough stall velocity to get airborne surfaced.

Thus, the airfoil selected was the Selig 2031. In switching to a thin laminar airfoil, the Clmax was increased for the chosen Reynold's number. With this airfoil, the chord was not reduced to the 6 inch proportionate length because it was feared that it would not produce enough lift at such a low Reynold's number (a situation not present with the RPV and its high powered turbulent trip design). A compromise between the chord length and aspect ratio was reached at a chord of 10 inches and aspect ratio of

8.2. Switching from a high to moderate aspect ratio increased the induced drag by 40%, increased the stall velocity, and lowered the lift curve slope, while still maintaining a comparable Clmax[1]. The increased sensitivity to pitch disturbances introduced with the thinner Selig airfoil was compensated for by this decrease in aspect ratio. Concurrently, the resulting wing area of 6 ft^2 produced a stall speed of 28.8 ft/sec, one of the limits of acceptable launch velocities.

The decreased control in roll and increased induced drag produced effects that necessitated changes to the control configuration implemented by larger vertical tailplanes. The ailerons were discarded in the design of the RPV, despite the loss in roll control, to keep the design structurally simple. The low wing design, twin boom, tail assembly, and wing dihedral were all incorporated into the technology demonstrator after these initial compensations were made. The fuselage was built to approximate that of the RPV within the existing construction expertise.

Analysis of the existing Astro-15 power plant for a variety of propellers set the climb velocity at 39 ft/sec for maximum performance and minimum power expended. After the initial hand launch, in which it is hoped that the stall velocity can be achieved through swift and nimble feet, the 12 in. diameter propeller will accelerate the demonstrator to an initial obstacle clearing velocity of 32 ft/sec. After the first 50 vertical feet are cleared, the motor speed will be increased to 6200 RPM and a corresponding velocity of 39 ft/sec to initiate the climb to 500 ft. In this maneuver, 0.18 amp-hrs will be expended. At cruise altitude, the RPM will be increased to 8243 to conserve power and the velocity will be decreased to 34 ft/sec. A series of 300 ft by 500 ft elliptical horizontal loops will be initiated, while the controls are tested and evaluated in their ability to maintain fixed, level flight. After 8 minutes of flight the proposed Delta Monster will enter a powerless glide profile with 10% reserve power. The glide will consist of series of slow gradual turns to dissipate energy. Finally, the demonstrator will be brought in at a moderate angle of approach and belly landed into soft grass. The folding propellor, which was modeled as the A12-6 for purposes of test calculations, would remain intact.

Flight test of the technology demonstrator was unsuccessful and furthermore proved inconclusive. Upon becoming airborne the RPV leveled

off and then initiated an extremely steep dive from an altitude of approximately 6 feet. It was speculated that this dive was a result of possible radio interference or inherent aerodynamic characteristics which could not be accounted for in the preliminary analysis.

REFERENCES

1. Simons, Martin, Model Aircraft Aerodynamics, Argus Books Limited, London, Second Edition, 1987, pp. 56-57.